

RESERVOIR AND DIAGENETIC
CHARACTERIZATION OF THE LOWER
COCHRANE MEMBER, HUNTON GROUP –
LINCOLN AND LOGAN COUNTIES, OKLAHOMA

By

CESAR SILVA

Bachelor of Science in Geology

Universidad Nacional de Colombia

Bogotá, Colombia

2005

Submitted to the Faculty of the
Graduate College of the
Oklahoma State University
in partial fulfillment of
the requirements for
the Degree of
MASTER OF SCIENCE
December, 2012

RESERVOIR AND DIAGENETIC
CHARACTERIZATION OF THE LOWER
COCHRANE MEMBER, HUNTON GROUP –
LINCOLN AND LOGAN COUNTIES, OKLAHOMA

Thesis Approved:

Jay M. Gregg

Thesis Adviser

James Derby

James O. Puckette

Darwin R. Boardman II

ACKNOWLEDGEMENTS

First of all, I want to acknowledge my family who are the foundation of my life

I wish to express my sincere thanks to my adviser Dr. Jay Gregg for his encouragement and support during the last two years

I also thank Dr. James Derby for all the ideas and material provided

I am deeply grateful to Dr. Jim Puckette for all his invaluable help

I also want to thank my committee member Dr. Darwin Boardman for his comments

I am grateful to John Chimahusky and Moe Nagaty from Equal Energy for the financial support to this project

Thanks to Marjo Operating Company for the material provided

I would like to thank Dr. Eliot Atekwana for his insights on isotopes data

I also want to thank Dr. Michael Grammer for his help on sedimentology and stratigraphy

I am thankful to Erin Roehrig for her help with the SEM and EDS analyses

I want to thank Brian Smith for his cooperation all the way through this thesis

I want to acknowledge Jackie Berryman for her help editing this thesis

I also thank Alex Fitzgerald, Cody Bacon and Sara Callner for their help with Petra

Thanks to all the faculty members at the Boone Pickens School of Geology – OSU

Finally, I take this opportunity to thank my good friends for the last two years: Drew Nelson, Malachi Lopez, Cody Bacon, Erin Roehrig, and Pride Abongwa whom made of my sojourn in Stillwater an enjoyable experience

Name: CESAR SILVA

Date of Degree: DECEMBER, 2012

Title of Study: RESERVOIR AND DIAGENETIC CHARACTERIZATION OF THE LOWER COCHRANE MEMBER, HUNTON GROUP – LINCOLN AND LOGAN COUNTIES, OKLAHOMA

Major Field: GEOLOGY

ABSTRACT: The Ordovician – Devonian Hunton Group is an important carbonate reservoir in central Oklahoma. The lower Cochrane member of the Hunton Group was affected by sea level changes during the Llandoveryian (Early Silurian), which favored early karsting throughout the reservoir. The dolomitization in the lower Cochrane member is the result of seawater migration through the reservoir at near surface temperatures. The dolomite carbon and oxygen isotopic signature (averaging $\delta^{18}\text{O} = -4.01\text{‰} \pm 0.69$ and $\delta^{13}\text{C} = 0.13\text{‰} \pm 0.76$) likely were partially reset during circulation of meteoric fluids that precipitated later calcite cements. Dolomite, together with calcite cements, was precipitated during the Silurian prior to the deposition of the Devonian Misener Sandstone and Woodford Shale. Sand, silt, and clay from Devonian siliciclastics occlude porosity, filling fractures and vugs after calcite cementation, and possibly after sparse silica cement. Stylolites, resulting from pressure-dissolution, represent the last diagenetic event recognized in the reservoir. Hydrocarbon production in the study area is likely related to fracturing and reservoir thickness rather than lithofacies. In general, the dolomite in the lower Cochrane member is more porous and permeable than limestone but its lack of uniformity affects overall reservoir quality.

TABLE OF CONTENTS

Chapter	Page
I. INTRODUCTION.....	1
II. GEOLOGICAL SETTING	4
Regional Structural and Stratigraphic Setting.....	4
Geological Setting of the Area of Study.....	5
III. DOLOMITIZATION.....	8
IV. METHODS.....	9
V. RESULTS	11
Petrophysical Mapping	11
Core Description	19
Anna 1-15 Core.....	20
Boone 1-4 Core.....	23
Carter Ranch 2-15 Core	23
Mary Marie 1-11 Core	24
McBride South 1-10 Core.....	24
Wilkerson 1-3 Core.....	25
Williams 1-3 Core.....	25
X-Ray Diffraction Analysis	26
Transmitted Light Petrography	28
Cathodoluminescence Microscopy	30
Stable Oxygen ($\delta^{18}\text{O}$) and Carbon ($\delta^{13}\text{C}$) Isotope Geochemistry	39
SEM and EDS Analyses	41
VI. DISCUSSION.....	44
Karsting – Fractures – Pressure-Solution	44
Dolomite – Calcite Cements – Silica Cement – Sand-mud infill	46
Dolomite Stable Isotope Geochemistry – SEM and EDS – XRD Analyses.....	47
Paragenetic Sequence of the Lower Cochrane Member	49
Reservoir Porosity and Permeability	51

Chapter	Page
VII. CONCLUSIONS	54
REFERENCES	55
APPENDICES	62

LIST OF TABLES

Table	Page
1. Core location, thicknesses and production.....	12
2. Samples with XRD analysis.....	27
3. Samples with carbon and oxygen isotope analyses	39
4. Mean isotope values for dolomite and brachiopods	40
5. Quant result for EDS spectrum of McBride South 1-10 core.....	41
6. Dolomite and limestone porosities and permeabilities	52

LIST OF FIGURES

Figure	Page
1. Location map of the study area.....	2
2. Map of the geological provinces of Oklahoma.....	6
3. Generalized stratigraphic column of the Hunton Group.....	7
4. Type log of the study area.....	13
5. Depth structural map at top of the Hunton Group.....	14
6. Depth structural map at top of the Sylvan Shale.....	15
7. Hunton reservoir thickness map.....	16
8. Dolomitic facies thickness map.....	17
9. Cross sections of the study area.....	18
10. Stratigraphic correlation between cores.....	21
11. Pictures of the Anna 1-15 core.....	22
12. XRD analyses of four samples from the Carter Ranch 2-15 core.....	27
13. Photomicrographs of dolomite and dolomitized limestone.....	29
14. Dolomite CL zones.....	31
15. Photomicrographs of dolomite and dolomitized limestone.....	32
16. CL variations on zone D1.....	34
17. Silica cement, skeletal allochems, and sand-mud infill.....	35
18. Fractures with respect to dolomite and calcite cements.....	36
19. Stylolites with respect to dolomite and limestone facies.....	37
20. Diagenetic events in the reservoir.....	38
21. Stable carbon and oxygen isotope data.....	40
22. SEM photomicrographs and EDS analyses.....	42
23. SEM photomicrographs.....	43
24. Paragenetic sequence of the lower Cochrane member.....	51
25. Porosity of dolomite facies vs. limestone facies.....	53

CHAPTER I

INTRODUCTION

The sedimentology and stratigraphy of the Hunton Group in Lincoln and Logan Counties are relatively well understood (West Carney Hunton Field – Derby *et al.*, 2002; Derby, 2007; Braimoh, 2010). Little is known, however, about the diagenetic processes that affected the Hunton Group reservoir. These processes are relevant to the overall understanding of the ultimate porosity and permeability of carbonate reservoirs. The study area is located in Lincoln and Logan counties (T. 15 N., R. 1 and 2 E.), and covers nearly 140 Km² (Fig. 1). Major production in the area comes from the Hunton Group, primarily from the basal Chimneyhill Subgroup (Late Ordovician – Early Silurian).

Since 1979, the Hunton reservoir has produced 4.9 MMBOE, and 41.3 MMCFG from the fields within the area of study (Fig. 1). Only the Silurian portion of the Chimneyhill Subgroup has been observed in the study area and is represented by the Cochrane Formation (Llandoveryan, Early Silurian). Based on conodont faunas, the Cochrane Formation is subdivided into three informal members: the lower Cochrane member, and two upper Cochrane members (Derby, 2007). Two macrofacies of the lower Cochrane member are the primary reservoirs in the study area, a dolomite facies containing more than 20% of the oil, and a fossiliferous limestone facies holding nearly 80% of the oil (Derby *et al.*, 2002).

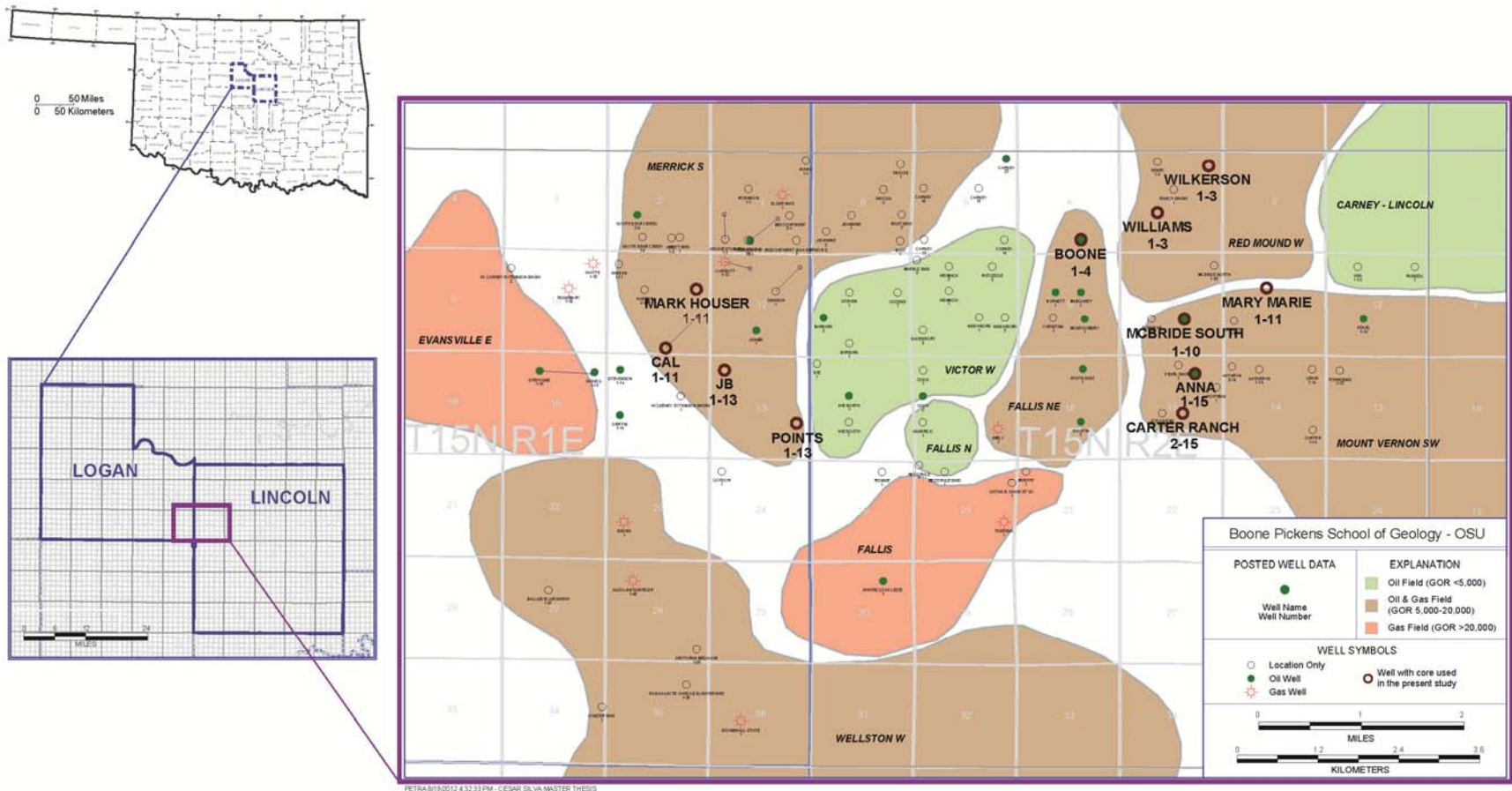


Figure 1. Map showing the study area in T15N, R 1 and 2 E, Lincoln and Logan Counties, Oklahoma. Boundaries of the oil and gas fields are modified from the map GM-36 by Boyd (2002), Oklahoma Geological Survey.

This project will determine the process or processes of dolomitization in the lower Cochrane member and addresses the question of why dolomitization is restricted to specific areas of the reservoir. Better understanding of these processes will help to determine the most appropriate reservoir stimulation method and potentially enhance secondary recovery. Reservoir characterization of the Hunton Group is timely as it is one of the major hydrocarbon producing reservoirs in central Oklahoma and represents an important target for oil and gas exploration and development.

Structural and isopach maps of the reservoir were generated from wireline logs. Core slabs from seven wells in Lincoln County were described in detail (Fig. 1). Transmitted light petrography, cathodoluminescence microscopy, x-ray diffraction analysis, stable isotope geochemistry, scanning electron microscopy, and energy-dispersive x-ray spectroscopy were conducted in order to establish the diagenetic history of the reservoir and the composition of the dolomitizing fluids.

CHAPTER II

GEOLOGICAL SETTING

Regional Structural and Stratigraphic Setting

During the Llandoveryan (Early Silurian Period), warm seawater temperatures favored the deposition of carbonates in Laurentia, northeastern Avalonia, Baltica, Siberia and equatorial Gondwana (Scotese and McKerrow, 1990). A shallow epicontinental sea covered most of the continent of Laurentia (Scotese, 2002), which was a restricted basin under arid conditions, with little to no siliciclastic input, favoring the production and deposition of carbonates. Sea level changes affected the carbonate stratigraphy with five major highstands during the Lower Silurian and three during the Upper Silurian (Johnson, 2006). Posterior collision of Laurentia with Avalonia and Baltica, during the Late Silurian – Early Devonian, resulted in the formation of the new continent Euramerica (Laurussia). This tectonic event may have modified the basin depocenter producing changes in carbonate thickness.

Johnson (1987) suggested that the Oklahoma Basin was the major depocenter in Oklahoma and northern Texas during the Early to Middle Paleozoic. Sediments from most parts of the Oklahoma Basin are widespread and laterally persistent. The uplift of the Nemaha Ridge and Ouachita Mountains during the Pennsylvanian split the Oklahoma Basin into the Anadarko Basin to the west, the Arkoma Basin to the southeast, and the Cherokee Platform to the northeast.

Charpentier (1995) sub-divided the Cherokee Platform Province into 6 conventional plays and 1 unconventional coalbed gas play. The most important play for this study is the *Pre-Woodford Paleozoic Play* that contains at least five different reservoir facies and two source facies, the Simpson Group shales (Ordovician), and the Woodford Shale (Late Devonian – Early Mississippian).

The present thesis concentrates on the Hunton Group as the reservoir of interest, which averages 12 m (39.4 ft) of net pay. Traps in the *Pre-Woodford Paleozoic Play* are primarily structural with some stratigraphic component involved throughout the Cherokee Platform Province (Charpentier, 1995). However, in the study area the trapping mechanism is primarily stratigraphic.

Geological Setting of the Area of Study

The study area is located on the Cherokee Platform, bounded by the Nemaha Ridge on the west, the Ozark Uplift on the east, and the Arkoma Basin and Arbuckle Uplift to the south (Fig. 2).

During the lower Paleozoic, the depositional slope of the Oklahoma Basin was southwestward into the Southern Oklahoma Aulacogen. Early Silurian structural movements have been suggested by the distribution and thickness of the carbonate reservoir (Derby *et al.*, 2002).

Posterior development of the Nemaha Uplift to the west and in the Arkoma Basin to the east tilted the study area eastward. This eastward tilting continued throughout the Upper Paleozoic. The study area was subsequently tilted southwestward during the Mesozoic resulting in the modern structural dip of about 8.5 m per km towards the southwest (Derby *et al.*, 2002). In the study area, the thickness of the Hunton Group ranges from 7 to 42 m (24 to 139 ft).

The shallow marine carbonates of the Chimneyhill Subgroup are the major reservoir in the study area (Derby *et al.*, 2002). Five megafacies have been recognized within the Chimneyhill Subgroup: (1) reef and reef-flank; (2) brachiopod biostrome; (3) lagoonal; (4) dolomitized shoal-

water grainstone; and (5) deepwater (Derby, 2007). The carbonates are unconformably overlain by the Late Devonian – Early Mississippian Misener Sandstone/Woodford Shale, and underlain by the Late Ordovician Sylvan Shale (Fig. 3). Three formations are defined within the Chimneyhill Subgroup: the Keel Formation (bottom), the Cochrane Formation (middle), and the Clarita Formation (top). Braimoh (2010) subdivided the Cochrane Formation into three informal units: the lower Cochrane member, the upper Cochrane A member, and the upper Cochrane B member (Fig. 3). This informal operational stratigraphy is adopted for this research.

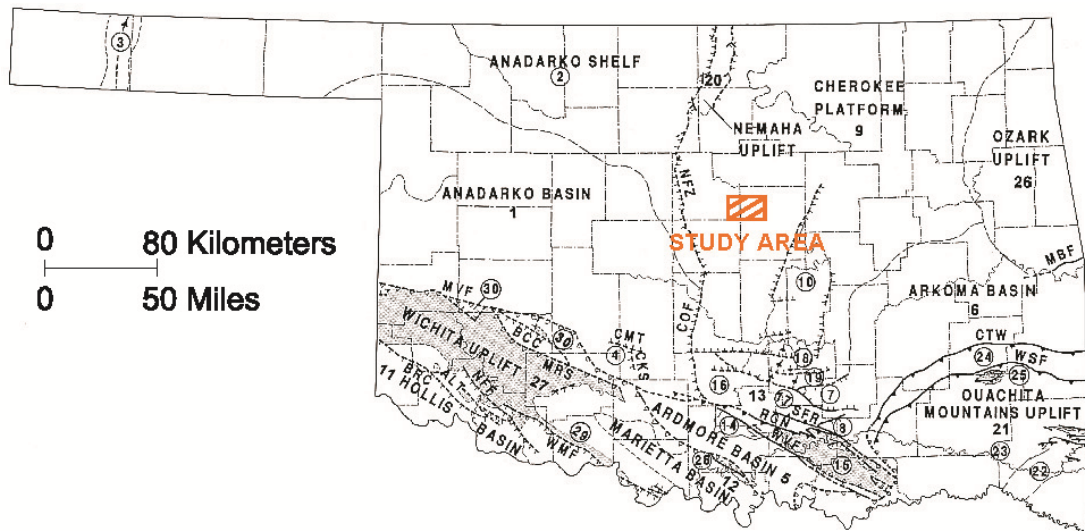


Figure 2. Map of the geological provinces of Oklahoma from Northcutt and Campbell (1995). Numbers correspond to geologic provinces listed by the referenced source.

The lower Cochrane member consists of brachiopod and crinoidal grainstones and packstones from the reef and reef-flank, and lagoonal megafacies (Derby, 2007). The upper Cochrane members and the Clarita Formation are seldom present to absent because of the relatively high paleo-topography in the study area (paleo-highs up to 30 m (98 ft), Braimoh (2010)). This paleo-

topography blocked the deposition of more carbonates overlying the lower Cochrane member and favored the unconformable contact with the overlying Misener Sandstone and Woodford Shale.

Derby (2007) describes the lower Cochrane member as a reef-dominated carbonate shoal that formed as an isolated platform into the early Silurian Sea. Stratigraphic continuity of the reef carbonates is poor, lateral transitions are abrupt, and traceable subdivisions within the unit are rare. Subaerial weathering of the reservoir, during lowstands of the Silurian Sea, resulted in the development of karst related porosity throughout the unit. Conventional interparticle porosity is developed in the dolomitic facies as well. Dolomitization here resulted in enhanced porosity and permeability. However, the dolomitic facies are not continuous across the field and the processes that lead to dolomitization are still unclear.

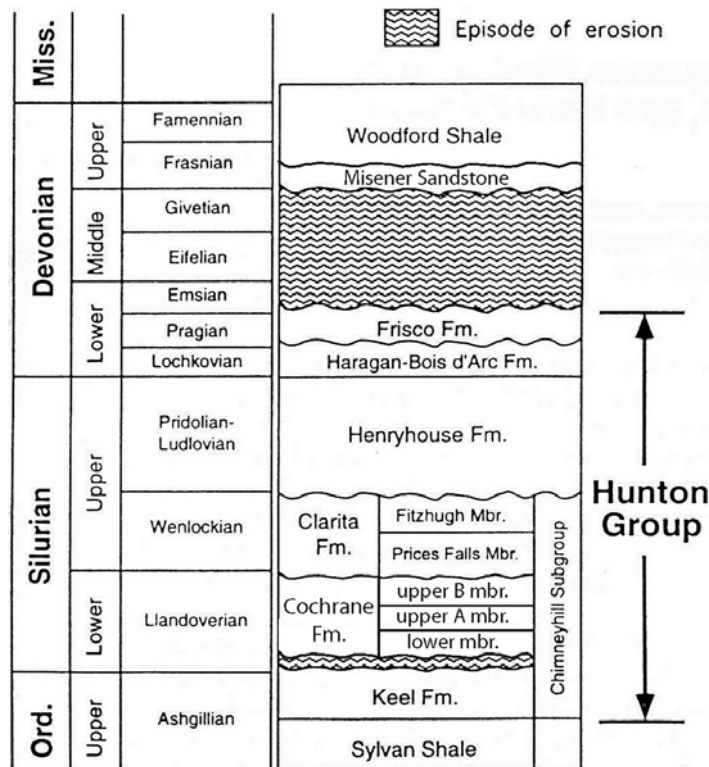


Figure 3. Generalized stratigraphic column of the Hunton Group in the Cherokee Platform. The lower Cochrane member of the Cochrane Formation is almost exclusively present within the study area. Modified from Barrick *et al.*, 1990.

CHAPTER III

DOLOMITIZATION

The diagenetic processes that resulted in dolomitization of the lower Cochrane member are not fully understood. Dolomitization is caused by post-depositional fluid migration and to a large extent determines the subsequent porosity and permeability of the reservoir. Dolomite is commonly porous and permeable, and hence a target for petroleum exploration (Tucker and Wright, 1990). However, dolomitization is not uniform throughout the study area and this lack of uniformity affects overall reservoir quality.

Four different types of fluids may cause dolomitization in any carbonate reservoir: (1) *normal seawater*: dolomite can be precipitated from normal seawater circulating through the precursor limestone (Saller, 1984); (2) *mixed seawater and freshwater*: dolomite may be formed by mixing meteoric water with up to 30% seawater causing undersaturation with respect to calcite and supersaturation with respect to dolomite (Badiozamani, 1973), or by alternating hypersaline seawater conditions with fresh water (Folk and Land, 1975); (3) *evaporitic reflux*: dolomite can be formed in underlying carbonates by downward refluxing hypersaline brines (Adams and Rhodes, 1960); and (4) *epigenetic fluids*: dolomitizing waters can be derived by dewatering of basinal strata at elevated temperature (Mattes and Mountjoy, 1980; Gregg, 1985; Machel, 2004).

CHAPTER IV

METHODS

Wireline logs from one hundred and four wells were correlated to generate structural and isopach maps of the reservoir. IHS Petra was used to correlate gamma ray, photoelectric, and porosity logs. Correlation was based upon determination of the top of the Hunton carbonates, top of the Sylvan Shale, and dolomitic facies within the reservoir. Structural and stratigraphic cross sections were also constructed for the study area.

Seven cores provided by Dr. James Derby and Marjo Operating Company were described in detail in order to identify dolomite and dolomitic limestone within the lower Cochrane member (Fig. 1, Table 1). The descriptions consisted of lithological identification, generalized fossil association, fabric determination using Dunham's (1962) classification, diagenetic features, and porosity classification by Choquette & Pray (1970). An emphasis was placed on selecting core from the dolomite facies rather than limestone facies.

X-ray diffraction (XRD) analyses of powdered dolomite were made with a Philips Analytical PW 1830/00 – copper PW 2273 tube diffractometer at Oklahoma State University. Seven samples of the Carter Ranch 2-15 core were used to quantify the amount of Mg substitution in the dolomite lattice, and establish the dolomite stoichiometry.

Fifty four polished thin sections were prepared from the cores. Sixteen additional oversized thin sections were provided by Dr. James Derby and Marjo Operating Company. The dolomite was described following Sibley and Gregg's (1987) classification. Total porosity was estimated from 600 point counts on each sample. Cathodoluminescence (CL) petrography was conducted using a CITL CL 8200 MK5-1 Optical Cathodoluminescence System. Photomicrographs from transmitted light and CL petrography were obtained with a Q Imaging Micropublisher 5.0 RTV cooled camera mounted on an Olympus BX51 petrographic microscope.

The isotope composition of the carbonates was determined using the Krishnamurthy *et al.*, (1997) method. Twenty eight powdered dolomite samples were measured using a Thermo-Finnigan Delta Plus gas-source isotope ratio mass spectrometer at Oklahoma State University. Prior to sampling, samples were stained with Alizarin red and described under the transmitted light and CL petrography in order to clearly identify dolomite. The $\delta^{13}\text{C}$ and $\delta^{18}\text{O}$ values (VPDB) have in-house standard errors of less than $\pm 0.1\%$. An emphasis was placed on selecting samples for isotopic analysis from which petrography is available.

Scanning electron microscopy (SEM) and energy-dispersive x-ray spectroscopy (EDS) of three dolomite samples were measured using a FEI Quanta 600 F field emission SEM at Oklahoma State University. The samples were coated with gold and palladium using a Balzers MED 100 coater. Photomicrographs were taken using a 14 MP image processor. A total of 20,428 counts were made for each EDS analysis, with a spot size of 4 nm, and a scan rate of 2,500 counts per second.

CHAPTER V

RESULTS

Petrophysical Mapping

Two tops were picked using gamma ray logs in the area of study, the top of the Hunton Group and the top of the Sylvan Shale (Fig. 4). The top of the Hunton Group was determined at the contact with the overlying Woodford Shale, a regional marker represented by its gamma ray values that exceed 150 API units (Fig. 4). The top of the Sylvan Shale was determined halfway from the low gamma ray values of the Hunton carbonates (approximate less than 30 API units) to the high values of the Sylvan Shale (approximate more than 80 API units). The dolomitic facies within the reservoir was determined from the porosity logs and photoelectric effect (Pe) values. Criteria used to identify dolomite from limestone establish that the neutron porosity (ϕ_N) reads higher than density porosity (ϕ_D) by at least 4 porosity units, and the Pe values ranging between 3 to 4.5 barns/electron (Fig. 4).

Structural contour maps on top of the Hunton Group (Fig. 5) and on top of the Sylvan Shale (Fig. 6) show a gentle dip towards the west – southwest. In the western part of the study area, both maps indicate a steeper westward dip towards the deepest part of the study area. A structural high with a northwest – southeast trend is observed in the middle of the Hunton structural map (Fig. 5).

API	Well name - number	Legal	Hunton thickness (m/ft)	Dolomite thickness (m/ft)	COP (BOE)	CGP (MCFG)
3508123606	Anna 1-15	S. 15, T15N, R2E	11.5 / 37.6	9.0 / 29.7	13,351	10,582
3508123567	Boone 1-4*	S. 4, T15N, R2E	9.0 / 29.5	1.6 / 5.3	16,055	90,375
3508123646	Carter Ranch 2-15	S. 15, T15N, R2E	8.9 / 29.1	4.8 / 15.8	8,291	82,238
3508123521	Mary Marie 1-11	S. 11, T15N, R2E	13.0 / 42.5	0.1 / 0.4	23,508	61,246
3508123593	McBride South 1-10	S. 10, T15N, R2E	10.4 / 34.3	1.0 / 3.4	26,921	218,742
3508123533	Wilkerson 1-3	S. 3, T15N, R2E	14.1 / 46.4	0.6 / 2.1	65,947	1,057,224
3508123562	Williams 1-3	S. 3, T15N, R2E	12.3 / 40.3	1.7 / 5.6	14,187	227,483

* Boone 1-4 produces from the Wilcox sandstone

Table 1. Seven cores described in this study from wells in Lincoln County, OK (See Fig. 1 for location map). All wells produce from the Hunton reservoir except the Boone 1-4 that produces from the Ordovician Wilcox Sandstone. Cumulative oil and gas production (COP and CGP) data corresponds to production since January 2000.

Subsea depth range for the Hunton Group structural map corresponds to 1483 – 1578 m (4866 – 5176 ft), and for the Sylvan Shale structural map corresponds to 1509 – 1616 m (4950 – 5301 ft).

The Hunton Group isopach map illustrates the heterogeneity in the reservoir thickness (Fig. 7). The reservoir is relatively thin in the eastern part with an average thickness of 15.2 m (50 ft), and thickens westward, reaching thicknesses of more than 40 m (130 ft). The thickness of the reservoir ranges from 7.4 m (24.3 ft of the Joe Givens 1-15 well – Sec. 15, T. 15 N., R. 2 E.) on the eastern part to 42.5 m (139.3 ft of the South Bear Creek 2-2 well – Sec. 2, T. 15 N., R. 1 E.) on the western part of the study area. The north – south oriented 24.4 m (80 ft) contour approximately delineates the change in thickness within the reservoir (Fig. 7). East from the 24.4 m (80 ft) contour line, the thickness is less than 24.4 m (80 ft); to the west the average thickness is around 30.5 m (100 ft). The dolomitic facies thickness map (Fig. 8) is consistent with the Hunton Group isopach map. The dolomitic facies thickens westward where the Hunton Group is the thickest, and is thinner eastward where the Hunton Group is the thinnest. The dolomite and dolomitized limestone thickness ranges from 0 to 20.1 m (0 to 65.8 ft), with the Algolian Suntiger 1-26 well (Sec. 26, T. 15 N., R. 1 E. – Fig. 8) containing the thickest section.

Structural and stratigraphic cross sections illustrate two structural domains within the area, and the heterogeneity in reservoir thickness (Fig. 9). The structural cross section (Fig. 9 a) shows two folds in the western part of the study area, an anticline and a syncline from Steffanie 1-15 well to Schwake 1-10 well. On the other hand, the eastern part of the study area is relatively flat with a gentle structural dip upward to the easternmost well, the Russell 1. The stratigraphic cross section (Fig. 9 b) illustrates how the reservoir thickens westward. The thicknesses from the Barbara 1 well to the Steffanie 1-15 well average more than 30.5 m (100 ft), and the thicknesses from the Davenport 2 well to the Russell 1 well are less than 24.4 m (80 ft).

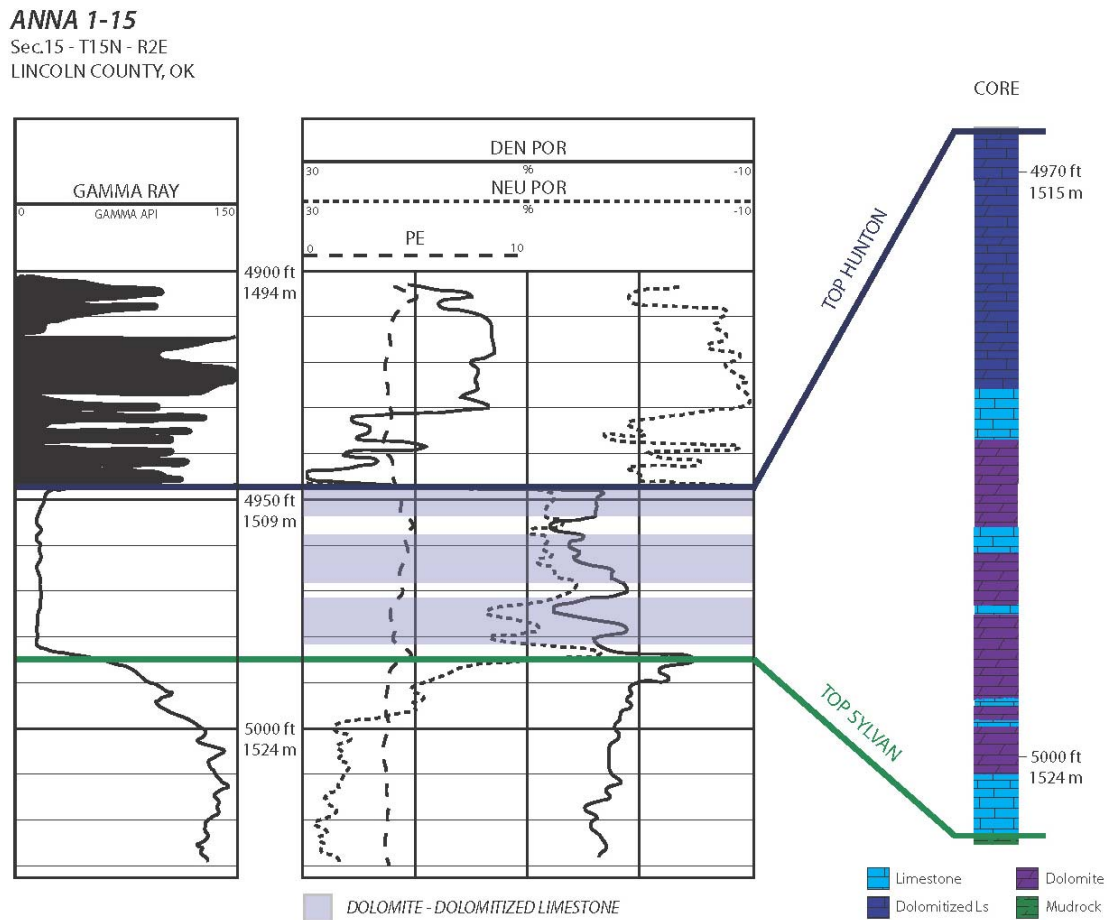
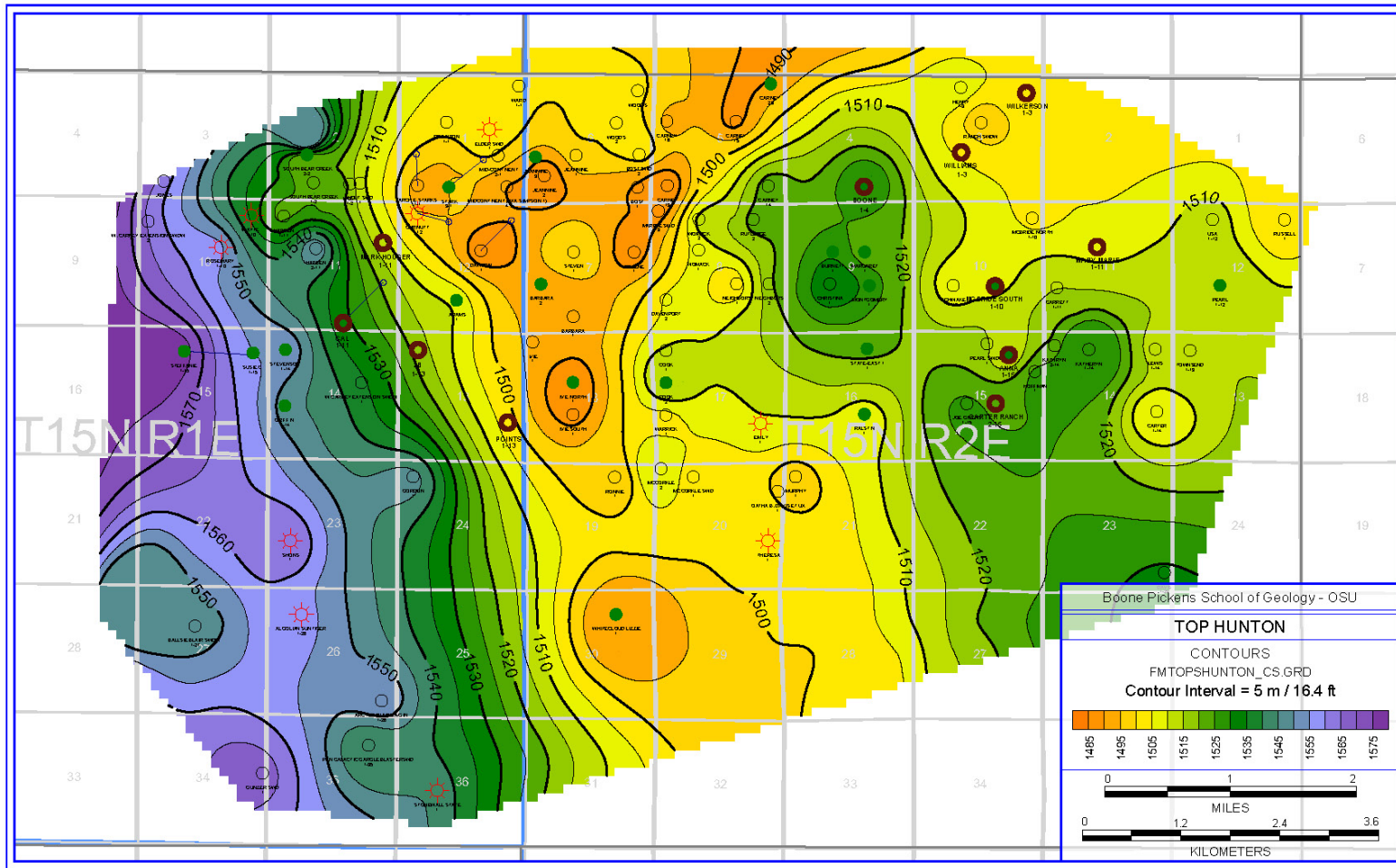
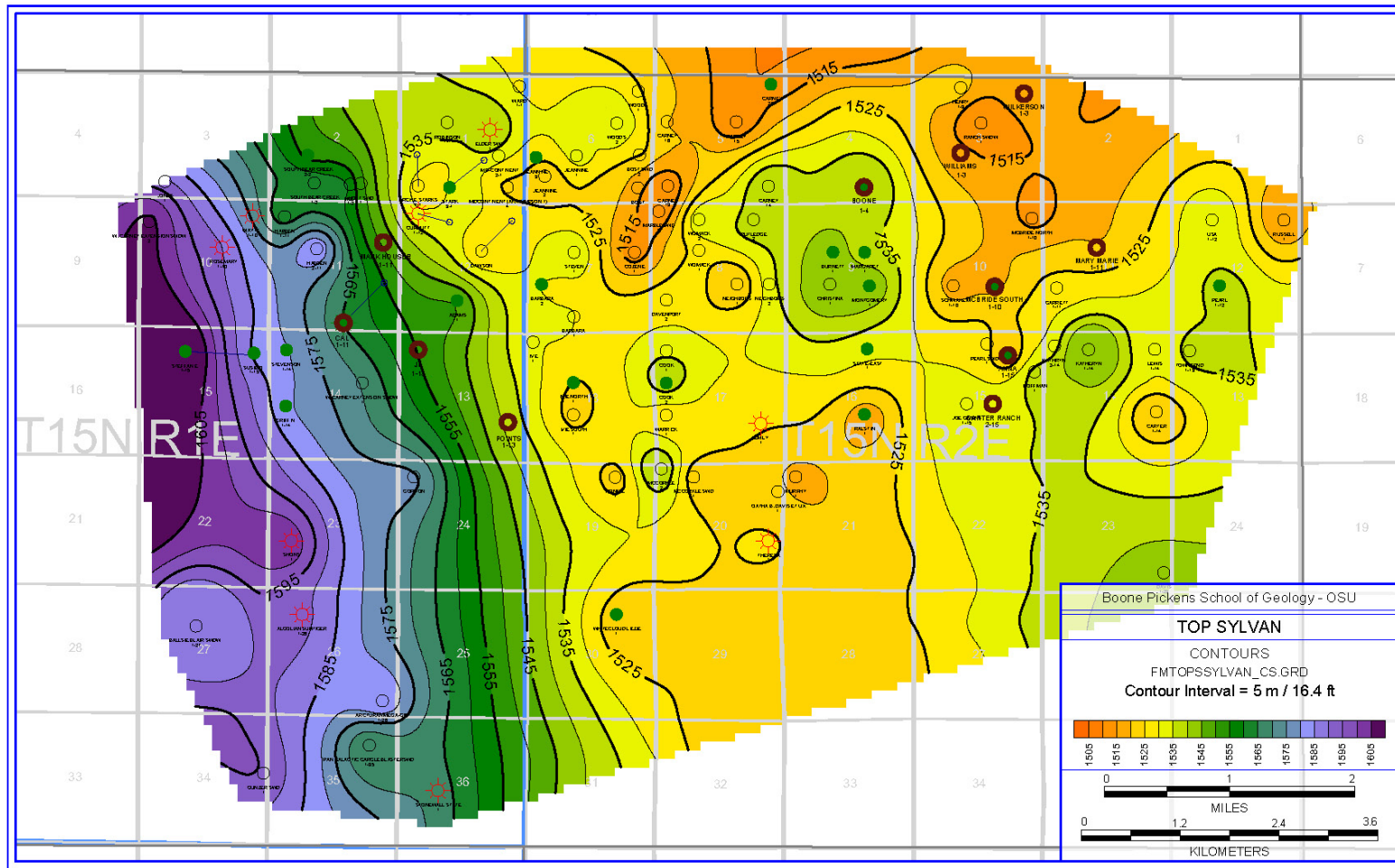


Figure 4. Type log of the study area showing the Hunton and Sylvan markers. Dolomite and dolomitized limestone are determined from Pe values and porosity logs (light purple). Core description (right) is correlated to the type log. The Anna 1-15 well is used as analog.



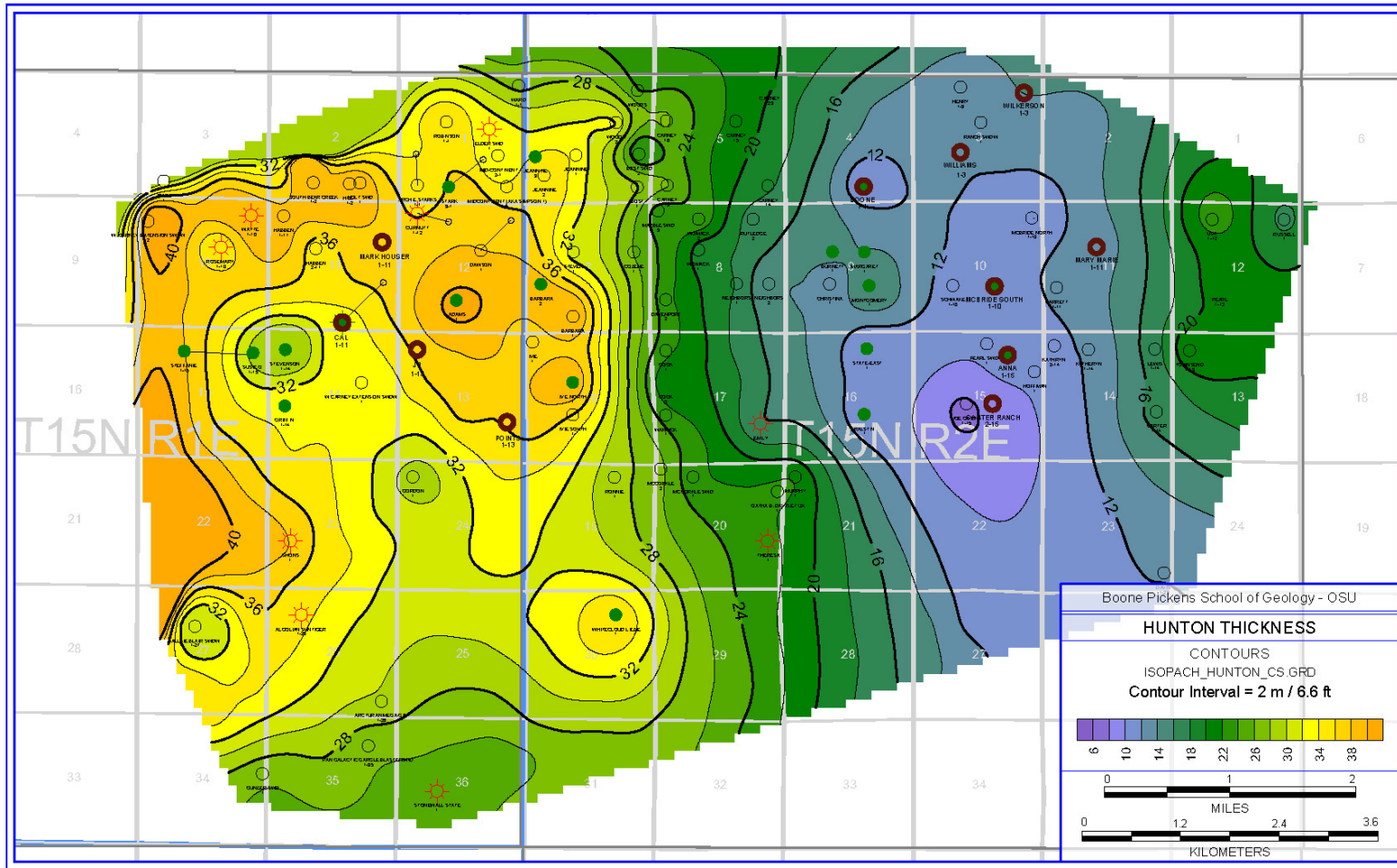
PETRA11/30/2012 11:03:57 AM - CESAR SILVA MASTER'S THESIS

Figure 5. Contour map on top of the Hunton Group. Regional dip is west–southwest towards the deepest part of the study area. Dip is gentle on the eastern side (10m/mile) and becomes steeper on the western side (30m/mile). Contour values are negative. Contour interval: 5m / 16.4ft.



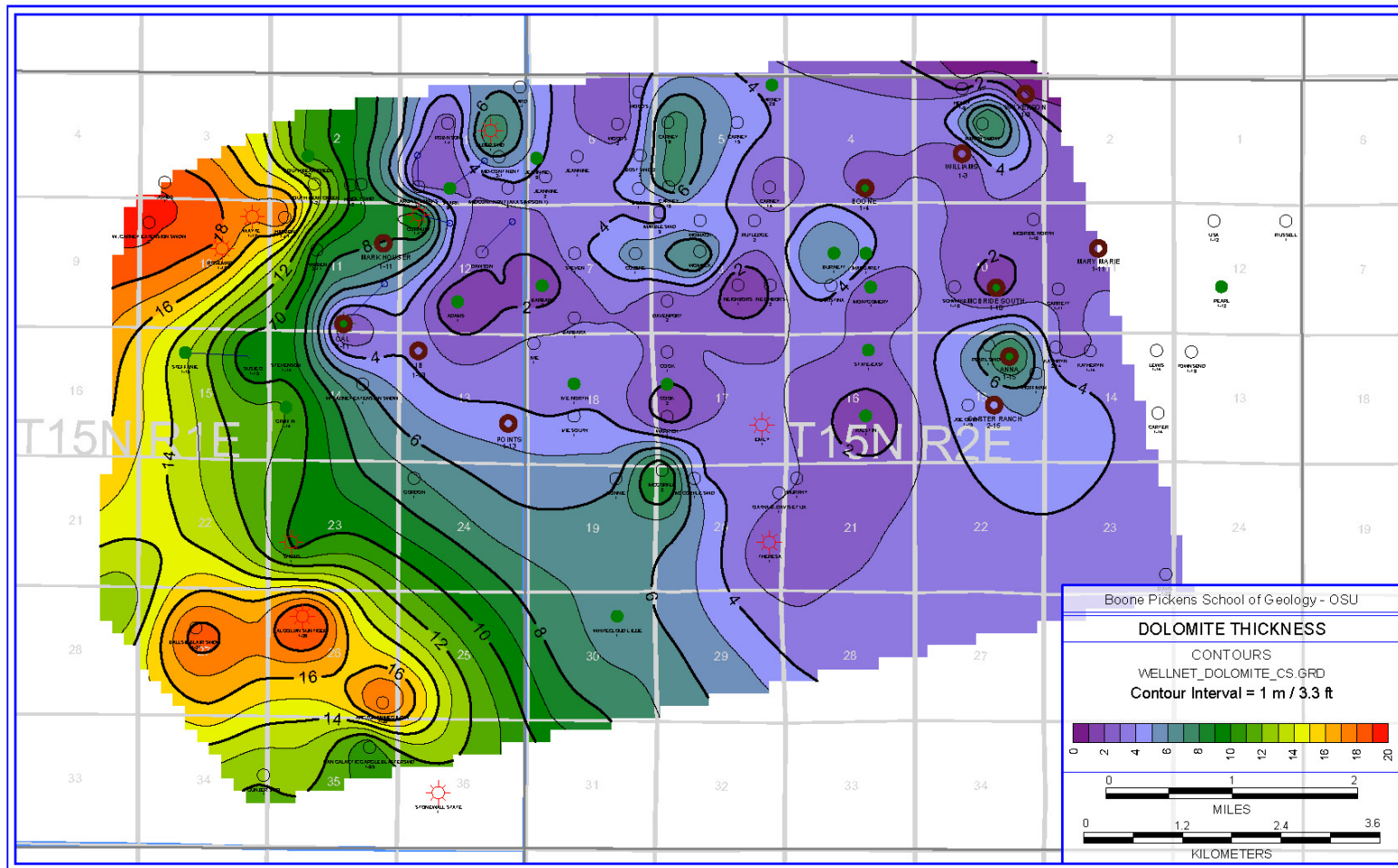
PETRA 12/22/2012 4:50:59 PM - CESAR SILVA MASTER'S THESIS

Figure 6. Contour map on top of the Sylvan Shale. Regional dip is west–southwest towards the deepest part of the area of study. Shallow dip on the eastern half of the study area becomes steeper on the western part. Contour values are negative. Contour interval: 5m / 16.4ft.



PETRA 12/2/2012 8:24:32 PM - CESAR SILVA MASTER'S THESIS

Figure 7. Hunton reservoir thickness map illustrating that the reservoir thickens westward, towards the deepest part of the study area. Contour interval: 2m / 6.6ft.



PETRA 12/2/2012 6:43:38 PM - CESAR SILVA MASTER'S THESIS

Figure 8. Total dolomitic facies thickness map. The cumulative thickness of the dolomitic facies is greatest to the west where the carbonates section is thicker. Contour interval: 1m / 3.3ft.

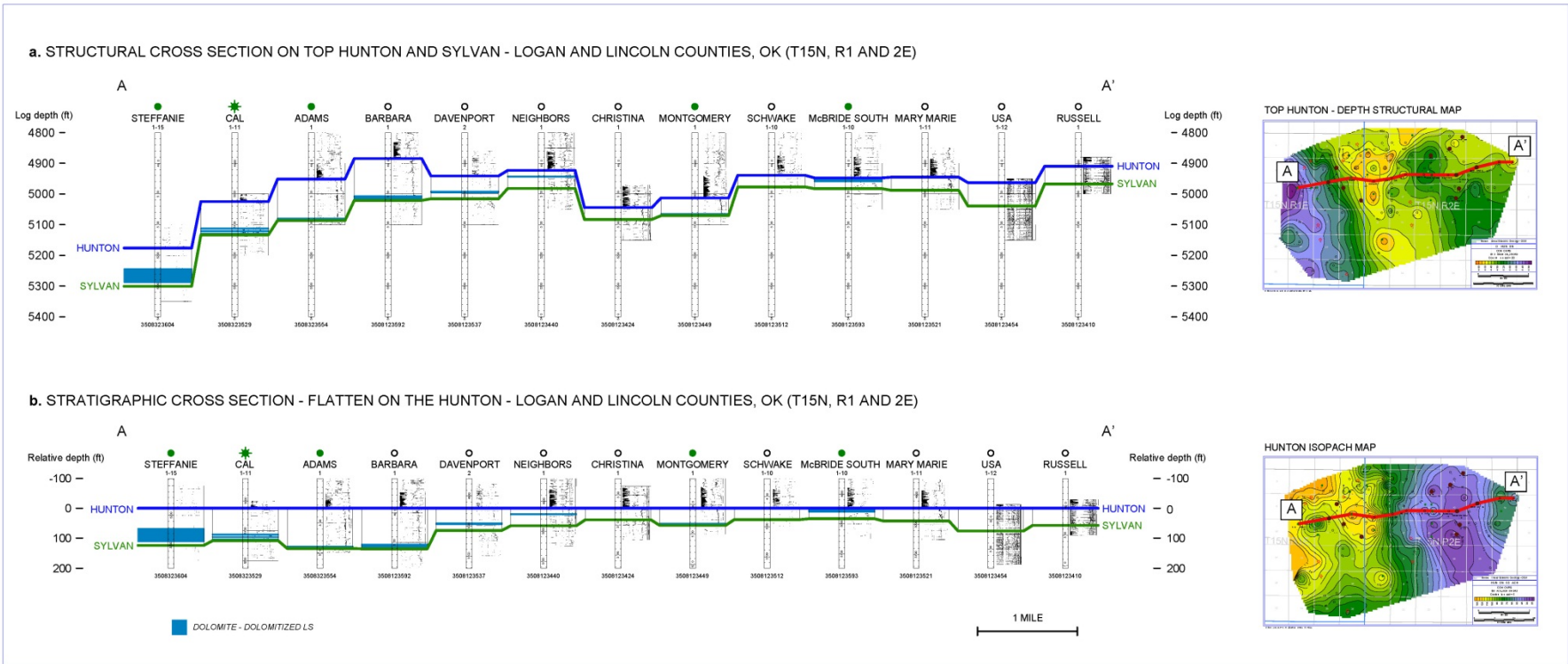


Figure 9. Cross sections from west to east across the study area (A to A'). **a.** Structural cross section showing two folds on the western side, and a relatively flat westward dip on the eastern side. **b.** Stratigraphic cross section flattened on the top of the Hunton Group illustrating how the section thickens westward.

Core Description

A total of 89.8 m (294.5 ft) of core from seven wells in Lincoln County were described in detail (Table 1, Plates 1 through 7). Core descriptions emphasized identification of dolomite and dolomitic limestone within the reservoir. Location, thicknesses, and cumulative oil and gas production from each well with core are summarized in Table 1. A stratigraphic correlation between the cores described in this study is shown in Figure 10. Photographs of the Anna 1-15 core are shown on Figure 11.

In general, the lower Cochrane member is made up of pink, yellow, tan and white grainstones and crystalline dolomite/limestone, less commonly packstones and boundstones, associated with pentamerid brachiopods (*Pentamerus sp.*, *Stricklandia sp.* from Derby (2010)), sparse crinoids, and occasional tabulate coral fragments (*Favosites sp.*, *Halysites sp.*, *Catenipora sp.* from Derby (2010)). Brachiopods are typically larger than 2mm and unreplaced by dolomite. However, the most common moldic porosity in the core is a result of brachiopods dissolution. Crinoids and corals are much less common and are frequently larger than 2 mm and unreplaced by dolomite. All described cores, except the Mary Marie 1-11, are slightly to highly dolomitized and described as yellowish-white dolomitized limestone, and grey crystalline dolomite with planar-e (sucrosic) texture. Areas of dolomitization are not uniform throughout the reservoir (Fig. 10).

The most common types of porosity in the dolomitic facies are intercrystal, moldic, solution-enlarged molds, vuggy, and shelter. On the other hand, the most common types of porosity in the limestone facies are interparticle, intraparticle, vuggy, shelter, and fracture. The porosity size ranges from large mesopores (0.0625 – 0.5 mm) to small megapores (4 – 32 mm) in both facies. Diagenetic features, such as stylolites and fractures are present in both facies. Stylolites are very frequent and range from less than 1mm to 25 mm of amplitude. These stylolites are commonly bounding the dolomitic facies (Fig. 11 B) indicating that dolomitization occurred prior to

pressure-solution. Fractures in the cores are filled with sand, silt, and mud that likely came from the overlying Devonian siliciclastics, and occasionally by calcite cement (base of the Anna 1-15 core). Vertical fractures crosscut the dolomite and limestone facies, and stylolites.

The thickness of the lower Cochrane member ranges from 8.9 m (29.1 ft) in the Carter Ranch 2-15 core to 14.1 m (46.4 ft) on the Wilkerson 1-3 core. The dolomitic facies thickness ranges from 0.12 m (0.4 ft) in the Mary Marie 1-11 core to 9 m (29.7 ft) in the Anna 1-15 core. Sharp unconformable contacts were observed with the underlying Sylvan Shale and with the overlying Misener Sandstone and Woodford Shale (Fig. 10).

Anna 1-15 Core [Sec. 15, T. 15 N., R. 2 E.]

The Anna 1-15 core is 11.7 m (38.4 ft) thick at a depth of 1514 – 1526 m (4967 – 5005.4 ft, Fig. 11). At the base of the core is 0.2 m (0.6 ft) of Sylvan Shale (Fig. 11 E); at the top is 0.05 m (0.15 ft) of the Misener Sandstone (Fig. 11 A). The Hunton carbonates are 11.5 m (37.6 ft) thick. The predominant carbonate lithology is grainstone and less common packstone and crystalline carbonates. Fauna associations are *Pentamerus sp.* and *Stricklandia sp.* brachiopods. The dolomite facies has sucrosic texture and is 9 m (29.7 ft) thick. It is often bounded by stylolites and contains moldic porosity. Other common types of porosities observed are fracture and vuggy forming large mesopores to small megapores; diagenetic features such as stylolites (up to 10 mm of amplitude), vertical fractures, and muddy sand infill (Fig. 11) are common in the dolomite and limestone facies. See Plate 1 for detailed descriptions.

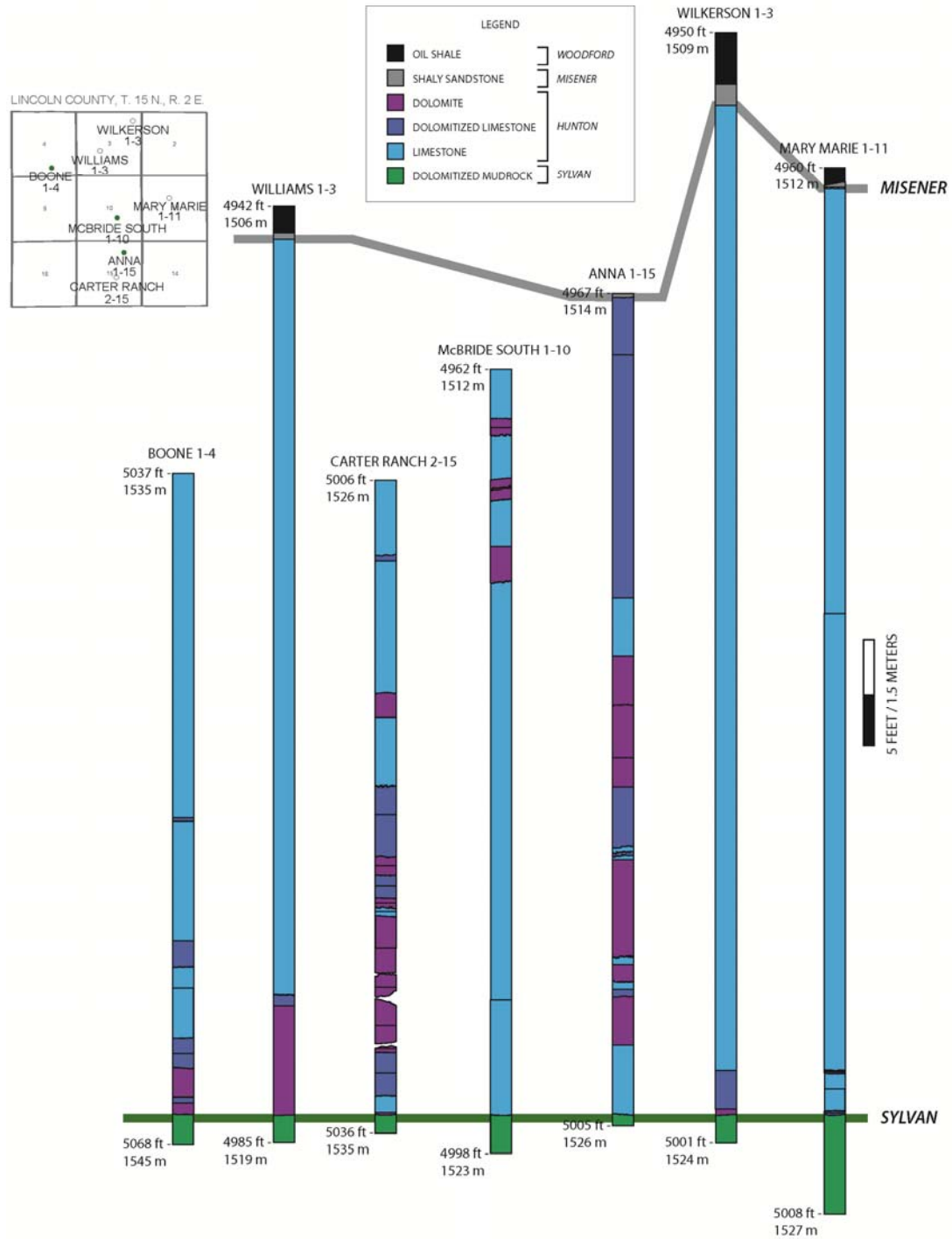


Figure 10. Stratigraphic correlation of the cores described in this study. The Sylvan Shale was cored in the seven wells. The Misener Sandstone and the Woodford Shale were cored in four wells. Note the lack of continuity and uniformity in the spatial distribution of the dolomitic facies within the Hunton Group.

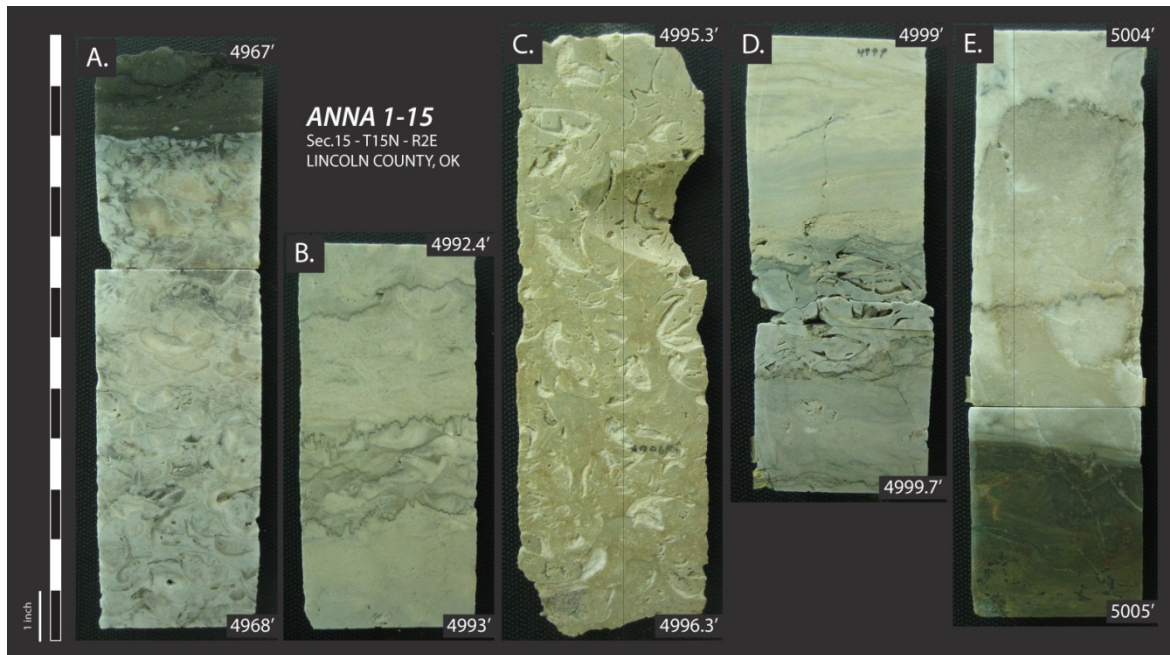


Figure 11. Photographs of representative samples of the lithofacies in the Anna 1-15 core. **A.** Misener Sandstone (dark grey), with silicified brachiopod fragments, unconformably overlies a dolomitized brachiopod grainstone of the Hunton Group (white-light grey). **B.** Dolomitized brachiopod grainstone (grey) bounded by stylolites. Limestones (white-light grey) are subjacent and above the dolomitic facies. **C.** Dolomite replacing matrix and partially dissolved brachiopods generating moldic porosity. **D.** Dolomite (grey) in contact with underlying slightly dolomitized limestone (white-light grey). Moldic porosity forms small megapores (5 to 20mm) within the dolomite. Low angle lamination is present in the dolomitized limestone. **E.** Crystalline limestone with stylolites (white-light brown) unconformably resting on the Sylvan Shale (dark green). Detailed description of the Anna 1-15 core is on Plate 1.

Boone 1-4 Core [Sec. 4, T. 15 N., R. 2 E.]

The Boone 1-4 core is 9.4 m (30.9 ft) thick at a depth of 1535 – 1545 m (5037 – 5067.9 ft). At the base is 0.4 m (1.4 ft) of Sylvan Shale. The Sylvan Shale is overlain by 9 m (29.5 ft) of Hunton carbonates on an abrupt unconformable contact. Neither the Misener Sandstone or the Woodford Shale were cored. The predominant carbonate lithology is pink, yellow, white grainstone and less commonly packstone and crystalline dolomite/limestone. Fauna associations are pentamerid brachiopods, crinoids, and tabulate corals (*Halysites sp.*). The dolomite facies is 1.6 m (5.3 ft) thick, and is recognized by its sucrosic texture, frequently bounded by stylolites, and contains dominantly moldic porosity. Other types of porosity observed are fracture and vuggy, forming large mesopores and small megapores in the dolomite and limestone facies. Stylolites (up to 16 mm amplitude) are present as well as vertical fractures filled with brownish-yellow muddy sandstone. At the depth of 1541 m (5055 – 5056 ft), a crystalline limestone shows wavy parallel lamination and a channel sand infill, which is interpreted as representing a paleo-slope or an uneven dissolution surface as a result of karsting. See Plate 2 for detailed descriptions.

Carter Ranch 2-15 Core [Sec. 15, T. 15 N., R. 2 E.]

The Carter Ranch 2-15 core is 9.1 m (30 ft) thick at a depth of 1526 – 1535 m (5006 – 5036 ft). At the base of the core is 0.3 m (0.9 ft) of Sylvan Shale. The Sylvan Shale is overlain by 8.9 m (29.1 ft) of Hunton Group carbonates that rest on an abrupt unconformable contact. Neither the Misener Sandstone or the Woodford Shale was cored. The predominant carbonate lithology is tan grainstone and less commonly crystalline carbonate and mudstone. Fauna associations are pentamerid brachiopods (*Pentamerus sp.*, *Stricklandia sp.*) and tabulate corals (*Favosites sp.*). The grey dolomite facies is 4.8 m (15.8 ft) thick, is often bounded by stylolites, and is distinguished by its characteristic moldic porosity. Other common types of porosity are fracture

and vuggy, forming large mesopores to small megapores in the dolomite and limestone facies. Diagenetic features such as stylolites (up to 24 mm of amplitude) are frequent. The core is highly fractured and near the top the fractures are filled by brownish-yellow muddy sublitharenite. See Plate 3 for detailed descriptions.

Mary Marie 1-11 Core [Sec. 11, T. 15 N., R. 2 E.]

The Mary Marie 1-11 core is 17.1 m (56 ft) thick at a depth of 1512 – 1529 m (4960 – 5016 ft). At the base of the core is 3.8 m (12.5 ft) of the Sylvan Shale. At the top, the core is 0.1 m (0.3 ft) of the Misener Sandstone overlain by 0.2 m (0.7 ft) of the Woodford Shale. The Hunton Group is 13 m (42.5 ft) thick, and composed of pink, white, and tan grainstone, and less commonly crystalline carbonate. Fauna associations are pentamerid brachiopods, tabulate corals (*Favosites sp.*, *Catenipora sp.*), sparse crinoids, and a bryozoan (?) fragment at 1524 m (5000.8 ft). Only 0.12 m (0.4 ft) of the dolomitic facies is present in this core as a grey crystalline dolomite with vuggy porosity (large mesopores up to 2mm). Common porosity types in the limestone facies are vuggy, fracture, and shelter, creating large mesopores to small megapores. Other diagenetic features consist of stylolites (up to 25 mm of amplitude), fractures, and grey muddy sand filling voids and fractures. See Plate 4 for detailed descriptions.

McBride South 1-10 Core [Sec. 10, T. 15 N., R. 2 E.]

The McBride South 1-10 core is 11 m (36 ft) thick at a depth of 1512 – 1523 m (4962 – 4998 ft). The base of the core contains 0.5 m (1.7 ft) of Sylvan Shale, which is overlain by 10.5 m (34.3 ft) of Hunton carbonates on an abrupt unconformable contact. Neither Misener Sandstone nor Woodford Shale was cored. The Hunton Group is composed of pink-tan grainstone, and less

commonly crystalline carbonate. Fauna associations are pentamerid brachiopods and infrequent crinoids. The grey dolomite facies is 1 m (3.4 ft) thick, is commonly bounded by stylolites, and is distinguished by its characteristic moldic porosity. Other porosity types in the dolomite and limestone facies are vuggy, interparticle, and shelter, forming large mesopores to small megapores. Stylolites (up to 10 mm amplitude), fractures, and brown to dark grey muddy sand infill of fractures and pores are frequently observed. At 1514 m (4967 ft), lamination between the limestone and the dolomite is inclined 15° to 20°, which could be a result of a paleo-slope or an uneven dissolution surface. See Plate 5 for detailed descriptions.

Wilkerson 1-3 Core [Sec. 3, T. 15 N., R. 2 E.]

The Wilkerson 1-3 core is 16.5 m (54.2 ft) thick at a depth of 1509 – 1525 m (4950 – 5004 ft). At the base of the core is 1.3 m (4.4 ft) of the Sylvan Shale. At the top of the core is 0.3 m (1 ft) of Misener Sandstone and 0.7 m (2.4 ft) of the Woodford Shale. The Hunton Group is 14.1 m (46.4 ft) thick, and is characterized by white, pink, and tan grainstones. Fauna associations are pentamerid brachiopods (*Pentamerus sp.*, *Stricklandia sp.*), tabulate corals (*Favosites sp.*), and sparse crinoids. The yellowish-grey dolomite facies is 0.6 m (2.1 ft) thick, is bounded by stylolites, and shows sucrosic texture. Common porosity types in the dolomite and limestone facies are moldic, vuggy and interparticle, forming large mesopores to small megapores. Diagenetic features such as stylolites (up to 3 mm of amplitude), vertical fractures, and sand infill towards the top of the section are also common. At the depth of 1510 to 1510.6 m (4954.5 to 4956 ft), a chaotic breccia is present indicating possible karstic collapse. See Plate 6 for detailed descriptions.

Williams 1-3 Core [Sec. 3, T. 15 N., R. 2 E.]

The Williams 1-3 core is 14.9 m (49 ft) thick at a depth of 1506 – 1521 m (4942 – 4991 ft). At the base of the core is 2.2 m (7.2 ft) of the Sylvan Shale. The top contains 0.1 m (0.4 ft) of Misener Sandstone and 0.3 m (1.1 ft) of the Woodford Shale. The Hunton Group is 12.3 m (40.3 ft) thick, and is composed of pinkish-grey grainstones. Fauna associations are pentamerid brachiopods (*Pentamerus sp.*, *Stricklandia sp.*), and coral (?) fragments at 1517 m (4977 ft). The dolomite facies in this core is grey and 1.7 m (5.6 ft) thick. Porosity types in the dolomite and limestone facies include vuggy, intraparticle, and shelter from large mesopores to small megapores. Stylolites (up to 8 mm of amplitude) and fractures with abundant sand infill from the overlying Misener Sandstone are frequent. See Plate 7 for detailed descriptions.

X-Ray Diffraction Analysis (XRD)

Dolomite, dolomitized limestone, and limestone from the Carter Ranch 2-15 core were sampled for XRD analysis (Table 2, Fig. 12). Determination of the mole % CaCO_3 was based on the Lumsden and Chimahusky (1980) equation:

$$N \text{CaCO}_3 = Md + B \quad \text{eq. 1}$$

where M equals to 333.33, B equals to -911.99, and d is the spacing in Å between the planes of the atomic lattice. The value of d is determined from Bragg's law:

$$d = n\lambda / 2\sin\theta \quad \text{eq. 2}$$

where n is an integer equals to 1, λ is the wavelength of the radiation, which equals 1.5418 Å, and θ is the scattering angle.

The average mole % CaCO_3 in the limestone is $99.1\% \pm 0.8$, and in the dolomite is $52.8\% \pm 1.5$. Values of 2θ , d , and mole % CaCO_3 for both minerals in each sample are listed in Table 2. XRD spectra of four characteristic samples are shown in Figure 12.

Well name-number	Depth (ft/m)	C a l c i t e				D o l o m i t e			
		2θ ($^\circ$)	d (\AA)	Mole % CaCO_3	Counts	2θ ($^\circ$)	d (\AA)	Mole % CaCO_3	Counts
Carter Ranch 2-15	5009.7 / 1527	29.41	3.03	99.5	56	30.81	2.90	54.6	249
Carter Ranch 2-15	5015.9 / 1529	29.35	3.04	99.7	59	30.83	2.90	54.0	284
Carter Ranch 2-15	5016.7 / 1529.1	29.33	3.04	100.0	254	30.85	2.90	53.4	289
Carter Ranch 2-15	5026.1 / 1532	29.35	3.03	99.3	526	30.89	2.89	52.2	447
Carter Ranch 2-15	5026.3 / 1532.1	29.43	3.03	98.8	62	30.91	2.89	51.5	450
Carter Ranch 2-15	5029.9 / 1533	29.31	3.03	99.1	22	30.85	2.90	53.4	216
Carter Ranch 2-15	5031.8 / 1534	29.47	3.03	97.5	49	30.95	2.89	50.3	635

Table 2. Samples with XRD analyses from the Carter Ranch 2-15 core. Mole % CaCO_3 was determined from Lumsden and Chimahusky's (1980) equation (Equation 1).

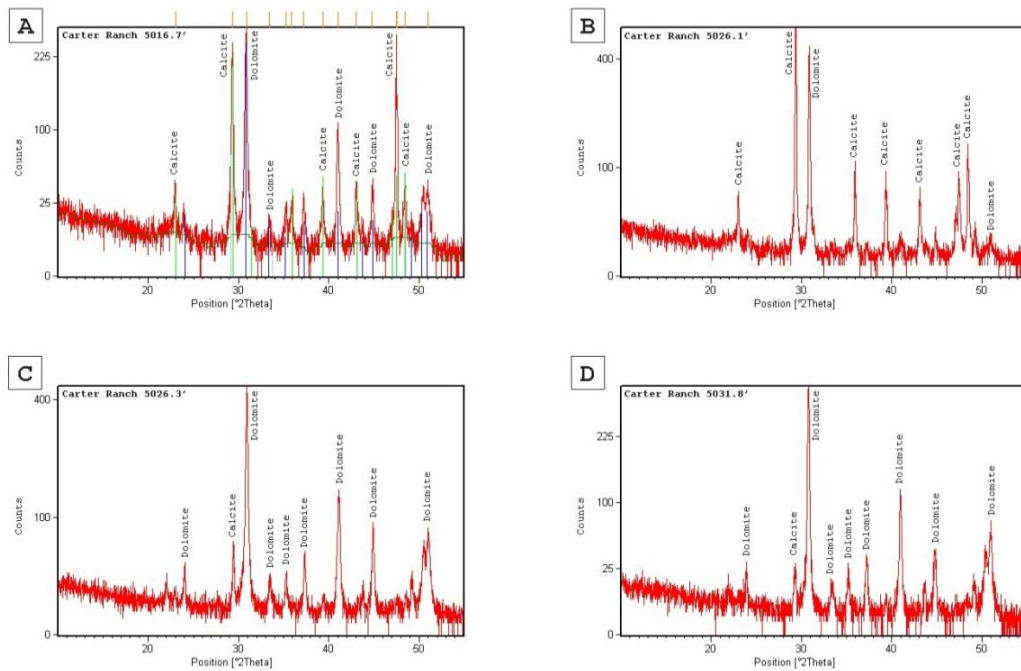


Figure 12. XRD analysis of four samples from the Carter Ranch 2-15 core. **A.** At 1529.1 m (5016.7 ft) – dolomitized limestone with 100% mole CaCO_3 for calcite and 53.4% mole CaCO_3 for dolomite; **B.** At 1532 m (5026.1 ft) – limestone with 99.3% mole CaCO_3 for calcite and 52.2% mole CaCO_3 for dolomite; **C.** At 1532.1 m (5026.3 ft) – dolomite with 98.8% mole CaCO_3

for calcite and 51.5% mole CaCO₃ for dolomite; **D.** At 1534 m (5031.8 ft) – dolomite with 97.5% mole CaCO₃ for calcite and 50.3% mole CaCO₃ for dolomite.

Transmitted Light Petrography

A total of seventy thin sections were used for petrographic descriptions. The dolomite and dolomitic limestone were classified using Sibley and Gregg's (1987) classification in combination with Dunham's (1962) classification. The porosity was described following Choquette and Pray's (1970) classification. See Appendix 1 for detailed descriptions of each thin section.

In general, the dolomite size distribution is unimodal with average crystal sizes from 0.04 mm in the Cal 1-11 core to 0.9 mm in the Wilkerson 1-3 core. Overall, the most common dolomite types observed are unimodal, planar-s and planar-e textures. Fossil assemblages are predominantly pentamerid brachiopods (*Pentamerus sp.* – Fig. 13 C to F, and *Stricklandia sp.*) with less common skeletal allochems such as crinoid fragments, tabulate corals (*Favosites sp.*, and *Halysites sp.*), sparse trilobites in the Points 1-13 core, very few bryozoans, and very scarce foraminifera (only observed in one thin section of the Cal 1-11 core). The brachiopods and corals are usually unreplaced by dolomite to partially replaced by calcite cements. Moldic porosity is mainly represented by the dissolution of brachiopods. Most of the crinoids are heavily cemented by syntaxial calcite cement overgrowths. The majority of the allochems are greater than 2 mm indicating biogenic deposits, probably reef and/or bioherm facies. The most frequent porosity types in the dolomitic facies are intercrystal (Fig. 13 A to D), vuggy, moldic, solution-enlarged molds, fracture, shelter (Fig. 13 C and D), intraparticle, and interparticle. The total porosity ranges from 0 to 24% in samples of the Carter Ranch 2-15 core (see Appendix 1 for total porosity values of each thin section).

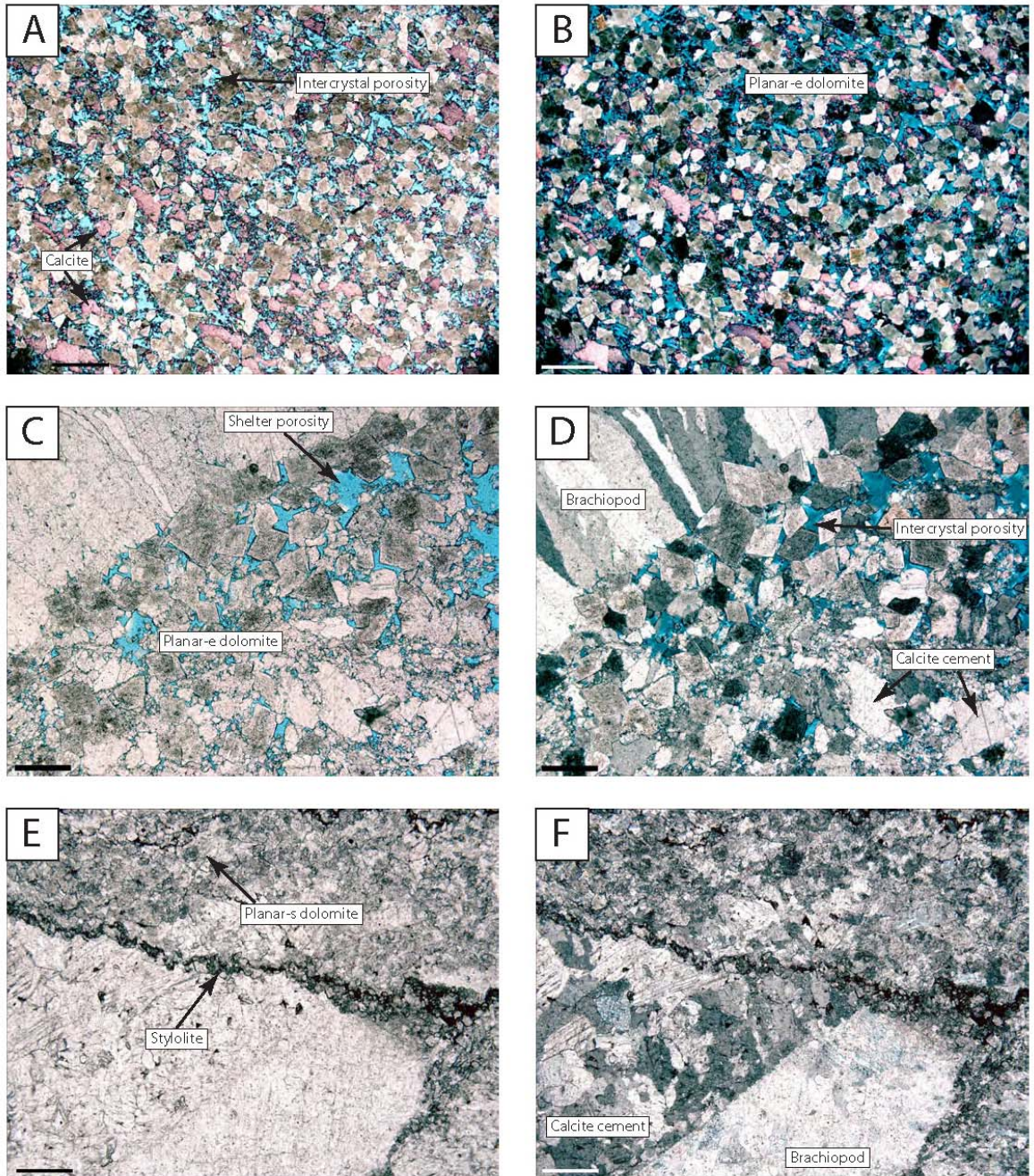


Figure 13. Photomicrographs of dolomite and dolomitized limestone. PPL to the left, and XPL to the right. See Appendix 1 for petrographic descriptions. **A – B.** Anna 1-15 at 1524.5 m (5001.8 ft) displaying planar-e dolomite, intercrystal porosity, and calcite in red – 2X, scale bar 1mm. **C – D.** Carter Ranch 2-15 at 1530.9 m (5022.5 ft) showing planar-e dolomite partially filling shelter porosity resulting in intercrystal porosity; calcite cement also occluding porosity; *Pentamerus sp.*

brachiopod – 4X, scale bar 0.5mm. **E – F.** McBride South 1-10 at 1513.3 m (4964.9 ft) displaying planar-s dolomite on top of brachiopod grainstone by a micro-stylolitic contact – 4X, scale bar 0.5mm.

Typically in the dolomitized sections, the precursor limestone matrix is partially to completely replaced by dolomite, and the primary void space is not filled to partially filled by dolomite (Fig. 13). Some dolomites display polymodal size distribution and nonmimic to mimic replacement of skeletal fragments. Microstylolites and stylolites with up to 2 mm of amplitude are common.

Calcite cements occur throughout the reservoir as syntaxial overgrowth of crinoid fragments, and more abundantly, as blocky cement with sharp edges. Silica cement is very sparse and only occurs at the Hunton Group – Sylvan Shale contact of three cores (Boone 1-4, Cal 1-11, and Williams 1-3). Sand-mud infill also occurs throughout the reservoir as sublitharenites formed by quartz, lithic fragments, and in some cases, with dolomite crystals as detrital fragments (Carter Ranch 2-15 core). The calcite and silica cements together with the sand-mud infill are occluding porosity and filling fractures resulted in diminished reservoir quality.

Cathodoluminescence Microscopy

Petrographic descriptions were complemented with cathodoluminescence (CL) microscopy. CL responses on dolomite display three distinctive zones (Fig. 14). The three dolomite CL zones, from earliest to latest are: CL Zone 1 (D1), an orange-red bright CL; CL Zone 2 (D2), dull CL; and, CL Zone 3 (D3), thin banded bright CL (Fig. 14). The three CL dolomite zones are seen in the Points 1-13, JB 1-13, and Carter Ranch 2-15 cores (Fig. 15 D and F). Nevertheless, the distribution of these zones varies from core to core.

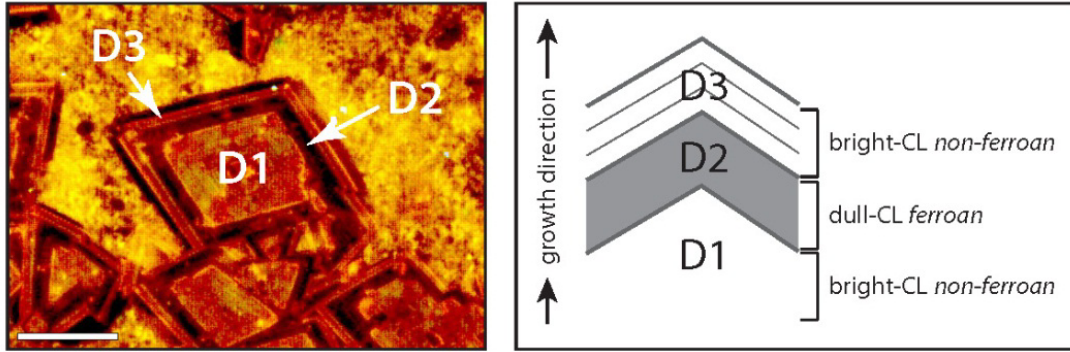


Figure 14. Dolomite CL Zones from the Points 1-13 at 1556.5 m (5106.5 ft). Zone D1 is the earliest, it displays orange-red bright CL, Zone D2 displays reddish-grey dull CL, and, Zone D3 is the latest, it displays thin bands of reddish-orange bright CL. Scale bar 0.2 mm.

The D1 zone is present in all cores (Fig. 16). However, variations within the D1 zone have been observed. Two inner, thin, orange bright CL bands are observed in the Anna 1-15, Boone 1-4, Cal 1-11, Mary Marie 1-11, McBride South 1-10 (Fig. 16 B) and Williams 1-3 core. Three inner yellowish-orange bright CL thin bands within the D1 zone are present in the Wilkerson 1-3 core (Fig. 16 D). The Mark Houser 1-11 core displays the D1 zone with no inner bands, and partially replaced by calcite cement (Fig. 16 F). On the other hand, the D2 and D3 zones do not exhibit variations in any of the cores where they were identified (Points 1-13, JB 1-13, and Carter Ranch 2-15 cores).

Calcite cements display three CL zones described in detail by Smith (2012). The three zones from earliest to latest are: CL Zone 1 (Z1), a non CL cement; CL Zone 2 (Z2), a thin yellow band of bright CL followed by a thin non CL cement; and, CL Zone 3 (Z3), yellow multi-banded cement consisting of alternating bright and dull CL bands (Smith, 2012). In the present study, Z1 largely occurs as syntaxial overgrowths on crinoid fragments (Figs. 15 B, and 17 D), Z2 follows Z1 (Fig. 16 F), and Z3 is the last generation of blocky calcite cement (Fig. 15 B). Calcite cements replace dolomite crystals as dedolomite throughout the reservoir and commonly occlude porosity (Figs. 15 A, B, and 16 F).

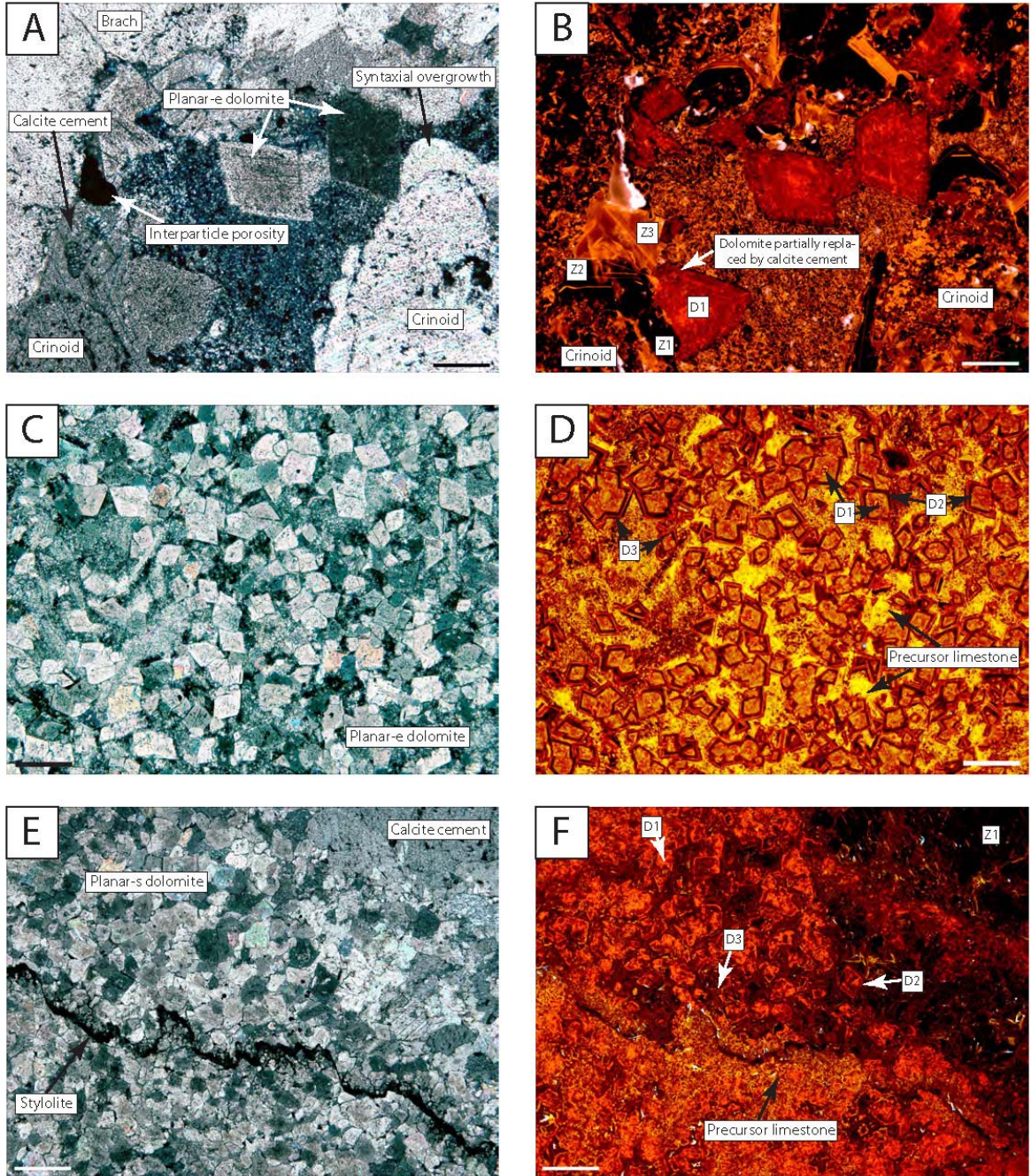


Figure 15. Photomicrographs of the dolomite and dolomitized limestone. XPL to the left, and CL to the right. **A – B.** Boone 1-4 core at 1540.1 m (5052.8 ft) showing planar-e dolomite (D1) partially replaced by calcite cements; syntaxial overgrowth on crinoid fragments (Z1), and calcite cements Z2 and Z3 occluding porosity – 10X, scale bar 0.2mm. **C – D.** Points 1-13 core at 1556.5 m (5106.5 ft) displaying planar-e dolomite with the D1, D2, and D3 zones, replacing the

precursor limestone (bright yellow CL) – 10X, scale bar 0.2mm. **E – F.** Carter Ranch 2-15 at 1528.8 m (5015.9 ft) with planar-s dolomite separated from the precursor limestone by a stylolitic contact – 4X, scale bar 0.5mm.

Silica cement displays dull CL (Fig. 17 A and B), is very rare and only found at the base of the Hunton Group (Cal 1-11 at 1559 m (5114 ft), and Williams 1-3 at 1519 m (4982.2 ft)), and in the uppermost section of the Sylvan Shale (Boone 1-4 at 1544 m (5066.4 ft)). The precursor limestone displays yellow bright CL (Fig. 15 C, D, E, F; 16 E, F; and 17 E, F). Other CL signatures that are recognized include: skeletal fragments such as brachiopods, corals and crinoids displaying yellow bright CL (Fig. 17 C and D), quartz from the sand–mud infill displaying blue bright CL, and non CL lithic fragments (Fig. 17 E and F).

Other observations relevant to diagenesis were made using CL petrography. Fractures are divided in two groups: the first group contains horizontal and vertical fractures filled by calcite cements (Z1 and Z3, Fig. 18 A and B), and by sand-mud infill; the second group comprises vertical open fractures that crosscut the dolomite and limestone facies (Fig. 18 C and D). This second group of fractures tends to cut through the reservoir with no distinction of lithology or diagenetic features. Stylolites typically characterize the contact between dolomite and limestone facies (Figs. 13 E, F; 15 E, F; and 19). Several voids in the Carter Ranch 2-15 core are filled by sand-mud infill that contains dolomite crystals as part of the detrital fragments (Fig. 20 A and B). A stunning CL photomicrograph of the Mark Houser 1-11 (Fig. 20 D) displays the sequence of at least three diagenetic events: the first (earliest) corresponds to the dolomite that is partially replaced as dedolomite by calcite cement (probably Z3), the second event is represented by calcite cements growing after dolomite (Z1, Z2 and Z3), and the third event (latest) corresponds to the sand-mud infill occluding porosity after the calcite cement Z3 (Fig. 20 C and D). Dedolomite is also observed in the Carter Ranch 2-15 core as euhedral dolomite crystals replaced by calcite cement Z1 (Fig. 18 A and B).

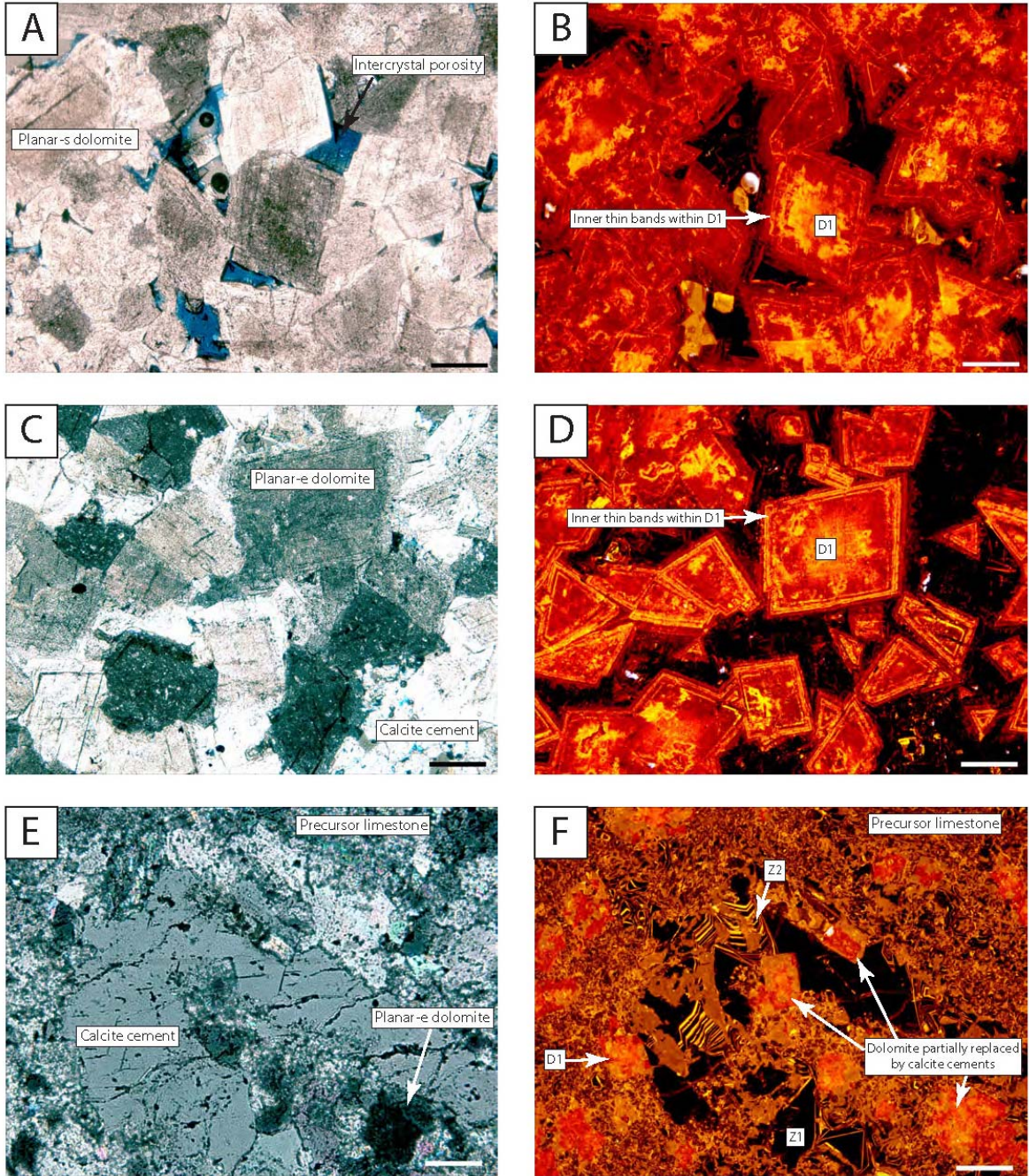


Figure 16. Photomicrographs of CL variations in the zone D1. XPL to the left, and CL to the right. All photomicrographs are taken at 10 X with a scale bar of 0.2 mm. **A – B.** McBride South 1-10 core at 1545.3 m (5070 ft) displaying planar-s dolomite with D1 zone and thin bright yellowish-orange CL bands in it. **C – D.** Wilkerson 1-3 core at 1523.6 m (4998.5 ft) displaying D1 planar-e dolomite with thin bright CL bands, surrounded by non-CL (Z1?) calcite cement. **E –**

F. Mark Houser 1-11 core at 1545.5 m (5070.5 ft) showing planar-e dolomite (D1) partially replaced by calcite cement (Z3?).

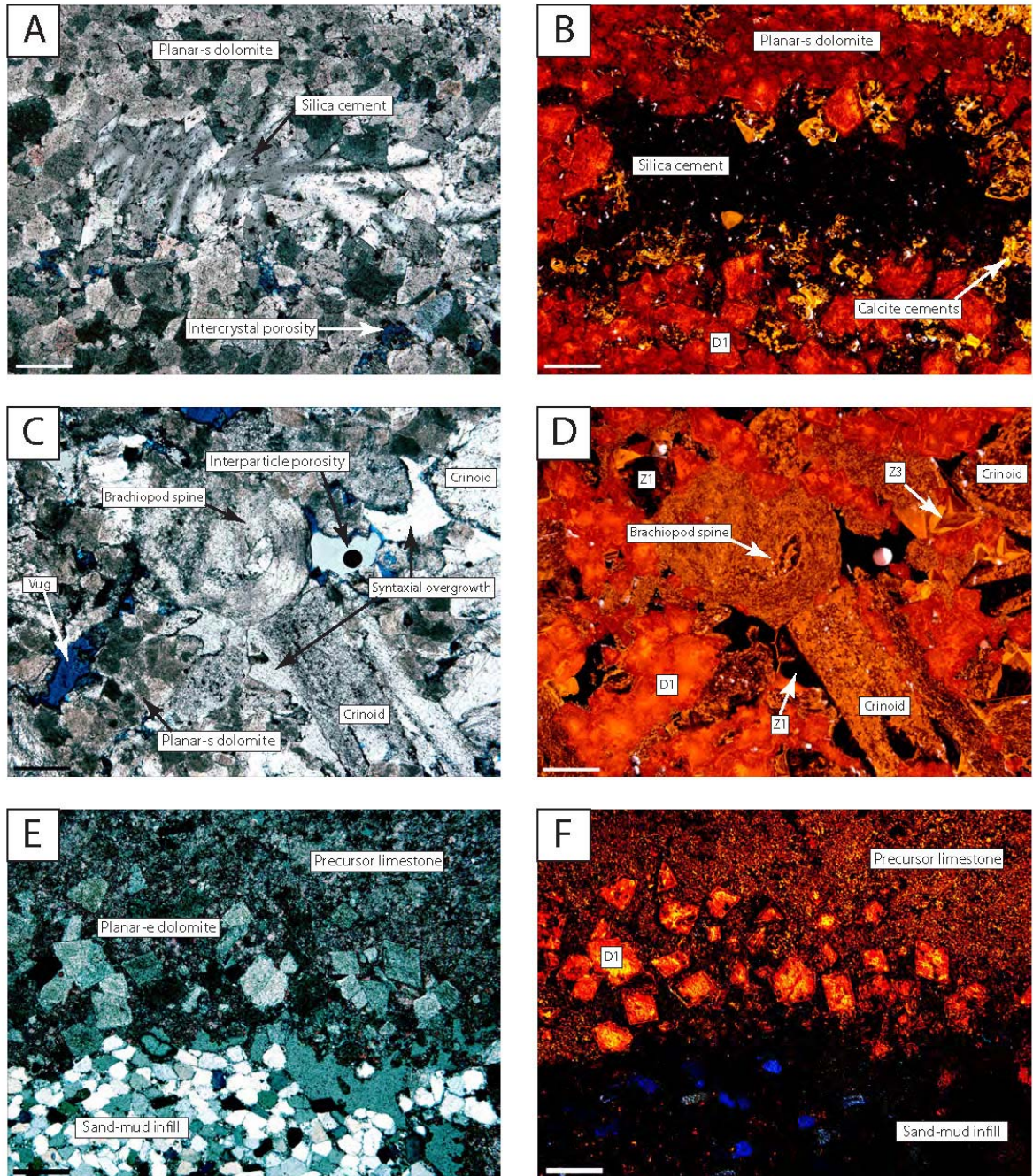


Figure 17. Silica cement, skeletal allochems, and sand-mud infill photomicrographs. XPL to the left, and CL to the right. All photomicrographs are taken at 4 X with a scale bar of 0.5 mm. A –

B. Williams 1-3 core at 1518.6 m (4982.1 ft) displaying silica cement filling vuggy porosity. **C – D.** Boone 1-4 core at 1538.3 m (5046.8 ft) displaying planar dolomite (D1), calcite cement (Z1 and Z3), and fossil assemblage (brachiopod and crinoids). **E – F.** Carter Ranch 2-15 core at 1534.2 m (5033.5 ft) showing sand-mud infill occluding porosity (blue CL), and planar-e dolomite (D1) replacing the precursor limestone.

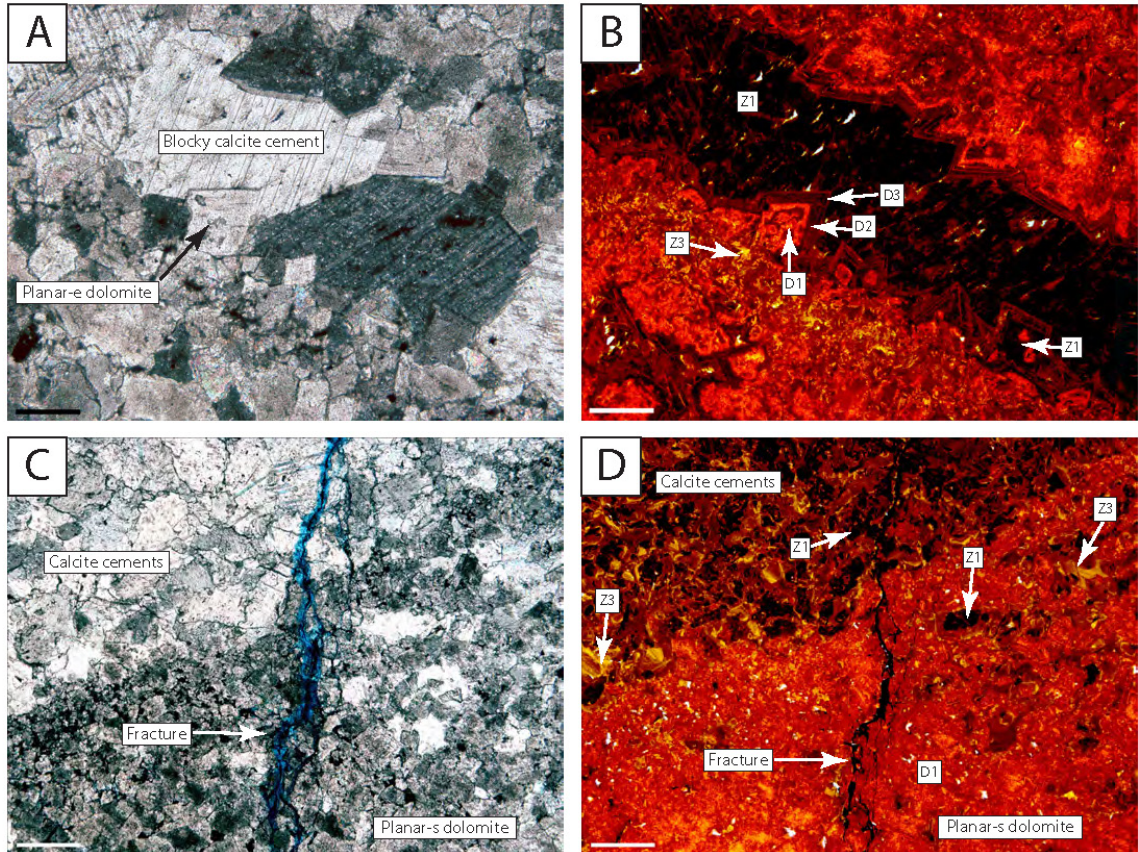


Figure 18. Photomicrographs of fractures in the Carter Ranch 2-15 core. XPL to the left, and CL to the right. **A – B.** Fracture filled with calcite cement Z1 at 1529 m (5015.8 ft). Note that calcite cement Z1 is also replacing dolomite crystals as dedolomite – Scale bar 0.2 mm (10X). **C – D.** Vertical fracture with no fill cutting through crystalline dolomite and limestone at 1527 m (5009.5 ft) – Scale bar 0.5 mm (4X).

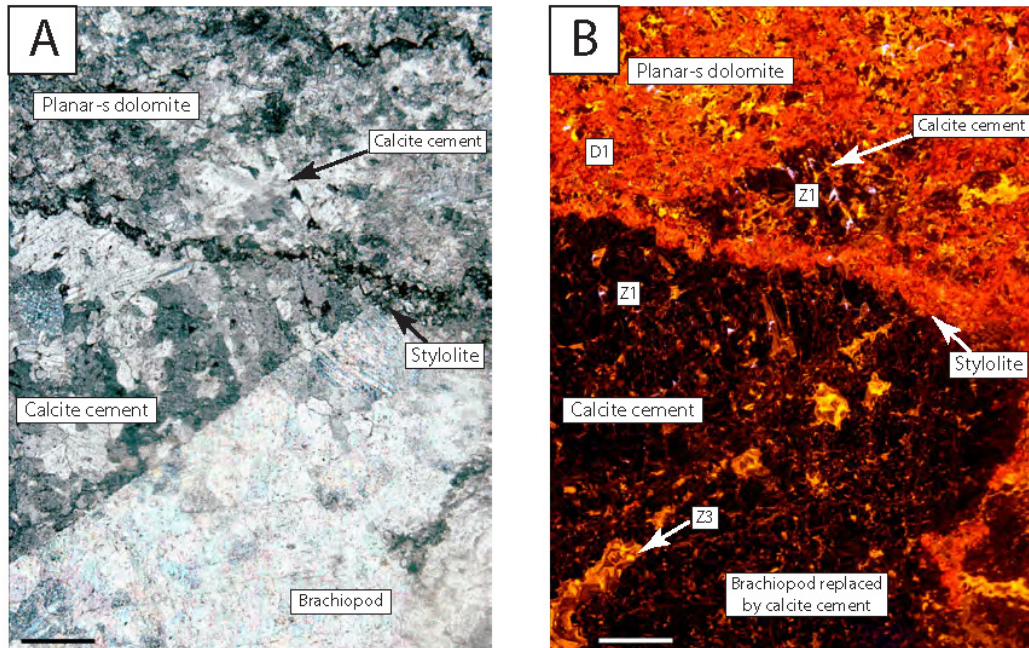


Figure 19. Photomicrographs of stylolites in the McBride South 1-10 at 1513.3 m (4964.9 ft) – Scale bar 0.5 mm (4X). **A.** XPL. Stylolitic contact between the crystalline dolomite with calcite cement (top) and the brachiopod grainstone with some dolomite (base). **B.** CL image of dolomite and limestone mostly restricted by the stylolitic contact.

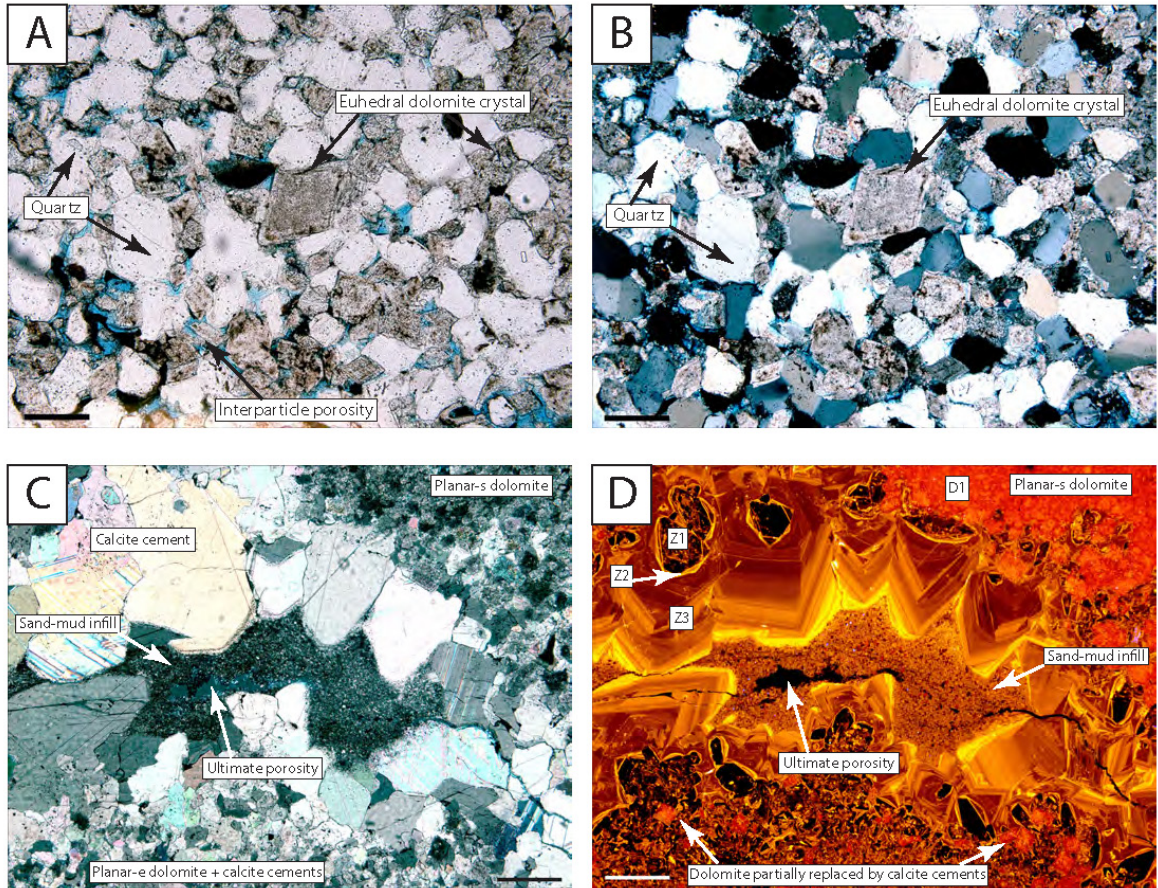


Figure 20. Diagenetic events observed in the Hunton Group. **A – B.** PPL and XPL photomicrograph of the Carter Ranch 2-15 at 1526.6 m (5008.6 ft) showing detrital dolomite within the sand-mud infill from the Misener Sandstone and the Woodford Shale (10X – scale bar 0.2 mm). **C – D.** XPL and CL photomicrographs of the Mark Houser 1-11 at 1545.7 m (5071.2 ft) illustrating the order of at least three diagenetic events which are: dolomite as the earliest event, calcite cements, and sand-mud infill as the latest event (4X – scale bar 0.5 mm).

Stable Oxygen ($\delta^{18}\text{O}$) and Carbon ($\delta^{13}\text{C}$) Isotope Geochemistry

The results of the stable isotope analysis of dolomite samples from ten cores are presented in Table 3 and Figure 21. The $\delta^{18}\text{O}$ and $\delta^{13}\text{C}$ ratios for the dolomite samples range from -5.40‰ to 2.81‰ and from -1.59‰ to 1.22‰ (Vienna Pee Dee Belemnite, VPDB), respectively (Table 4, Figure 21). Ten brachiopod samples were analyzed in order to estimate the carbon and oxygen isotope composition of the Silurian seawater (Smith, 2012). The $\delta^{18}\text{O}$ and $\delta^{13}\text{C}$ values for the unaltered brachiopods range from -5.21‰ to -3.56‰ and from -0.79‰ to 1.86‰ (VPDB), respectively (Table 4, Figure 21).

Sample	Well name - number	Depth (ft / m)	$\delta^{13}\text{C}$ (VSMOW)	$\delta^{13}\text{C}$ (VPDB)	$\delta^{18}\text{O}$ (VSMOW)	$\delta^{18}\text{O}$ (VPDB)
1	Anna 1-15	4969.8 / 1515	31.80	0.86	26.89	-3.90
2	Anna 1-15	4994.2 / 1522	31.01	0.09	27.51	-3.30
3	Anna 1-15	4999.5 / 1524	30.95	0.04	27.33	-3.47
4	Anna 1-15	5001.3 / 1525	30.54	-0.36	25.78	-4.98
5	Boone 1-4	5052.8 / 1540	31.44	0.51	25.81	-4.95
6	Boone 1-4	5063.6 / 1543	31.38	0.46	25.85	-4.91
7	Boone 1-4	5065.6 / 1544	30.01	-0.88	26.10	-4.67
8	Boone 1-4	5066.4 / 1545	30.90	-0.01	28.02	-2.81
9	Cal 1-11	5115.5 / 1559	32.02	1.07	27.08	-3.71
10	Carter Ranch 2-15	5009.7 / 1527	31.85	0.91	26.11	-4.65
11	Carter Ranch 2-15	5015.9 / 1529	31.49	0.56	27.24	-3.56
12	Carter Ranch 2-15	5020.6 / 1530	31.17	0.25	25.34	-5.40
13	Carter Ranch 2-15	5026.9 / 1532	31.04	0.13	27.29	-3.51
14	Carter Ranch 2-15	5031.5 / 1533	31.07	0.16	27.52	-3.29
15	Carter Ranch 2-15	5032.2 / 1534	31.08	0.16	27.18	-3.61
16	JB 1-13	5000.5 / 1524	30.20	-0.69	27.80	-3.01
17	JB 1-13	5022.5 / 1531	32.10	1.16	27.07	-3.73
18	Mark Houser 1-11	5070.7 / 1545	32.08	1.14	26.26	-4.51
19	Mark Houser 1-11	5072.2 / 1546	32.17	1.22	27.07	-3.72
20	McBride South 1-10	4964.9 / 1513	28.81	-2.03	24.18	-6.53
21	McBride South 1-10	4967.8 / 1514	30.04	-0.85	27.03	-3.76
22	McBride South 1-10	4970.4 / 1515	31.65	0.72	27.27	-3.53
23	McBride South 1-10	4971.2 / 1515	31.38	0.45	26.87	-3.92
24	Points 1-13	5106.5 / 1556	32.25	1.30	29.44	-1.43
25	Wilkerson 1-3	4998.1 / 1523	29.97	-0.92	27.08	-3.71
26	Wilkerson 1-3	4999.2 / 1524	30.26	-0.63	25.69	-5.06
27	Williams 1-3	4979.1 / 1518	29.27	-1.59	26.30	-4.47
28	Williams 1-3	4982.8 / 1519	30.18	-0.71	26.75	-4.04

Table 3. Stable carbon and oxygen isotope ratios for twenty-eight powdered dolomite samples from ten cores.

Average values for $\delta^{18}\text{O}$ of $-4.16\text{‰} \pm 0.45$ for the brachiopods and $-4.01\text{‰} \pm 0.69$ for the dolomite indicate 0.15‰ enrichment of $\delta^{18}\text{O}$ in the dolomite with respect to the brachiopods. The average values for $\delta^{13}\text{C}$ of $0.82\text{‰} \pm 0.76$ for the brachiopods and $0.13\text{‰} \pm 0.76$ for the dolomite indicate 0.69‰ depletion of the $\delta^{13}\text{C}$ in the dolomite with respect to the brachiopods.

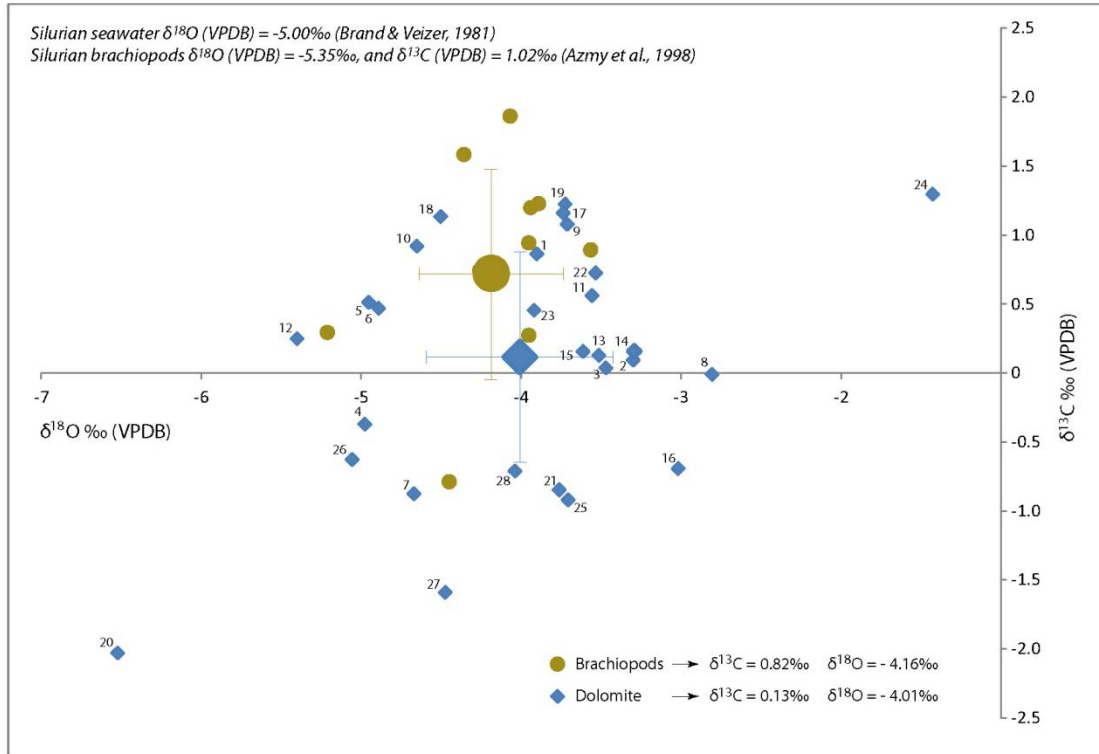


Figure 21. Stable carbon and oxygen isotope data from brachiopods of the Points 1-13 core (brown dots), and dolomite samples from ten cores (blue rhombs, see Table 3). Both clusters of data display unimodal distribution. The average values of $\delta^{18}\text{O}$ for the brachiopods ($-4.16\text{‰} \pm 0.45$) and for the dolomite ($-4.01\text{‰} \pm 0.69$) are very close, and the average values of $\delta^{13}\text{C}$ show that the dolomite ($0.13\text{‰} \pm 0.76$) is depleted with respect to the brachiopods ($0.82\text{‰} \pm 0.76$). Dolomite samples 20 and 24 were not used for the mean value calculation.

Sample	Isotope	Mean (VPDB/VSMOW)	Max. (VPDB/VSMOW)	Min. (VPDB/VSMOW)	Std. Dev.	n
Dolomite	$\delta^{13}\text{C}$	0.13 / 31.04	1.22 / 32.17	-1.59 / 29.27	0.76	26
Dolomite	$\delta^{18}\text{O}$	-4.01 / 26.78	-2.81 / 28.02	-5.40 / 25.34	0.69	26
Brachiopods	$\delta^{13}\text{C}$	0.82 / 31.76	1.86 / 32.83	-0.79 / 30.10	0.76	10
Brachiopods	$\delta^{18}\text{O}$	-4.16 / 26.62	-3.56 / 27.24	-5.21 / 25.54	0.45	10

Table 4. Carbon and Oxygen stable isotopes maximum, minimum, and mean values with standard deviation for the dolomite and brachiopod samples. Samples 20 and 24 were not used for the

dolomite average values (see Table 3 and Figure 21). Brachiopods average values were taken from Smith (2012) and represent the Early Silurian seawater composition.

Scanning Electron Microscopy (SEM) and Energy-Dispersive X-ray Spectroscopy (EDS)

Three dolomite samples were analyzed by SEM and EDS techniques (Figs. 22 and 23).

Photomicrographs of the McBride South 1-10 core display well-formed dolomite crystals together with clay associated with sand-mud infill from the Misener Sandstone and the Woodford Shale. EDS analysis on one sample of the McBride South 1-10 reveals that the dolomite contains iron with up to 10% atomic percentage for that specific sample. The clay is evidenced by the silicon and aluminum content and the sheet shaped crystals (Table 5, Fig. 22). Planar dolomite crystals with intercrystal porosity are observed in the McBride South 1-10 core (Fig. 23 C).

Photomicrographs of the Carter Ranch 2-15 core display well-formed dolomite crystals together with sand infill (quartz euhedral crystals) associated with karsting (Fig. 23 A and B). The Points 1-13 photomicrographs expose subhedral dolomite crystals together with clay associated to the sand-mud infill (Fig. 23 D).

<i>Element</i>	<i>WT (%)</i>	<i>AT (%)</i>	<i>K_A</i>	<i>K_Z</i>	<i>Intensity</i>	<i>P/bkg</i>
Mg	8.09	12.74	0.403	1.003	25.511	4.1
Al	2.56	3.63	0.494	1.006	10.159	1.1
Si	5.41	7.37	0.609	1.008	31.465	2.8
Ca	69.3	66.21	0.966	1.005	395.623	26.7
Fe	14.6	10.04	0.935	1.000	40.491	4.3

Table 5. Quantified result of the EDS spectrum (Fig. 19 G) for one dolomite sample of the McBride South 1-10 core.

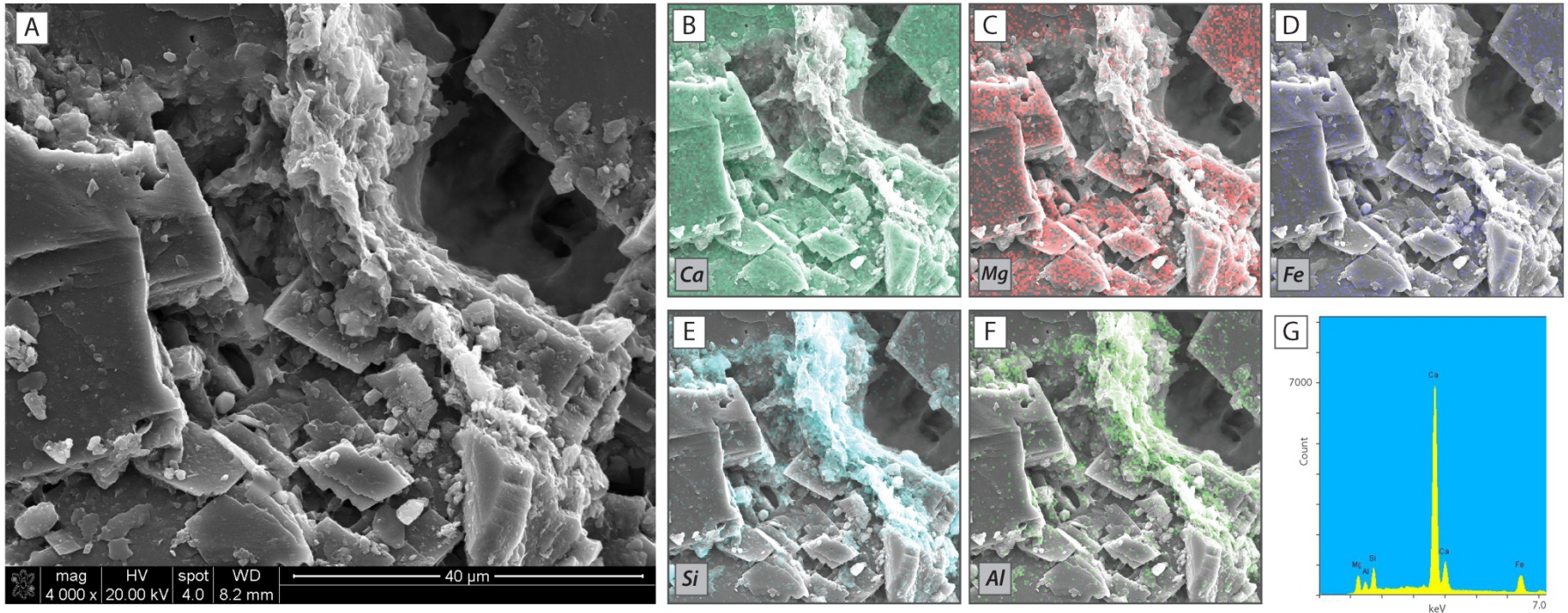


Figure 22. **A.** SEM photomicrograph of dolomite crystals with mud infill from the McBride South 1-10 core at 1513.3 m (4964.9 ft). EDS analyses are shown on photomicrographs B to F. **B.** Calcium distribution in green; **C.** Magnesium distribution in red; **D.** Iron distribution in purple; **E.** Silicon distribution in blue; **F.** Aluminum distribution in light green. **G.** Spectrum identification of elements existing in the dolomite crystals and mud infill (See Table 5 for values from each peak).

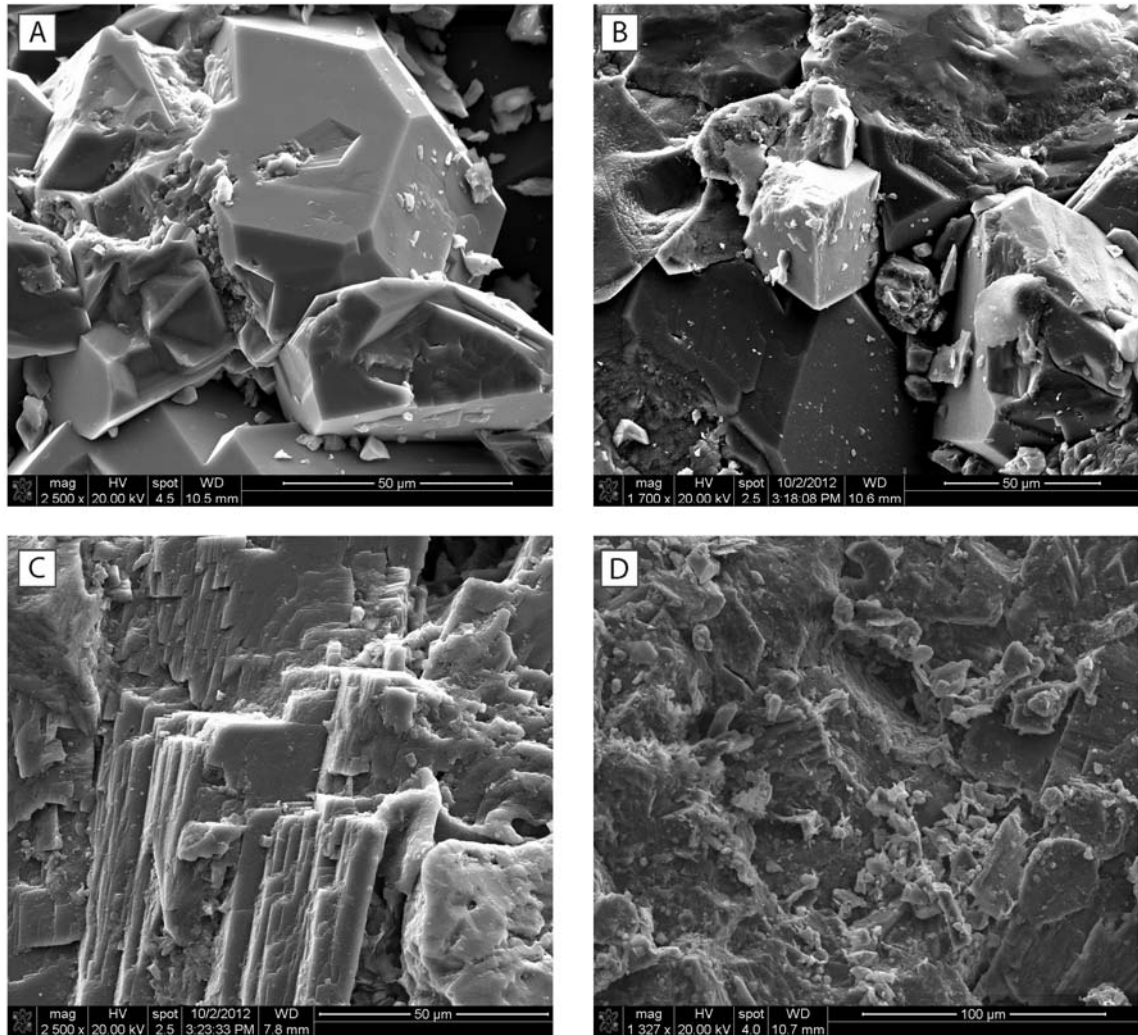


Figure 23. SEM photomicrographs of three samples of the dolomitic facies. **A – B.** Carter Ranch 2-15 at 1528.8 m (5015.9 ft) – **(A)** quartz euhedral crystal of the sand-mud infill occluding porosity; and **(B)** euhedral dolomite crystals with intercrystal porosity. **C.** McBride South 1-10 at 1513.3 m (4964.9 ft) – planar dolomite with void at the upper-right corner. **D.** Points 1-13 at 1556.3 m (5106 ft) – subhedral dolomite with clay from the sand-mud infill.

CHAPTER VI

DISCUSSION

The following discussion is focused on determining the paragenetic sequence and the origin of the dolomite in the lower Cochrane member, Chimneyhill Subgroup, Hunton Group.

Observations made from subsurface maps, core descriptions, transmitted light petrography, CL microscopy, SEM, XRD analyses, and geochemistry provided sufficient information to interpret the diagenetic history of the reservoir.

Karsting – Fractures – Pressure-Solution

Sea level fluctuations during the Silurian have been reported by several authors (Grahn and Caputo, 1992; Azmy *et al.*, 1998; Johnson, 2006). The reservoir stratigraphy was affected by karsting due to five major highstands and lowstands of the sea level during the lower Silurian (Johnson, 2006). Karst features such as breccias, interconnected vugs, and caves filled by sediments from the Devonian siliciclastics and calcite cements are observed in the cores. Other possible evidence of karsting includes the random distribution of the dolomitic facies (Fig. 10) that may have precipitated as a consequence of fluid migration following karst conduits. This observation indicates that karsting occurred early and prior to dolomitization, calcite cementation, and sand-mud infill from Devonian units.

The vast majority of the fractures observed in the cores are horizontal, followed by less common vertical fractures. Fractures in the cores are generally open or filled by sand, silt, or mud. Only the Anna 1-15 core has a fracture filled by calcite at the base of the reservoir (see Plate 1). Two groups of fractures are observed: fractures filled by calcite cements (Fig. 18 A and B), and open fractures that affect the reservoir with no distinction to lithology, sedimentological or other diagenetic features (Fig. 18 C and D). Fractures filled by calcite cements correspond to a fracturing event prior to calcite cementation. The open fractures are largely vertical and may have been formed together with the filled fractures or during a later fracturing event. These open fractures sometimes are filled by sand and mud from Devonian sediments. However, more evidence is needed to determine the temporal relation between these two types of fractures. For the purpose of this study, we will assume the fracturing to be one event that occurred prior to calcite cementation. These fractures may have been reactivated later in the paragenetic sequence.

Stylolites cause changes in thickness comparable with the results of erosion (reduction of thickness due to pressure dissolution in a vertical direction amounting to 20–35% are commonplace in limestones (Bathurst, 1975)). Additionally, stylolites act as permeability barriers that influence the distribution of reservoir rock and the CaCO_3 released by stylolite growth is a major source of late diagenetic cement (Bathurst, 1975). The dolomitic facies identified in the cores is frequently bounded by stylolites that form the contact between dolomite and limestone (Figs. 11 B; 13 E, F; 15 E, F; and 19). Stylolites are also present within the dolomite and limestone facies (Figs. 11 B, D, and E). Throughout the reservoir, stylolites clearly represent a post dolomitization event and pressure-solution likely is a source of CaCO_3 for calcite cementation. Some stylolites contain quartz and mud indicating that the growth of these stylolites, and perhaps all, occurred after the sand-mud infill event.

Summarizing, karsting represents an early diagenetic event prior dolomitization. Dolomitization occurred prior the fracturing and pressure-solution events. Fracturing started prior the calcite

cementation and sand-mud infill, and could be reactivated later in the diagenesis. The pressure-solution events may have been coetaneous with calcite cementation. If this is the case, calcite cements correspond to overburdens of 600–900 m (1968–2953 ft) or greater, the depth which is required to generate stylolites (Bathurst, 1975).

Dolomite – Calcite Cements – Silica Cement – Sand-Mud Infill

Transmitted light petrography and CL observations indicate the relative timing of dolomitization, calcite cementation, and sand-mud infill. CL also provides information on the spatial distribution of Fe^{2+} (dull CL) and Mn^{2+} (bright CL) in the dolomite and calcite cements (Scholle and Ulmer-Scholle, 2003). CL zones are inferred as time representative for calcite cements, where calcite cement closer to the substrate is interpreted as older than those cements which precipitate adjacent to open space (Meyers, 1991). The same concept is applied for dolomite, the earlier dolomite CL zones are followed by younger dolomite zones (Fig. 14). The dolomite in the lower Cochrane member exhibits three major CL zones, D1, D2, and D3. The D1 zone is the earliest, is bright CL indicating the absence of Fe^{2+} , and contains up to three thin bright CL bands (Figs. 16 B and D). D2 is later than D1, and is dull CL indicating the presence of Fe^{2+} (Figs. 15 D and 18 B). The D3 zone is the latest, and consists of thin banded bright CL dolomite indicating the absence of Fe^{2+} (Figs. 15 D and 18 B). Variations of the Fe^{2+} content in the dolomite may represent a response to sea level fluctuations during dolomitization.

Calcite cements petrography and CL characteristics are described in detail by Smith (2012). The calcite cements replace and corrode dolomite crystals throughout the reservoir (Figs. 15 A, B; 16 E, F; 18 A, B; and 20 C, D), indicating dolomitization prior to calcite cementation. Smith (2012) reported a cave filled with calcite cements Z1, Z2, and Z3 in the Mark Houser 1-11 providing evidence that karsting occurred prior to calcite cementation.

Infrequently voids are filled with silica cement at the base of the reservoir. In the Boone 1-4 core, silica cement fills vuggy porosity in a crystalline dolomite following calcite cement Z3 (Fig. 17 A and B). This indicates that dolomite and calcite cements precipitated prior to silica cement. The relationship of the silica cement to other diagenetic events such as stylolitization and fracturing could not be determined.

Sand-mud infill frequently occludes porosity, filling voids lined by the latest calcite cement Z3 (Figs. 20 C and D). Dolomite crystals are found as detrital fragments within the sand-mud infill, together with quartz grains and lithic fragments (Figs. 20 A and B). The source of the sand-mud infill is the Devonian Misener Sandstone and the Woodford Shale, and occurs more frequently upward towards the contact with the overlying Devonian units. This evidence indicates that the sand-mud infill occurred after calcite cementation, and well after dolomitization.

Dolomite Stable Isotope Geochemistry – SEM and EDS – XRD Analyses

Smith (2012) obtained stable $\delta^{13}\text{C}$ and $\delta^{18}\text{O}$ isotope data for pentamerid brachiopods (Table 4, Fig. 21). Brachiopods are originally composed of low-Mg calcite, which is typically the most diagenetically stable form of calcium carbonate (Bathurst, 1975). It is inferred that brachiopods will be the least altered by later diagenetic effects and will reflect the isotopic compositions of the seawater from which they precipitated (Rush and Chafetz, 1990). Nevertheless, it is suggested that only the innermost fibers of mature brachiopod shells should be included in proxy calculation of seawater temperatures (Cusack and Huerta, 2012).

The $\delta^{18}\text{O}$ values of the brachiopods analyzed by Smith (2012) range from -5.21‰ to -3.56‰ VPDB and the $\delta^{13}\text{C}$ values range from -0.79‰ to 1.86‰ VPDB, with average values of $\delta^{18}\text{O} = -4.16\text{‰}$ and $\delta^{13}\text{C} = 0.82\text{‰}$. Dolomite $\delta^{18}\text{O}$ values range from -5.40‰ to -2.81‰ VPDB and $\delta^{13}\text{C}$ values range from -1.59‰ to 1.22‰ VPDB, with average values of $\delta^{18}\text{O} = -4.01\text{‰}$ and $\delta^{13}\text{C} =$

0.13‰ (Table 4). The $\delta^{18}\text{O}$ values obtained for the brachiopods (Smith, 2012) fall within the range of those values used by Azmy *et al.*, (1998) to calculate the isotopic composition for Llandoveryian seawater.

In modern environments, tropical sea-surface temperature ranges from 23°C to 27°C (Milliman, 1974). Since the study area is located in tropical paleolatitudes of less than 30°S (Scotese and McKerrow, 1990), and is associated with inner platform facies, it is reasonable to assume a comparable range of temperatures for the tropical Silurian seas. Using the dolomite-water fractionation factor of 1.03038 (Land, 1980), the carbonate-water fractionation equations of Fritz and Smith (1970), and Friedman and O'Neil (1977), and assuming a Silurian seawater $\delta^{18}\text{O}$ value of -3.5‰ SMOW for warm episodes and -2.5‰ SMOW for glacial episodes (Azmy *et al.*, 1998), the calculated temperatures of dolomitizing fluids range between 32°C and 44°C. These high temperatures are not realistic for the following reasons: (I) the preponderance of petrographic evidence suggests that the dolomite is a result of an early diagenetic event and not consistent with a burial dolomitization model at elevated temperatures; (II) the dolomitization of the lower Cochrane member is matrix selective and fabric retentive (Figs. 15, and 16 C, D) which are common features of low temperature dolomitization (Machel, 2004); and, (III) if a seawater dolomitization model at these temperatures were invoked, such warm conditions would have had to exist during glacial times in the Silurian seas (Azmy *et al.*, 1998).

The dolomite $\delta^{18}\text{O}$ values also indicate that the dolomite was not precipitated from evaporitic reflux of hypersaline brines, which is characterized by enriched $\delta^{18}\text{O}$ values with respect to seawater. The average $\delta^{18}\text{O}$ value of the brachiopods ($-4.16\text{‰} \pm 0.45$ VPDB) is very close to the average $\delta^{18}\text{O}$ value of the dolomite ($-4.01\text{‰} \pm 0.69$ VPDB), which suggests seawater as the main dolomitizing fluid. Added to that, the bathymetry of Silurian pentamerid brachiopods and crinoids range from 10 to 90 m (33 to 295 ft – Johnson, 1987) indicating shallow water depths which is a favorable condition for the formation of dolomite from seawater (Machel, 2004). Additionally,

seawater and/or chemically slightly modified seawater are the principle agents of dolomitization at shallow depths and commensurate temperatures (Machel, 2004). The $\delta^{13}\text{C}$ average value for the dolomite is slightly depleted with respect to the average value of the brachiopods (Table 4). This depletion in $\delta^{13}\text{C}$ could be interpreted as a result of a small scale meteoric flow that generated calcite cements Z1 and Z2, and likely reset the $\delta^{13}\text{C}$ of the dolomite.

Three factors may have affected the isotopic signatures of the dolomite. (I) The dolomite isotope signature was partially reset to isotopically lighter values during circulation of meteoric fluids that precipitated Z1 and Z2 calcite cements, and during intermediate burial when calcite cement Z3 was precipitated (Smith, 2012). (II) The dolomite fractionation factor of Land (1980) applies for open systems. In a rock buffered system, such as the lower Cochrane member, fractionation of ^{18}O is not likely to have been complete resulting in values for dolomite close to values of the replaced limestone. (III) The dolomite samples may have been contaminated by small amounts of calcite cements or precursor limestone.

Photomicrographs of the dolomite facies from SEM (Figs. 22 A and 23), together with EDS analysis (Fig. 22, Table 5) indicate the presence of some iron in the non CL zones of the dolomite. The presence of iron in the dolomite crystal lattice would explain the slight nonstoichiometry of the dolomite indicated by x-ray analysis (Fig. 12, Table 2). The ferroan CL zone D2 likely is related to Fe^{2+} enrichment occurring as a consequence of a sea-level highstand when more reducing conditions were favored during dolomitization.

Paragenetic Sequence of the Lower Cochrane Member

The paragenetic sequence of the reservoir is established as seven main events represented on Figure 24, and briefly described as follows:

1. Karsting – sea level changes during carbonate production and deposition resulted in karsting as the earliest diagenetic event. Calcite cements and Devonian sediments filling caves indicate that the karsting continued until the deposition of the Misener Sandstone and the Woodford Shale.
2. Dolomitization – dolomite is an early product of diagenesis in the reservoir. CL zones D1 to D3 may reflect sea level fluctuations during the Silurian. The bright CL zones D1 and D3 may reflect sea-level lowstands at cold conditions, and the dull CL zone D2 likely reflects a sea-level highstand at warmer conditions. Most of the moldic porosity and the planar-e (sucrosic) dolomite texture were generated during dolomitization.
3. Fracturing – fractures filled by calcite cements and sand-mud from Devonian sediments started to form before calcite cementation. They may have been reactivated later during diagenesis.
4. Calcite cementation – calcite cements Z1 and Z2 were precipitated in a meteoric phreatic environment; Z3 was precipitated at intermediate burial depth (Smith, 2012). Calcite cements Z1 and Z3 replace dolomite crystals as dedolomite, fill fractures, and occlude porosity throughout the reservoir.
5. Silica cement – silica cement is very sparse and formed after dolomite and calcite cementation. No other relationships with later diagenetic events were observed for the silica cement. The source of the silica is may be chert beds or adjacent shales.
6. Sand-mud infill of fractures and porosity – sediments from the Misener Sandstone and Woodford Shale, as well as eroded dolomite crystals, occlude porosity following the latest calcite cement Z3.
7. Pressure-solution – stylolites bound dolomite to limestone transitions as well as crosscut both of these lithologies. Some stylolites contain quartz and mud indicating that the stylolites growth was after the sand-mud infill from Devonian sediments.

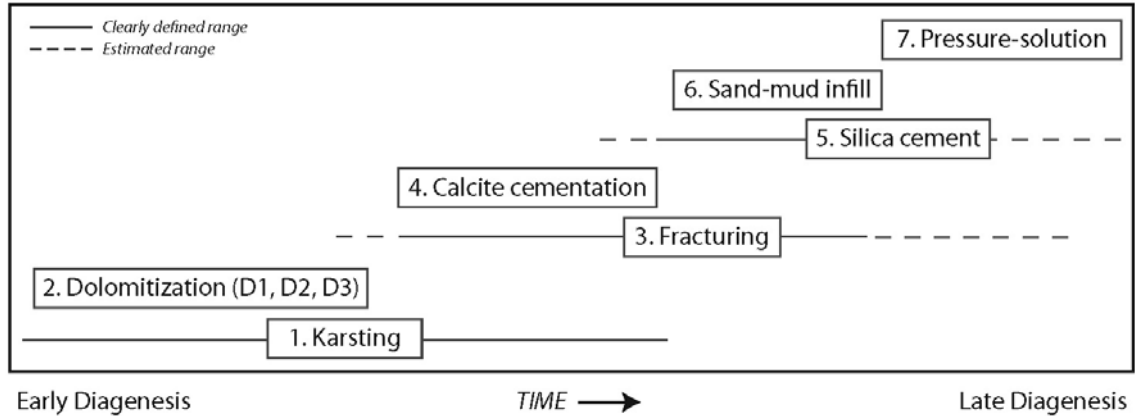


Figure 24. Paragenetic sequence of diagenetic events for the lower Cochrane member from the earliest event (1) to the latest (7).

Reservoir Porosity and Permeability

Core analyses data provided by Dr. James Derby and Marjo Operating Company were used to characterize the porosity and permeability of the dolomite and limestone within the reservoir. The dolomitic facies are generally more porous and permeable than the limestone facies (Table 6). Maximum effective porosity values for the dolomitic facies range from 7.8% to 13.2%, and for the limestone facies range from 4.4% to 11.2%. Maximum permeability values for the dolomitic facies range from 18.1 to 976 millidarcies, and for the limestone range from 3.8 to 798 millidarcies. Nevertheless, hydrocarbon production in the lower Cochrane member tends to be controlled by the total reservoir thickness where the highest cumulative oil production corresponds to the thickest section (Points 1-13 well – Table 6), and the lowest oil production corresponds to the thinnest section (Carter Ranch 2-15 well – Table 6). Vertical fractures are also an important host and conduit for fluids in the study area (James Derby, verbal communication). That is to say, the production of the reservoir in the study area is not restricted to specific facies. It is more likely related to the thickness of the reservoir and the vertical fractures affecting it.

Ratios between porosity and thickness were calculated from porosity logs of sixty-eight wells in the study area (Fig. 25). A minimum of 6% porosity was assumed for this ratio, which is the minimum value of porosity where carbonate reservoirs commonly produce hydrocarbons. It is inferred from these ratios that the thicker the carbonate section, the thicker the reservoir with more than 6% porosity. The linear regression points out that the trend line of the dolomite has a steeper slope compared with the limestone trend line. This is an indication that dolomite develop more porous reservoirs with respect to limestone. For instance, at 12 m (40 ft) of reservoir thickness, 8.5 m (28 ft) of dolomite will have more than 6% porosity, and only 3.4 m (11 ft) of limestone will have more than 6% porosity (Fig. 25).

Well name - number	Max. Helium Porosity (%)		Max. Permeability (md)		Hunton thickness (m/ft)	COP (BOE)	CGP (MCFG)
	Dolomite	Limestone	Dolomite	Limestone			
Anna 1-15	13.2	11.2	454	88.4	11.5 / 37.6	13,351	10,582
Boone 1-4*	8.1	10.6	18.1	29.5	9.0 / 29.5	16,055	90,375
Cal 1-11	----	4.4	----	7.9	31.0 / 101.8	61,055	596,620
Carter Ranch 2-15	12.7	9.0	760	33	8.9 / 29.1	8,291	82,238
JB 1-13	----	4.8	----	3.8	26.5 / 86.9	25,151	321,771
Mark Houser 1-11	----	4.9	----	9.9	35.5 / 116.6	42,991	754,780
Mary Marie 1-11	----	8.1	----	278	13.0 / 42.5	23,508	61,246
McBride South 1-10	7.8	6.5	976	74.8	10.4 / 34.3	26,921	218,742
Points 1-13	----	8.5	----	798	35.8 / 117.4	84,265	296,295
Wilkerson 1-3	11.2	10.4	100	88	14.1 / 46.4	65,947	1,057,224
Williams 1-3	9.2	4.9	21.2	9.8	12.3 / 40.3	14,187	227,483

* Boone 1-4 produces from the Wilcox Sandstone

Table 6. Maximum effective porosity and permeability for dolomite and limestone, reservoirs thickness, and cumulative oil and gas production for each of the eleven cored wells (see Figure 1 for location).

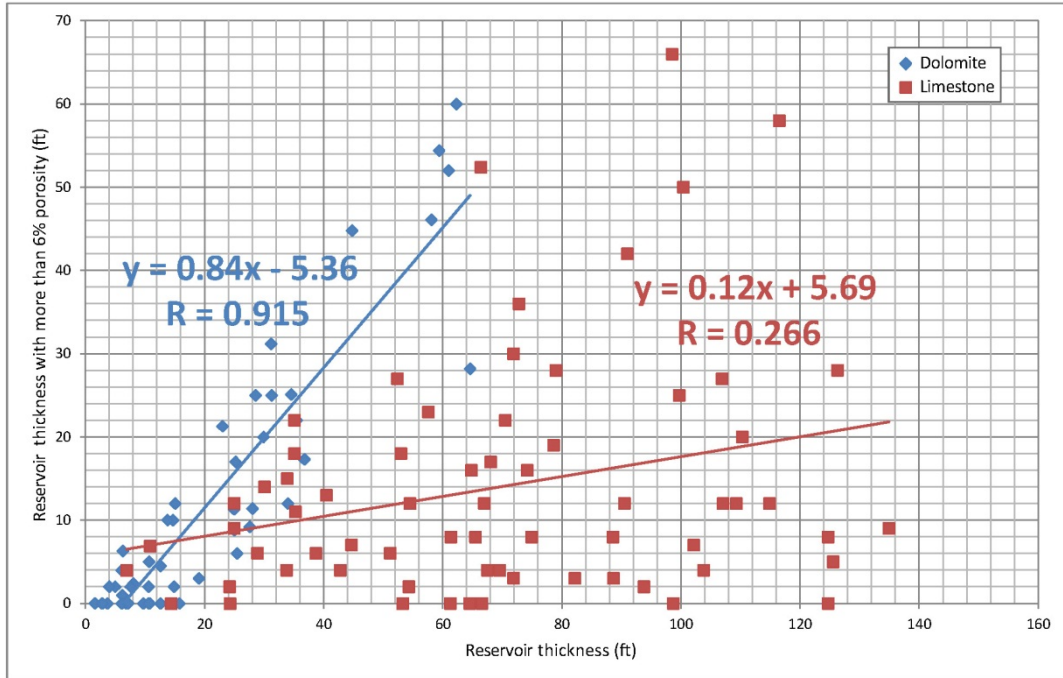


Figure 25. Linear regression of the reservoir thickness vs. reservoir thickness with more than 6% porosity. The dolomite (blue rhombs) shows a trend line with a steep positive slope and high correlation coefficient ($R=0.915$), which indicates a high significant correlation. The limestone (red squares) shows a trend line with a gentle positive slope and moderate correlation coefficient ($R=0.266$), which indicates a significant correlation.

CHAPTER VII

CONCLUSIONS

1. The lower Cochrane member was affected by early karsting attributed to sea level fluctuations in the Llandoveryan (Early Silurian).
2. Dolomitization in the reservoir is a result of seawater migration through the reservoir during early diagenesis. The dolomite isotopic signature may have been partially reset by circulation of meteoric fluids that precipitated calcite cements.
3. The paragenetic sequence determined for the lower Cochrane member indicates that karsting is the earliest diagenetic event. The dolomite and the calcite cements were precipitated before sand-mud infill from Devonian sediments. Therefore, the dolomitization and calcite cementation are pre-Devonian in age. Pressure-solution events occurred after the deposition of the Devonian units and represent the latest diagenetic event recognized in the reservoir.
4. Hydrocarbon production in the study area is likely more related to fracturing and reservoir thickness rather than lithofacies. Dolomite is frequently more porous and permeable than limestone. However, dolomite distribution is not uniform throughout the reservoir and this lack of spatial uniformity affects overall reservoir quality.

REFERENCES

- Adams, J. E., and M. L. Rhodes, 1960, Dolomitization by seepage refluxion: AAPG Bulletin, v. 44, no. 12, p. 1912–1920.
- Azmy, K., J. Veizer, M. G. Bassett, and P. Copper, 1998, Oxygen and carbon isotopic composition of Silurian brachiopods: Implications for coeval seawater and glaciations: GSA Bulletin, v. 110, no. 11, p. 1499-1512.
- Badiozamani, K., 1973, The Dorag dolomitization model – application to the Middle Ordovician of Wisconsin: Journal of Sedimentary Petrology, v. 43, no. 4, p. 965–984.
- Barrick, J.E., G. Klapper, and T.W. Amsden, 1990, Late Ordovician – Early Devonian conodont succession in the Hunton Group, Arbuckle Mountains and Anadarko Basin, Oklahoma: *in* S. M. Ritter ed., Early to Middle Paleozoic conodont biostratigraphy of the Arbuckle Mountains, southern Oklahoma, Oklahoma Geological Survey, Guidebook 27, p. 55-62.

Bathurst, R. G., 1975, Carbonate sediments and their diagenesis: Elsevier Scientific Publishing Company, 658 p.

Boyd, D.T., 2002, Map of Oklahoma Oil and Gas Fields (Distinguished by G.O.R. and Conventional Gas vs. Coalbed Methane) – Map GM36: *in* Oklahoma Geological Survey webpage [www.ogs.ou.edu/fossilfuels/MAPS/GM-36.pdf]

Braimoh, K., 2010, Deepwater, shoalwater, and lagoonal facies in the Silurian upper Cochrane member, Hunton Group, Chimneyhill Subgroup, West Carney Hunton Field, Oklahoma: unpublished M. S. Thesis, University of Tulsa.

Brand, U., and J. Veizer, 1981, Chemical diagenesis of a multicomponent carbonate system -2: Stable isotopes: *Journal of Sedimentary Petrology*, v. 51, no. 3, p. 987-997.

Charpentier, R. R., 1995, Cherokee Platform Province, National Assessment of United States Oil and Gas Resources: CD-ROM from the U.S.G.S. as Digital Data Series DDS-30, United States Geological Survey.

Choquette, P. W., and L. C. Pray, 1970, Geological nomenclature and classification of porosity in sedimentary carbonates: *AAPG Bulletin*, v. 54, p. 207-250.

Cusack, M., and A. P. Huerta, 2012, Brachiopods recording seawater temperature – a matter of class or maturation?: *Chemical Geology*, doi: 10.1016/j.chemgeo.2012.20.021

Derby, J., 2007, Geologic studies of West Carney Hunton Field: *in* M. Kelkar (ed.), *Exploitation and optimization of reservoir performance in Hunton Formation, Oklahoma – Final Technical Report*: University of Tulsa, Department of Petroleum Engineering, DOE Contract No. DE-FC26-00NT15125, U.S. Department of Energy, August 27 of 2007, p. 42-65.

Derby, J., 2010, Unpublished personal notes.

Derby, J., F. Podpechan, J. Andrews, and S. Ramakrishna, 2002, U.S. DOE-sponsored study of West Carney Hunton Field, Lincoln & Logan counties, Oklahoma: a preliminary report (Part I): *The Shale Shaker*, July - August, p. 9-19.

Dunham, R. J., 1962, Classification of carbonate rocks according to their depositional texture: *in* W. E. Ham, ed., *Classification of Carbonate Rocks-a symposium*: Tulsa, OK, AAPG Memoir 1, p. 108-121.

Folk, R. L., and L. S. Land, 1975, Mg/Ca ratio and salinity: two controls over crystallization of dolomite: *AAPG Bulletin*, v. 59, no. 1, p. 60–68.

Friedman, I., and J. R. O'Neil, 1977, Compilation of stable isotope fractionation factors of geochemical interest: USGS Professional Paper 440, 12 p.

Fritz, P., and D. G. W. Smith, 1970, The isotopic composition of secondary dolomites: *Geochim. Cosmochim. Acta*, v. 34, p. 1161-1173.

Grahn, Y., and M. V. Caputo, 1992, Early Silurian glaciations in Brazil: *Palaeogeography, Palaeoclimatology, Palaeoecology*, v. 99, p. 9-15.

Gregg, J. M., 1985, Regional epigenetic dolomitization in the Bonneterre Dolomite (Cambrian), southern Missouri: *Geology*, v. 13, p. 503–506.

Johnson, M. E., 1987, Extent and bathymetry of North American platform seas in the Early Silurian: *Paleoceanography*, v. 2, no. 2, p. 185-211.

Johnson, M. E., 2006, Relationship of Silurian sea-level fluctuations to oceanic episodes and events: *GFF*, v.128, no. 2, p. 115-121.

Krishnamurthy, R. V., E. A. Atekwana, and H. Guha, 1997, A simple, inexpensive carbonate – phosphoric acid reaction method for the analysis of carbon and oxygen isotopes of carbonates: *Analytical Chemistry*, v. 69, no. 20, p. 4256-4258, doi: 10.1021/ac9702047.

Land, L. S., 1980, The isotopic and trace element geochemistry of dolomite: the state of the art: SEPM Special Publication, no. 28, p. 87-110.

Lumsden, D. N., and J. S. Chimahusky, 1980, Relationship between dolomite nonstoichiometry and carbonate facies parameters: SEPM Special Publication, no. 28, p. 123-137.

Machel, H. G., 2004, Concepts and models of dolomitization: a critical reappraisal: *in* C.J.R. Braithwaite, G. Rizzi. & G. Darke eds., The geometry and petrogenesis of dolomite hydrocarbon reservoirs: Geological Society of London, Special Publication, no. 235, p. 7–63.

Mattes, B. W., and E. W. Mountjoy, 1980, Burial dolomitization of the Upper Devonian Miette buildup, Jasper National Park, Alberta: SEPM Special Publication, no. 28, p. 259–297.

Meyers, W. J., 1991, Calcite cement stratigraphy: An overview: SEPM Luminescence Microscopy and Spectroscopy: Qualitative and Quantitative Applications (SC25)

Milliman, J. D., 1974, Marine carbonates: Springer-Verlag, New York, 375 p.

Northcutt, R., and J. Campbell, 1995, Geological Provinces of Oklahoma: Oklahoma Geological Survey website, Open File Report OF5-95
[www.ogs.ou.edu/geolmapping/Geologic_Provinces_OF5-95.pdf]

Rush, P. F., and H. S. Chafetz, 1990, Fabric-retentive, non-luminescent brachiopods as indicators of original $\delta^{13}\text{C}$ and $\delta^{18}\text{O}$ composition: a test: *Journal of Sedimentary Petrology*, v. 60, n. 6, p. 968-981.

Saller, A. H., 1984, Petrologic and geochemical constraints on the origin of subsurface dolomite, Enewetak Atoll: an example of dolomitization by normal seawater: *Geology*, v. 12, p. 217–220.

Scholle, P. A., and D. S. Ulmer-Scholle, 2003, A color guide to the petrography of carbonate rocks: grains, textures, porosity, diagenesis: *AAPG Memoir 77*, 474 p.

Scotese, C. R., 2002, PALEOMAP Project website [<http://www.scotese.com/newpage2.htm>]

Scotese, C. R., and W. S. McKerrow, 1990, Revised world maps and introduction: *in* W.S. McKerrow, and C.R. Scotese eds., *Paleozoic palaeogeography and biogeography*, Geological Society of London, Memoir 12, p. 1-21.

Sibley, D. F., and J. M. Gregg, 1987, Classification of dolomite rock texture: *Journal of Sedimentary Petrology*, v. 57, p. 967-975.

Smith, B. J., 2012, Effects of sea level fluctuations on porosity and permeability of the lower Cochrane member, Hunton Group, Chimneyhill Subgroup, West Carney Hunton Field, OK: unpublished M. S. Thesis, Oklahoma State University, p. 46.

Tucker, M. E., and V. P. Wright, 1990, *Carbonate Sedimentology*: Blackwell Science Ltd, 482 p.

APPENDICES

APPENDIX 1

Tables with detail petrographic descriptions and dolomite classification

Thin section number	Well name-number	Depth	Size distribution		Dolomite texture		Allochans					Matrix			Void filling		Average crystal size (mm)	Porosity (%)	Porosity classification (Choquette & Pray, 1970)
			Unimodal	Polymodal	Planar-e	Planar-s	Unreplaced	Molds	Partial	Replaced		Unreplaced	Partial	Replaced	Unreplaced	Partial			
										Mimic	Nonmimic								
1	Anna 1-15	4969.5' - 69.6'															0.25 to 0.75	14	bc, fr, wp
2	Anna 1-15	4969.6' - 69.7'															0.25 to 0.8	9	bc, fr, vug, wp
3	Anna 1-15	4983.4'															0.2 to 0.6	11	sh, bc, wp
4	Anna 1-15	4989' - 89.1'															0.18 to 0.7	6	sh, bc, vug
5	Anna 1-15	4989.1' - 89.2'															0.2 to 0.5	9	fr, bc
6	Anna 1-15	4994.3' - 94.4'															0.2 to 0.6	21	bc, wp, fr, mo (partially)
7	Anna 1-15	4994.4' - 94.5'															0.2 to 0.6	16	bc, wp, fr, mo (partially)
8	Anna 1-15	4999.2' - 99.2'															0.15 to 0.6	21	bc, vug, fr, mo (partially)
9	Anna 1-15	5001' - 01.2'															0.2 to 0.5	10	bc, fr, vug
10	Anna 1-15	5001.8' - 01.9'															0.2 to 0.6	12	bc, vug, mo
11	Boone 1-4	5046.8'															0.25 to 0.75	16	wp, bc, vug
12	Boone 1-4	5052' 10" - 5053'															0.15 to 0.6	6	bc, vug
13	Boone 1-4	5063' 10" - 5064'															0.2 to 0.7	13	bc, wp, vug, mo (partially)
14	Boone 1-4	5065' 4" - 65' 6"															0.4 to 0.8	10	sx-mo, vug, fr
15	Boone 1-4	5065' 10.5" - 5066'															0.25 to 0.7	16	mo, sx-mo, vug
16	Boone 1-4	5066.4' - 66.5'															0.15 to 0.85	3	vug
17	Cal 1-11	5114'															0.04 to 0.12	0.5	fr, tight
18	Cal 1-11	5115'															0.1 to 0.2	0	tight - non porous
19	Cal 1-11	5121'															0.06 to 0.22	0	tight - non porous
20	Cal 1-11	5128.2'															0.1 to 0.25	0.5	fr, tight
21	Carter Ranch 2-15	5008.6'															0.12 to 0.35	6	sh, bp, wp
22	Carter Ranch 2-15	5009' 6" - 09' 7"															0.25 to 0.5	3	fr, bc, vug
23	Carter Ranch 2-15	5009' 7" - 09' 8"															0.1 to 0.5	7	fr, bc, vug
24	Carter Ranch 2-15	5015' 9.5" - 15' 10.5"															0.3 to 0.4	0	fr, tight
25	Carter Ranch 2-15	5015' 11" - 5016'															0.25 to 0.5	0	tight - non porous
26	Carter Ranch 2-15	5016' 9.5" - 16' 10.5"															0.1 to 0.4	4	vug, bc, fr
27	Carter Ranch 2-15	5016' 11" - 5017'															0.2 to 0.6	0	tight - non porous
28	Carter Ranch 2-15	5020' 10.5" - 5021'															0.2 to 0.6	6	vug, bc, wp
29	Carter Ranch 2-15	5023.5' - 23.7'															0.2 to 0.6	7	bc, sh
30	Carter Ranch 2-15	5025' 4" - 25' 6"															0.2 to 0.6	17	vug, bc
31	Carter Ranch 2-15	5026' 0.5" - 26' 1.5"															0.45 to 0.6	6	bc, vug
32	Carter Ranch 2-15	5026' 2" - 26' 3"															0.3 to 0.7	7	vug, bc, mo (partially)
33	Carter Ranch 2-15	5026.8' - 26.9'															0.15 to 0.65	10	bc, sx-mo, vug
34	Carter Ranch 2-15	5031' 4" - 31' 5"															0.3 to 0.5	24	mo, sx-mo
35	Carter Ranch 2-15	5033.5'															0.25 to 0.55	10	wp
36	Carter Ranch 2-15	5035' - 35.2'															0.1 to 0.45	1	bc, tight
37	JB 1-13	5004'															0.15 to 0.35	4	bp, wp, bc, vug
38	JB 1-13	5022'															0.1 to 0.35	0	tight - non porous
39	Mark Houser 1-11	5070.5'															0.2 to 0.4	2	bc, vug
40	Mark Houser 1-11	5070.7'															0.15 to 0.45	8	bc, vug, fr
41	Mark Houser 1-11	5070.8'															0.1 to 0.7	11	sx-mo, vug, bc
42	Mark Houser 1-11	5071.2'															0.05 to 0.4	16	mo, sx-mo, vug, fr
43	Mark Houser 1-11	5072'															0.05 to 0.4	10	bc, sx-mo, vug, fr
44	Mark Houser 1-11	5072.2'															0.1 to 0.35	10	mo, sx-mo, vug, bc, fr
45	Mary Marie 1-11	5001.6'															0.2 to 0.3	5	vug, fr
46	Mary Marie 1-11	5003.5' - 03.6'															0.15 to 0.4	1	fr, tight
47	McBride South 1-10	4964' 10.5" - 4965'															0.2 to 0.6	14	vug, fr
48	McBride South 1-10	4967' 8" - 67' 9"															0.16 to 0.55	6	bc, vug
49	McBride South 1-10	4970' 1" - 70' 2"															0.25 to 0.4	12	mo, sx-mo
50	McBride South 1-10	4970' 2" - 70' 3"															0.2 to 0.7	22	mo, sx-mo, vug, bc
51	McBride South 1-10	4971' - 71' 1"															0.15 to 0.6	14	wp, vug, bc
52	McBride South 1-10	4971' 1.5" - 71' 2.5"															0.2 to 0.5	15	mo, sx-mo, vug, wp, bc
53	Points 1-13	5106'															0.1 to 0.2	2	wp, tight
54	Points 1-13	5106.5'															0.1 to 0.2	2	vug, tight
55	Points 1-13	5106.8'															0.1 to 0.4	0.5	fr, tight
56	Points 1-13	5107'															0.05 to 0.2	0.5	fr, tight
57	Wilkinson 1-3	4997' 9" - 97' 10"															0.12 to 0.55	6	vug, bc, wp
58	Wilkinson 1-3	4998' 7" - 98' 8"															0.35 to 0.85	9	vug, bc, wp, mo (partially)
59	Wilkinson 1-3	4999' 5" - 99' 6"															0.18 to 0.7	13	mo, vug, bc
60	Wilkinson 1-3	4999' 7" - 99' 8"															0.2 to 0.9	12	sx-mo, vug, bc
61	Wilkinson 1-3	4999.7'															0.3 to 0.55	4	bc
62	Williams 1-3	4978' 8.5" - 78' 9.5"															0.25 to 0.6	9	bc, sh, fr
63	Williams 1-3	4978' 10" - 78' 11"															0.25 to 0.65	12	vug, bc, wp, mo (partially)
64	Williams 1-3	4978' 11" - 4979'															0.2 to 0.4	15	mo, sx-mo, vug, bc
65	Williams 1-3	4981' - 81' 1"															0.2 to 0.65	9	vug, bc, mo (partially)
66	Williams 1-3	4981' 2.5" - 81' 3.5"															0.2 to 0.65	13	vug, bc, fr, mo (partially)
67	Williams 1-3	4982' 1.5" - 82' 2.5"															0.2 to 0.7	4	bc, mo (partially)
68	Williams 1-3	4982' 3" - 82' 4"															0.2 to 0.7	12	vug, bc
69	Williams 1-3	4982.6'															0.4 to 0.6	11	bc, wp, fr
70	Williams 1-3	4983.1'															0.25 to 0.5	12	bc, wp

bc: intercrystal; bp: interparticle; wp: intraparticle; sh: shelter; mo: moldic; sx-mo: solution-enlarged molds; vug: vuggy; fr: fracture

Thin section number	Well name-number	Depth	Fossil Assemblage	Dolomite Classification (Sibley & Gregg, 1967; Wright, 1992)	Observations
1	Anna 1-15	4969.5' - 69.6'	Brachiopods (few mm to 2cm)	unimodal, planar, rudstone	Sand and mud infill; calcite cement filling fractures
2	Anna 1-15	4969.6' - 69.7'	Brachiopods (few mm to 2cm)	unimodal, planar, rudstone	Porosity filled by sand and mud (karst infill); calcite cement replacing brachs
3	Anna 1-15	4983.4'	Brachiopods (centimetric size)	unimodal, planar-e, rudstone	Dolomite replacing matrix; calcite cement filling porosity
4	Anna 1-15	4989' - 89.1'	Brachiopods (centimetric size)	unimodal, planar, rudstone	Planar dolomite replacing matrix
5	Anna 1-15	4989.1' - 89.2'	Brachiopods (centimetric size)	unimodal, planar, rudstone	Fractures up to 0.75mm wide; micro-stylolites
6	Anna 1-15	4994.3' - 94.4'	Brachiopods (centimetric size)	unimodal, planar-s, rudstone	Sucrosic dolomite texture
7	Anna 1-15	4994.4' - 94.5'	Brachiopods (few mm to 2cm)	unimodal, planar, rudstone	Sucrosic dolomite texture
8	Anna 1-15	4999.2' - 99.4'	Brachiopods (larger than 2mm)	unimodal, planar-s, float/sparstone	Brachs partially replaced; sucrosic texture
9	Anna 1-15	5001' - 01.2'	Brachiopods (larger than 2mm)	unimodal, planar-e, floatstone	Planar-e dolomite partially replacing matrix and brachs
10	Anna 1-15	5001.8' - 01.9'	Brachiopods	unimodal, planar, sparstone	Moldic porosity from dissolved brachs; calcite cement; sucrosic texture
11	Boone 1-4	5046.8'	Corals, brachiopods, crinoids (> 2mm)	unimodal, planar-e, rudstone	Calcite cement filling imp porosity and syntaxial overgrowth crinoids
12	Boone 1-4	5052' 10" - 5053'	Crinoids, brachiopods (> 2mm)	unimodal, planar-e, rudstone	Calcite cement showing syntaxial overgrowth on crinoids and replacing brachs
13	Boone 1-4	5063' 10" - 5064'	Crinoids, brachiopods (> 2mm)	unimodal, planar-e, rudstone	Calcite cement showing syntaxial overgrowth on crinoids
14	Boone 1-4	5065' 4" - 65' 6"	None	unimodal, planar-s, sparstone	Planar-s dolomite replacing matrix; no fossils remain
15	Boone 1-4	5065' 10.5" - 5066'	Brachiopods	unimodal, planar-s, sparstone	No fossils remain, replaced by calcite cement or dissolved
16	Boone 1-4	5066.4' - 66.5'	None	unimodal, planar-s, sparstone	Planar-s dolomite replacing matrix; no fossils remain
17	Cal 1-11	5114'	Crinoids, brachiopods, forams	unimodal, planar-e, pack/sparstone	Green fossiliferous chert; silica cement occluding imp porosity
18	Cal 1-11	5115'	Crinoids, brachiopods	unimodal, planar-e, wackestone	Sand, mud, and detrital dolomite infill; planar-s dolomite following proto-stylolite (?)
19	Cal 1-11	5121'	Brachiopods, crinoids (up to 3mm)	unimodal, planar-s, pack/floatstone	Calcite cement replacing brachs and crinoids; stylolites
20	Cal 1-11	5128.2'	Crinoids, brachiopods	unimodal, planar-e, packstone	Calcite cement filling vugs and silica cement occluding imp porosity; brach spines
21	Carter Ranch 2-15	5008.6'	Brachiopods (centimetric size)	unimodal, planar-e, rudstone	Large brachs; imp porosity occluded by sand infill, Qz, mud, and dolomite crystals (detrital dolomite)
22	Carter Ranch 2-15	5009' 6" - 09' 7"	None	unimodal, planar-s, sparstone	Calcite cement at top
23	Carter Ranch 2-15	5009' 7" - 09' 8"	None	unimodal, planar-s, sparstone	Merely dolomite; stylolites and fractures
24	Carter Ranch 2-15	5015' 9.5" - 15' 10.5"	Brachiopods (larger than 2mm)	unimodal, planar-s, rud/sparstone	Dolomitized Ls at top in 'stylolite' contact with brach rudstone at base; calcite cement
25	Carter Ranch 2-15	5015' 11" - 5016'	None	unimodal, planar-s, sparstone	Planar-s dolomite at base grading to crystalline Ls at top; sand-mud infill; stylolites
26	Carter Ranch 2-15	5016' 9.5" - 16' 10.5"	Brachiopods (centimetric size)	unimodal, planar-s, rudstone	Calcite cement replacing brachs; pyrite
27	Carter Ranch 2-15	5016' 11" - 5017'	Brachiopods (centimetric size)	unimodal, planar-s, rudstone	Brown planar dolomite; calcite cement partially replacing brachs
28	Carter Ranch 2-15	5020' 10.5" - 5021'	Brachiopods, crinoids (larger 2mm)	unimodal, planar-s, rudstone	Dolomite replacing matrix
29	Carter Ranch 2-15	5022.5' - 22.7'	Brachiopods (centimetric size)	unimodal, planar, float/sparstone	Large punctate brachs (base); stylolite
30	Carter Ranch 2-15	5025' 4" - 25' 6"	None	unimodal, planar, sparstone	Merely dolomite
31	Carter Ranch 2-15	5026' 0.5" - 26' 1.5"	Brachiopods (centimetric size)	polymodal, planar-s, floatstone	Dolomite partially replacing matrix
32	Carter Ranch 2-15	5026' 2" - 26' 3"	None	unimodal, planar-s, sparstone	Stylolites at top
33	Carter Ranch 2-15	5026' 8" - 26' 9"	None	unimodal, planar-s, sparstone	Dolomite replacing matrix; sparse calcite cement; no fossils remain
34	Carter Ranch 2-15	5031' 4" - 31' 5"	Brachiopods (larger than 2mm)	unimodal, planar-s, sparstone	Dissolved brachs generating moldic porosity
35	Carter Ranch 2-15	5033.5'	Tabulate coral	unimodal, planar-e, bafflestone	Sparse planar-e dolomite crystals within the Ls, next to a sand infill; Tabulate coral (<i>Favosites</i> sp.)
36	Carter Ranch 2-15	5035' - 35.2'	Brachiopods, crinoids (larger 2mm)	unimodal, planar-e, rudstone	Dolomite at the Sylvan - Hunton contact
37	JB 1-13	5004'	Brachiopods, crinoids, bryozoans	unimodal, planar, rudstone	Dolomite replacing matrix; calcite cement replacing crinoids and occluding imp porosity
38	JB 1-13	5022'	Coral, brachiopods, crinoids, bryozoan	unimodal, planar, baffle/floatstone	Planar dolomite on top of a <i>Favosites</i> coral; <i>Halysites</i> coral and other organisms at top; calcite cement
39	Mark Houser 1-11	5070.5'	Crinoids	unimodal, planar, packstone	Calcite cement replacing crinoids and filling vugs (base); planar dolomite at top
40	Mark Houser 1-11	5070.7'	Brachiopods, crinoids	unimodal, planar-s, grainstone	Planar dolomite (top); brach grainstone (base); calcite cement replacing brachs and filling vugs
41	Mark Houser 1-11	5070.8'	None	unimodal, planar-s, sparstone	No fossils remain; solution enlarged molds and vugs
42	Mark Houser 1-11	5071.2'	Brachiopods (larger than 2mm)	polymodal, planar-s, rud/sparstone	Dolomite replacing matrix (top); brach rudstone (base); calcite cement replacing some brachs
43	Mark Houser 1-11	5072'	None	polymodal, planar-s, sparstone	Planar-s dolomite replaces matrix
44	Mark Houser 1-11	5072.2'	Brachiopods, crinoids (larger 2mm)	polymodal, planar-s, floatstone	Brach-crinoidal rudstone (base) in contact with dolomitic floatstone (top)
45	Mary Mane 1-11	5001.6'	Crinoids, brachiopods	unimodal, planar-s, grain/sparstone	Crinoidal-brach grainstone (base and top); dolomite + calcite cement (middle)
46	Mary Mane 1-11	5003.5' - 03.6'	None	unimodal, planar-e, sparstone	Dolomitic Ls on top of the Sylvan - Hunton unconformity
47	McBride South 1-10	4964' 10.5" - 4965'	Brachiopods (centimetric size)	unimodal, planar-s, float/sparstone	Brach floatstone (base) in contact, by a fracture, with the dolomitic Ls
48	McBride South 1-10	4967' 8" - 67' 9"	Brachiopods (centimetric size)	unimodal, planar-s, rudstone	Calcite cement partially replacing brachs
49	McBride South 1-10	4970' 1" - 70' 2"	Brachiopods (larger than 2mm)	unimodal, planar, rud/sparstone	Brach rudstone (top) in contact with the dolomite sparstone; sucrosic texture; glauconite
50	McBride South 1-10	4970' 2" - 70' 3"	Brachiopods (larger than 2mm)	unimodal, planar-s, sparstone	Sand infill between Ls and planar dolomite; sucrosic texture; brachs dissolved away
51	McBride South 1-10	4971' - 71' 1"	Brachiopods (larger than 2mm)	unimodal, planar-s, rud/sparstone	Calcite cement filling moldic porosity
52	McBride South 1-10	4971' 1.5" - 71' 2.5"	Brachiopods	unimodal, planar-s, sparstone	Brachs dissolved away, only moldic porosity remain
53	Points 1-13	5106'	Crinoids, brachiopods, bryozoan, coral	unimodal, planar-e, rudstone	Sparse planar-e dolomite crystals, corroded boundanes, within the rudstone; calcite cement
54	Points 1-13	5106.5'	Crinoids, brachs, bryozoan, trilobites	unimodal, planar, packstone	Planar dolomite replacing matrix; grainstone at the very top
55	Points 1-13	5106.8'	Crinoids, trilobites, bivalves, brachs	unimodal, planar, floatstone	Crinoidal-trilobite wackestone (base), crinoidal dolomitic packstone (top); glauconite
56	Points 1-13	5107'	Crinoids, brachiopods, coral	unimodal, planar, wackestone	Planar dolomite partially replacing matrix and fossils; glauconite and pyrite
57	Wilkerson 1-3	4997' 9" - 97' 10"	Brachiopods, crinoids (larger 2mm)	unimodal, planar-e, rudstone	Syntaxial overgrowth dolomite (top); brach-crinoid rudstone (base); calcite cement replacing fossils
58	Wilkerson 1-3	4998' 7" - 98' 8"	Brachiopods (larger than 2mm)	unimodal, planar, floatstone	Syntaxial overgrowth dolomite; brachs partially dissolved and replaced by calcite cement
59	Wilkerson 1-3	4999' 5" - 99' 6"	Brachiopods (larger than 2mm)	unimodal, planar-s, sparstone	Euhedral dolomite crystal ghosts; dolomitic cement, calcite cement occluding porosity
60	Wilkerson 1-3	4999' 7" - 99' 8"	None	unimodal, planar-s, sparstone	Euhedral dolomite crystal ghosts; dolomitic cement
61	Wilkerson 1-3	4999.7'	None	polymodal, planar, sparstone	Euhedral dolomite with crystal overgrowth; pyrite; glauconite; calcite veins; Sylvan contact
62	Williams 1-3	4978' 8.5" - 78' 9.5"	Brachiopods (centimetric size)	unimodal, planar, grainstone	Planar dolomite crystals replacing matrix
63	Williams 1-3	4978' 10" - 78' 11"	Brachiopods, crinoids (larger 2mm)	unimodal, planar-s, rudstone	Dolomite replacing matrix enhancing porosity; calcite cement replacing crinoids
64	Williams 1-3	4978' 11" - 4979'	Brachiopods, crinoids (larger 2mm)	unimodal, planar-s, rud/sparstone	Dolomite replacing matrix enhancing porosity; fossils partially and/or completely dissolved away
65	Williams 1-3	4981' - 81' 1"	Brachiopods, crinoids (larger 2mm)	unimodal, planar-s, rudstone	Dolomite replacing matrix enhancing porosity; fossils partially dissolved
66	Williams 1-3	4981' 2.5" - 81' 3.5"	Brachiopods (centimetric size)	unimodal, planar-s, rudstone	Dolomite replacing matrix; calcite cement partially occluding porosity and replacing brachs
67	Williams 1-3	4982' 1.5" - 82' 2.5"	Brachiopods (centimetric size)	unimodal, planar-s, rudstone	Sparse silica cement filling vugs; calcite cement replacing brachs
68	Williams 1-3	4982' 3" - 82' 4"	Brachiopods (larger than 2mm)	unimodal, planar, grain/rudstone	Dolomite replacing matrix enhancing porosity
69	Williams 1-3	4982.6'	Brachiopods (larger than 2mm)	unimodal, planar, rud/sparstone	Planar-s dolomite surrounding large brachs; planar-e dolomite replacing matrix; calcite cement
70	Williams 1-3	4983.1'	Brachiopods, crinoids	unimodal, planar-e, grainstone	Dolomite replacing matrix

VITA

César Augusto Silva Cárdenas

Candidate for the Degree of

Master of Science

Thesis: RESERVOIR AND DIAGENETIC CHARACTERIZATION OF THE LOWER COCHRANE MEMBER, HUNTON GROUP – LINCOLN AND LOGAN COUNTIES, OKLAHOMA

Major Field: Geology

Biographical:

Education:

Completed the requirements for the Master of Science in Geology at Oklahoma State University, Stillwater, Oklahoma in December 2012.

Completed the requirements for the Bachelor of Science in Geology at Universidad Nacional de Colombia, Bogotá, Colombia in 2005.

Experience:

Geological Intern, Occidental Petroleum Corporation, Houston, TX, Summer 2012

Field Geologist, Smithsonian Tropical Research Institute, Panama City, Republic of Panama, January 2008 – July 2010

Field Geologist, Corporación Geológica Ares, Bogotá, Colombia, August 2004 – December 2007







Professional Memberships:

Asociación Colombiana de Geólogos y Geofísicos del Petróleo

American Association of Petroleum Geologists









































Geological Society of America

Society of Exploration Geophysicists

	Brachiopod		Limestone		Dolomite
	Shaly sandstone		Dolomitized limestone		Dolomitized mudrock

smg - small megapore
 lms - large mesopore
 T.S. - Thin Section
 ISO - Isotope geochemistry

CORE DESCRIPTION

Fm.	Depth	Lithology	Fossils	Fabric	Diagenetic Features	Pore type	Sample	Descriptions		
MISENER	4967							Dark grey sandstone interlaminated with shale and chert; silicified <i>Pentamerid</i> brachiopods		
	4968			Packstone	Veins	Intraparticle & vuggy, lms [3mm]		Greyish tan packstone, karst infill, brachs (up to 3cm), silicified at the very top, calcite veins (up to 1mm wide)		
	4969				Fracture	Intraparticle, shelter, vuggy, moldic & sol. enlarged molds, lms to smg		Brownish grey packstone, brachs (up to 3.5cm), calcareous mud filling shelter & intraparticle porosity		
	4970			Packstone		Intraparticle, vuggy, shelter, smg [10mm]	T.S. ISO	Greyish tan packstone, brachs, black fine grained sand by karst infill Grey packstone, slightly dolomitized Yellowish brown packstone, <i>Pentamerid</i> brachs (up to 3.5cm)		
	HUNTON GROUP	4971				Fracture Stylolite: 1mm Stylolite: 0.5mm	Intraparticle, lms [2mm] Shelter, lms [2mm]		Greyish brown brachiopod packstone, karst infill from Misener sandstone Greyish tan brachiopod packstone, karst infill Brownish grey packstone, brachs replaced by siderite?, dolomite?	
		4972			Packstone		Shelter, smg [6mm]		Brownish grey packstone, brown brachs replaced by siderite?, dolomite?; slightly dolomitized	
		4973			Packstone	Stylolite: 2mm Vertical stylolite Stylolites [2]: .5mm	Shelter, smg [4mm] Vuggy, lms [3mm] Reduced mold, smg [5mm]		Brownish grey packstone, complete brown brachs (up to 3cm) replaced by siderite?, dolomite?; randomly oriented	
		4974			Grainstone	Fracture	Reduced mold, smg [5mm] partially infill		Tan grainstone, brachs (up to 3.2cm)	
		4975			Grainstone		Moldic, smg [10mm]		Brownish grey grainstone, brown brachs replaced by calcareous mud; slightly dolomitized	
		4976			Grainstone		Vuggy, lms [1mm]		Yellow grainstone, micro-vugs in brachs, slightly dolomitized	
		4977			Grainstone	Stylolite: 2mm Fracture Stylolite: 1mm	Shelter, lms [3mm]		Grey grainstone bounded by stylolites and fractures	
		4978			Grainstone	Vertical fractures Stylolite: 1mm	Intraparticle, smg [6mm]		Brownish tan grainstone, mud ~40%	
		4979			Grainstone		Vuggy & shelter, smg [7mm]		Tan grainstone, <i>Pentamerid</i> brachs (up to 3.5cm), slightly dolomitized	
		4980			Grainstone	Stylolite: 0.5mm Horizontal and vertical fractures	Intraparticle, lms to smg Vuggy, lms [3mm] Fracture, 15cm long 1mm open		Tan grainstone, <i>Pentamerid</i> brachs (up to 5cm), slightly dolomitized	
		4981			Packstone	Vertical fractures	Intraparticle, lms [3mm] Shelter, lms [3mm]		Brownish yellow packstone, <i>Pentamerid</i> brachs (up to 4cm); slightly dolomitized	
		4982			Wackestone	Stylolite: 0.5mm	Vuggy, lms [3mm]		Greyish tan wackestone, brachs (up to 2.5cm); slightly dolomitized	
		4983			Packstone	Stylolite: 1mm	Intraparticle, lms [3mm]		Greyish tan packstone, brachs (up to 4cm), brown, mud filling intraparticle porosity; slightly dolomitized	
		4984			Packstone	Stylolite: 3mm Vertical fractures 1mm wide	Intraparticle & shelter, smg [6mm] Vuggy, smg [5mm]		Greyish tan packstone, brachs (up to 4cm); slightly dolomitized Tan packstone, brachs (up to 4.5cm)	
		4985			Wackestone	Stylolite: 3mm Stylolite: 2mm Fracture	Moldic, smg [10mm]		Grey wackestone	
		4986			Packstone	Vertical fractures	Intraparticle, smg [6mm] Shelter, smg [4mm]		Yellow packstone, <i>Pentamerid</i> brachs (up to 4cm), tight; slightly dolomitized Tan packstone, <i>Pentamerid</i> brachs (up to 3.5cm)	
		4987			Packstone		Vuggy, lms [0.5mm] Shelter, lms [1.5mm]		Yellow packstone, <i>Pentamerid</i> brachs, slightly dolomitized Tan brachiopod packstone <i>Pentamerid</i> brachiopod (7cm long)	
		4988			Packstone	Fracture Stylolite: 0.5mm Stylolite: 1mm	Vuggy, lms [1mm]		Tan brachiopod packstone	
		4989			Wackestone		Vuggy, lms [3mm]	T.S.	Tan brachiopod packstone (up to 4.5cm)	
		4990			Wackestone		Intraparticle, lms [5mm] Shelter, smg [5mm] Vuggy, smg [5mm]		Yellow packstone, <i>Pentamerid</i> brachs (up to 4cm), tight, slightly dolomitized Grey brachiopod (up to 4.5cm) packstone; slightly dolomitized	
		4991			Packstone	Fracture	Intraparticle, lms [2mm]		Yellowish grey packstone, <i>Pentamerid</i> brachs (up to 4.5cm), dolomitized	
		4992			Packstone	Stylolites [2]: 8mm Stylolite: 2mm	Shelter, smg [4mm] Vuggy, smg [5mm]		Yellowish grey packstone, <i>Pentamerid</i> brachs (up to 4.5cm), dolomitized	
		4993			Grainstone		Intraparticle, smg [10mm] Vuggy, lms [2mm]		Grey packstone/wackestone bounded by stylolites	
		4994			Packstone	Fracture, 16cm long 1mm open Interparticle, smg [8mm] Fractures	Vuggy, smg [13mm]		Yellowish grey packstone, <i>Pentamerid</i> brachs (up to 3.5cm), grey mud filling some brach molds; dolomitized	
		4995			Wackestone		Moldic, lms [3mm] Vuggy, smg [5mm]		Yellowish grey packstone, mud filling brach's shelter porosity; dolomitized Yellowish grey brachiopod packstone	
		4996			Wackestone	Stylolites [3]: 3mm	Vuggy, smg [5mm] Intraparticle, lms [2mm]	T.S. T.S.	Yellowish grey brachiopod packstone Greyish yellow wackestone bounded by stylolites Yellowish white brachiopod grainstone	
		4997			Packstone	Vertical fractures Stylolite: 1mm Stylolite: 0.5mm Stylolite: 2mm	Fracture, 9cm long <1mm open Moldic, smg [15mm] Vuggy, lms [3mm]		Yellowish grey brachiopod packstone, dolomitized Greyish white wackestone bounded by stylolites Grey brachiopod packstone	
		4998			Packstone	Stylolites [3]: .5mm	Intraparticle, lms [3mm] Solution enlarged mold, smg [10mm] Shelter, smg [5mm] Vuggy, lms [3mm]		Greyish yellow <i>Pentamerid</i> brachs packstone, calcareous mud filling shelter porosity; dolomitized	
		4999			Grainstone	Stylolite: 1mm Stylolite: 10mm Stylolite: 1mm Stylolite: 5mm	Shelter, smg [8mm]		Greyish white packstone; brachs (up to 4cm); mud filling shelter porosity White brachiopod grainstone Grey brachiopod packstone White brachiopod grainstone bounded by stylolites	
		5000			Packstone/Grainstone	Horizontal and vertical fractures	Fenestral, 1cm long 1mm wide		Large dolomitized brachs (up to 5 cm) Tan brachiopod packstone/grainstone; trilobites?	
		5001			Packstone/Grainstone		Intraparticle, smg [6mm] Vuggy, smg [4mm] Moldic, smg [25mm]	T.S. ISO T.S.	Yellowish brown brachiopod packstone/grainstone; dolomitized Tan brachiopod packstone/grainstone, partially diluted, dolomitized matrix	
		5002			Packstone		Vuggy, smg [5mm] Moldic, smg [22mm]		Yellowish brown packstone, brachs partially to complete diluted, dolomitized matrix	
		5003			Wackestone	Stylolite: 5mm	Moldic, smg [29mm] Vuggy, smg [6mm]		Tan wackestone, partially diluted white brachs, dolomitized matrix	
		5004			Mudstone	Fractures	Fracture, 7.5cm long 1mm open Fenestral, 7mm long <1mm wide		Greenish grey dolomitized mudstone, micro-stylolites, dolomitized Light yellow brachiopod grainstone	
		5005			Grainstone	Stylolite: 10mm	Moldic, smg [13mm] Micro-vugs Fracture, 30cm long 1mm open		Greenish grey dolomitized mudstone, slightly laminated, moldic porosity of brachs Yellowish white crystalline Ls with <i>Pentamerid</i> brachs	
		SYLVAN	5006				Fractures Stylolite: 1mm Stylolite: 4mm			Greyish tan laminated mudstone
			5007			Packstone	Fracture Stylolite: 5mm Stylolite: 1mm	Fracture, 4.5cm long <1mm open Moldic, smg [20mm] Vuggy, lms [2mm] Fracture, 4cm long <1mm open	T.S. ISO	Grey dolomitized brachiopod packstone Grey dolomitized crystalline carbonate
			5008			Crystalline carbonate	Stylolite: 0.5mm Fracture	Moldic, smg [7mm]		Yellowish grey dolomitized wackestone
5009				Crystalline carbonate	Stylolites [2]: 1mm	Vuggy, smg [13mm]				
5010				Crystalline carbonate	Fracture Stylolite: 1mm	Fracture, 5cm long <1mm open Moldic, smg [20mm] Vuggy, lms [1mm]	T.S. ISO T.S.	Brownish yellow dolomitized wackestone, porous <i>Pentamerid</i> brachiopods		
5011				Crystalline carbonate		Fracture, 15cm long 1mm open Vuggy, smg [5mm]		White to light grey crystalline Ls, slightly laminated; mud filling lamination planes		
5012				Crystalline carbonate	Stylolites [2]: 1mm Stylolite: 8mm Stylolite: 3mm	Fractures, 2cm long <1mm open		Greyish white, slightly pink crystalline Ls with trilobites replaced by mud; abundant stylolites and joints		
5013				Grainstone	Stylolites [2]: 4mm Fractures filled w/ calcite crystals	Fractures, 2cm long 2mm open	T.S.	White grainstone with brachiopods at the base, tight Pyrite replacing brachs Brownish white brachiopod grainstone, fractured, calcite crystals partially filling joints Mud infill bounded by joints		
5014						T.S.	Green dolomitized mudrock, fractured, pyrite veins, slightly laminated			



- Brachiopod
- Crinoid
- Coral
- Limestone
- Dolomitized limestone
- Dolomite
- Dolomitized mudrock

- smg - small megapore
- lms - large mesopore
- T.S. - Thin Section
- ISO - Isotope geochemistry

CORE DESCRIPTION

Fm.	Depth	Lithology	Fossils	Fabric	Diagenetic Features	Pore type	Sample	Descriptions	
LOWER COCHRANE MEMBER - CHIMNEYHILL SUBGROUP - HUNTON GROUP	5037			Packstone	Stylolite: 4mm Stylolite: 1mm Highly fractured	Vuggy, smg [10mm] Fracture, 19cm long 2mm wide		Light brown packstone, large coral frags (2cm), crinoids, and brachs; highly fractured	
	5038			Packstone	Stylolite: 0.5mm Stylolite: 10mm Stylolites[3]: 1mm Stylolites[2]: 2mm	Vuggy, lms [1.5mm]		Light brown packstone, large brach frags (4cm), sand infill along fractures	
	5039			Packstone	Fracture Stylolite: 1mm	Vuggy, smg [5mm]		Light brown packstone, brachs (up to 1.5cm), crinoids (up to 7mm), sparse sand infill by karsting	
	5040			Packstone/ grainstone	Fractures Stylolite: 16mm Stylolite: 2mm	Vuggy, lmg [35mm]		Brownish tan packstone/grainstone with brachs; brown sand infill by karsting	
	5041			Grainstone	Stylolite: 1mm Stylolites[2]: 3mm Fracture			Tan grainstone with mainly crinoids and sparse brachs; tight; calcite crystals filling fractures at the top	
	5042			Grainstone	Stylolite: 1mm	Moldic, smg [6mm] Micro-vugs		Tan grainstone with crinoid and brach fragments	
	5043			Crystalline carbonate/ grainstone	Stylolite: 3mm Stylolite: 1mm Fracture	Vuggy, smg [5mm]		White crystalline Ls/grainstone with <i>Halysites</i> coral and sparse brachs	
	5044			Grainstone	Stylolites[3]: 2mm Fracture	Vuggy, smg [20mm]		Brownish tan packstone/grainstone with corals (up to 1.8cm), brachs (up to 1.2cm), and crinoid fragments; vugs partially infilled with calcite crystals; calcareous sand infill fractures	
	5045			Grainstone	Stylolites[2]: 3mm			White-grey-pink grainstone with brachs (up to 3cm); tight	
	5046			Grainstone	Stylolites[3]: 2mm Stylolites[4]: 2mm Stylolite: 6mm Fracture				
	5047			Packstone	Stylolite: 2mm	Micro-vugs Intraparticle, smg [4mm] Vuggy, smg [18mm]	T.S.	Tan (slightly green-pink) packstone with <i>Halysites</i> coral (up to 1.5cm), crinoids (up to 1cm), and brach fragments	
	5048			Grainstone	Stylolites[8]: 1mm Stylolite: 3mm	Vuggy, smg [12mm]		Tan (grey at the top) grainstone, brachs (up to 1.5cm), crinoids (up to 1cm), and corals (up to 1.5cm) slightly yellow (oil stained?)	
	5049			Grainstone	Stylolites[3]: 1mm Fracture Stylolites[3]: 1mm	Vuggy, smg [4mm]		Large channel sand infill (7 cm long) Tan grainstone with crinoids, brachs, and coral fragments oil stained?	
	5050			Grainstone	Stylolites [6]: 2mm	Micro-vugs		Tan grainstone, mainly crinoids and sparse brachs; tight channel sand infill (by karsting)	
	5051			Grainstone	Stylolites[4]: 1mm Fracture Stylolites[3]: 1mm	Vuggy, lms [3mm] Intraparticle, smg [4mm]		Tan crinoidal grainstone (up to 3.5cm); calcareous silt infill along fractures (karsting) oil stained?	
	5052			Grainstone	Fracture Fracture	Micro-vugs Fracture, 8cm long 1mm wide		Tan crinoidal grainstone (up to 2.5cm); calcareous silt infill along fractures and channels (karsting) oil stained?	
	5053			Grainstone	Stylolites[7]: 1mm	Micro-vugs	T.S. ISO	Tan grainstone, mainly crinoids (up to 1cm), and sparse brach fragments; calcareous silt infill along fractures; tight oil stained?; slightly dolomitized	
	5054			Grainstone	Fracture Stylolites [5]: 2mm	Micro-vugs		Tan grainstone, brachs (up to 1.7cm), crinoids (up to 1.2cm), and coral fragments; channel calcareous silt infill (karsting) Grey brown crystalline Ls	
	5055			Crystalline carbonate/ grainstone	Stylolites [2]: 1mm Stylolites [2]: 1mm	Vuggy, smg [6mm]		Brownish grey crystalline Ls/grainstone, sparse brach and crinoid fragments (up to 0.5cm) oil stained?	
	5056			Crystalline carbonate	Fracture			Tan crystalline carbonate, wavy parallel lamination, channel filled with yellow sand Yellow crystalline carbonate slightly laminated, oil stained?	
	5057			Rudstone	Horizontal vertical fractures Stylolite: 1mm	Fracture, 2cm long <1mm wide Intraparticle, smg [4mm]		Tan rudstone with pentamerid brachs (up to 2.5cm), slightly laminated, fractured, brown sand infill (karsting?) Yellow grainstone; oil stained	
	5058			Grainstone	Stylolite: 1mm Fracture	Shelter, lms [2mm] Micro-vugs		Tan grainstone with pentamerid brachs; fracture filled with yellowish brown silt Yellow grainstone; oil stained	
	5059			Grainstone	Stylolite: 2mm	Vuggy, smg [7mm]		Tan grainstone with brachs and crinoids; tight	
	5060			Grainstone	Fracture Stylolites [7]: 1mm	Vuggy, lms [2mm]		Pinkish grey grainstone with crinoids (up to 2.5cm), and sparse brachs; tight with seldom micro-vugs	
	5061			Grainstone	Fracture Stylolite: 10mm Stylolites [3]: 2mm Vertical fracture 19 cm long 1mm wide	Vuggy, lms [3mm] Fracture, 19cm long 1mm wide		Pink grainstone, brachs (up to 2cm) and crinoids (up to 2.5cm) fractures filled with yellow muddy sand; tight	
	5062			Grainstone	Stylolites [6]: 2mm	Micro-vugs		Pink grainstone with brachs and crinoids (up to 0.5cm); tight	
	5063			Grainstone	Fracture Fracture Stylolite: 2mm	Micro-vugs		Tan grainstone with brachs (up to 1.5cm), crinoids; tight	
	5064			Grainstone	Fracture Stylolite: 3mm	Vuggy, smg [15mm]	ISO	Tan grainstone, partly dolomitized, brachs (up to 2.5cm), sparse vugs partially filled with calcite crystals	
	5065			Crystalline carbonate	Fracture	Crystalline carbonate Mudstone	T.S.	Tan crystalline carbonate partly dolomitized; micro-vugs oil stained Grey dolomite mudstone, micro-vugs, slightly laminated	
	5066			Wackestone	Fracture Stylolite: 2mm	Moldic, smg [20mm] Vuggy, smg [30mm] Moldic, smg [20mm] Solution enlarged mold, smg [21mm] Vuggy, smg [10mm]	T.S. ISO	Greenish grey wackestone, moldic porosity of brachs, slightly laminated, and highly dolomitized	
	5067			Crystalline carbonate		Vuggy, lms [3mm]	T.S.	Yellowish tan dolomitized wackestone, oil stained Greenish tan crystalline carbonate, muddy sandstone replacing brachs, partly dolomitized, micro-vugs Tan crystalline dolomite with irregular lenses of brownish yellow muddy sandstone; micro-vugs	
	SYLVAN	5067							Green dolomitized mudrock, fractured, pyrite veins, light brown laminae

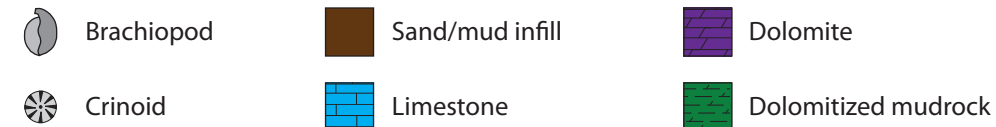


smg - small megapore
 lms - large mesopore
 T.S. - Thin Section
 ISO - Isotope geochemistry
 XRD - X-ray diffraction
 SEM - Scanning Electron Microscopy

- Brachiopod
- Limestone
- Dolomite
- Coral
- Dolomitized limestone
- Dolomitized mudrock

CORE DESCRIPTION

Fm.	Depth	Lithology	Fossils	Fabric	Diagenetic Features	Pore type	Sample	Descriptions
LOWER COCHRANE MEMBER - CHIMNEYHILL SUBGROUP - HUNTON GROUP	5006			Packstone	Stylolite: 1mm Stylolites[2]: 7mm Stylolites[3]: 1mm	Vuggy, lms [3mm]		Pinkish grey packstone, coarse <i>Pentamerid</i> brachs up to 4cm, some brachs have pyrite, sand infill on shelter porosity (karsting)
	5007			Packstone	vertical & horizontal micro-stylolites Stylolite: 2mm Fracture	Shelter, smg [10mm] Vuggy, smg [5mm] Intraparticle, smg [4mm]		Brownish tan packstone, coarse <i>Pentamerid</i> brachs (<i>Pentamerus</i>) Breccia with brown fine grained sand infill by karsting
	5008			Packstone	Micro-stylolites 0.25 mm Fracture	Shelter, smg [4mm] Vuggy, smg [5mm] Intraparticle, sms [0.5mm]	T.S.	Brownish tan packstone, <i>Pentamerid</i> brachs up to 4.2cm, sand infill on shelter porosity and along fractures
	5009			Grainstone Mudstone	Stylolite: 3mm vertical & horizontal fractures	Shelter, lms [1mm] Vuggy, lms [1mm]	T.S. ISO XRD	Greyish pink packstone, brachs up to 4.5cm, sand infill on shelter porosity Pink brachiopod grainstone, tight Grey dolomite mudstone, slightly laminated
	5010			Grainstone	Stylolites[2]: 1mm	Shelter, lms [1mm] Fracture, 2cm long 1mm wide		Pink brachiopod grainstone, tight, fractured
	5011			Packstone	Stylolites[2]: 3mm Fracture	Vuggy, lms [3mm]		Pink-brown-white brachiopod packstone, fine grained sand infill on shelter and interparticle porosities (karsting) Brownish tan packstone, brachs up to 3cm, micro-vugs in the brown matrix
	5012			Packstone	Stylolite: 4mm Fracture	Shelter, lms [2mm] Micro-vugs		Pinkish brown packstone, <i>Pentamerid</i> brachs up to 4cm with pink calcite cement in shelter porosity
	5013			Packstone	Stylolites[2]: 2mm Stylolite: 2mm Stylolite: 3mm	Micro-vugs Vuggy, smg [4mm]		Pinkish grey-brown packstone, <i>Pentamerid</i> brachs up to 4cm, micro-vugs in the brown matrix sand infill interparticle porosity by karsting
	5014			Packstone	Fracture Micro-stylolites Fracture			Pinkish grey-brown brachiopod packstone, sand infill on shelter and intraparticle porosity
	5015			Packstone	Stylolites[8]: 2mm	Vuggy, lms [1mm] Shelter, smg [4mm]		Pinkish grey packstone, brachs up to 3.5cm, mostly tight, sand infill along voids by karsting <i>Pentamerid</i> brach coquina
	5016			Packstone	Micro-stylolites Fracture	Vuggy, lms [1mm] Moldic, smg [4mm]		Pinkish grey packstone, brachs up to 3cm, fine grained sand filling voids and vugs (karsting)
	5017			Grainstone	Stylolites[3]: 1mm	Vuggy, lms [3mm]	T.S. ISO XRD SEM	Brown brachs replaced by dolomite Grey dolomite grainstone, brachs up to 6 cm, sand & mud filling voids (karsting)
	5018			Packstone	Stylolites[4]: 1mm Fracture Stylolite: 1mm Stylolite: 3mm	Vuggy, lms [3mm]	T.S.	Pinkish grey packstone, brachs up to 3 cm, tight, sand & mud infill on shelter porosity
	5019			Grainstone	Stylolite: 4mm Fracture Stylolites[5]: 1mm	Vuggy, smg [5mm] Fracture		Pinkish grey grainstone, brachs up to 5 cm, calcite crystals partially filling vugs
	5020			Packstone	Stylolite: 1mm Stylolite: 3mm Stylolites[3]: 1mm	Vuggy, smg [20mm] Fracture		Pinkish grey-brown packstone, <i>Pentamerid</i> brachs (up to 4cm), mud and very fine sand filling vugs and voids (karsting)
	5021			Grainstone	Stylolite: 0.5mm Stylolite: 2mm	Micro-vugs Vuggy, smg [20mm] Shelter, smg [10mm]	ISO	Yellowish pink-grey brachiopod grainstone, oil stained(?) Pinkish grey grainstone, partly dolomitized, brachs up to 5 cm
	5022			Grainstone	Stylolite: 4mm Fracture Stylolites[5]: 1mm	Vuggy, smg [9mm]	T.S.	Grey dolomitized brachiopod grainstone
	5023			Grainstone	Fractures Stylolites [2]: 2mm	Shelter, lms [3mm] Micro-vugs Vuggy, smg [4mm] Moldic, shelter smg [7mm]	T.S.	Yellowish grey dolomitized brachiopod grainstone, oil stained Dolomite cement Grey dolomitized grainstone, brachs up to 4 cm oil stained? Yellowish tan grainstone, brachs up to 3 cm
	5024			Grainstone	Stylolite: 2mm	Shelter, vuggy lms [3mm]		Tan grainstone, brachs up to 6cm
	5025			Mudstone	Stylolite: 0.5mm Stylolite: 3mm	Micro-vugs		Grey crystalline dolomite
	5026			Crystalline carbonate	Stylolites [2]: .5mm Fracture Stylolite: 2mm Stylolite: 1mm	Moldic, smg [5mm] Vuggy, lms [1mm]		Crystalline dolomite/grainstone, moldic porosity from brachs Grey crystalline carbonate, partly dolomitized, slightly laminated (red laminae)
	5027			Grainstone	Stylolite: 3mm Stylolite: 0.5mm	Micro-vugs Moldic, smg [16mm]	T.S.	Tan grainstone, brachs up to 2cm, partly dolomitized
	5028			Wackestone	Fracture Stylolite: 1mm	Vuggy, smg [13mm]		Grey dolomite wackestone, brachs up to 2cm becoming moldic porosity
	5029			Grainstone	Stylolite: 1mm Vertical stylolite	Shelter, smg [10mm]		Yellowish tan brachiopod grainstone, brachs up to 3.5 cm
	5030			Mudstone	Stylolite: 2mm Stylolite: 4mm Fracture Stylolites [2]: .5mm	Vuggy, lms [2mm]	T.S. XRD XRD	Tan dolomite mudstone, slightly laminated
	5031			Crystalline carbonate	Fracture Stylolites [5]: .5mm Fracture	Vuggy, smg [4mm] Micro-vugs	T.S. ISO	Yellowish tan crystalline dolomite, oil stained (?) Tan crystalline dolomite, brachs ghosts (?)
	5032			Packstone	Stylolite: 0.5mm Fracture Stylolite: 0.5mm Stylolite: 24mm	Fracture Vuggy, smg [5mm] Moldic, smg [20mm] Fracture		Yellowish tan crystalline dolomite, slightly laminated, oil stained? Grey dolomite packstone, moldic porosity from brachs Yellow-grey crystalline dolomite, slightly laminated, oil stained?
	5033			Mudstone	Vertical fracture	Vuggy, lms [1mm]		Light grey dolomite mudstone
	5034			Grainstone	Large fracture	Moldic, smg [10mm]	XRD	Grey dolomite grainstone, moldic porosity from brachs
	5035			Wackestone		Moldic, smg [7mm]		Grey dolomite wackestone, moldic porosity from brachs and coral fragments (5030' 3" to 4")
	5036			Mudstone	Fractures	Vuggy, smg [11mm] Fracture		Grey dolomite mudstone, green wavy discontinuous lamination
	5037			Grainstone	Fractures	Vuggy, smg [13mm] Moldic, smg [10mm]	T.S. ISO	Grey dolomite grainstone, moldic porosity from brachs
	5038			Mudstone/wackestone	Large fracture	Vuggy, lms [3mm]	XRD	Grey dolomite mudstone/wackestone highly fractured
	5039			Grainstone	Stylolites [7]: .5mm	Moldic, vuggy smg [5mm]	ISO	Grey grainstone, partly dolomitized, sublitharenite filling voids (Miserer Ss?)
	5040			Grainstone/crystalline dolomite	Stylolite: 0.5mm Fractures	Fracture, smg [5mm] Intraparticle, lms [2mm]	T.S.	White grainstone/boundstone, partly dolomitized, large tabulate coral colony (<i>Favosites</i>); sublitharenite filling voids Tabulate coral fragments (up to 8 cm)
5041			Grainstone	Fractures Stylolites [4]: 2mm Fracture	Shelter, lms [3mm] Vuggy, lms [3mm]		Partly dolomitized grainstone; lith- to sublith-arenites filling fractures	
5042			Grainstone	Fracture	Vuggy, lms [1mm]		Tan grainstone, brachs (up to 3cm); tight	
SYLVAN						T.S.	Light grey dolomitized grainstone	
5043							Green dolomitized mudrock, fractured, pyrite veins, light brown laminae	



smg - small megapore
 lms - large mesopore
 T.S. - Thin Section
 ISO - Isotope geochemistry
 SEM - Scanning Electron Microscopy

CORE DESCRIPTION

Fm.	Depth	Lithology	Fossils	Fabric	Diagenetic Features	Pore type	Sample	Descriptions
LOWER COCHRANE MEMBER - CHIMNEYHILL SUBGROUP - HUNTON GROUP	4962				Stylolite: 4mm	Shelter, smg [7mm] Vuggy, lms [3mm]		Pinkish brown packstone, coarse <i>Pentamerid</i> brachs; tight
				Packstone	Stylolites [5]: 1mm	Interparticle, smg [9mm] Intraparticle, lms [2mm]		Brownish grey packstone, merely brachs, highly porous, mud ~30%
	4963			Packstone	Vertical fracture Stylolite: 1mm	Interparticle, smg [5mm] Moldic, smg [4mm] Vuggy, smg [9mm] Fracture, 12cm long <1mm open		Greyish brown packstone, merely brachs, relatively high porous, mud ~35%
	4964			Packstone	Stylolites [2]: 1mm Vertical fracture	Intraparticle, lms [3mm] Shelter, lms [3mm] Fracture, 20cm long <1mm open Moldic, smg [9mm]	SEM T.S. ISO	Brownish green dolomitized mudstone, tight Grey dolomitized packstone, white brachs, fractured, less porous than the one at the base Grey dolomitized packstone, <i>Pentamerid</i> brachs, moldic porosity from brachs
	4965			Grainstone	Stylolite: 4mm Stylolites [2]: 2mm	Vuggy, smg [4mm]		Pinkish white brachiopod grainstone, tight
	4966			Packstone	Stylolite: 2mm Stylolite: 3mm Stylolites [2]: .5mm	Intraparticle, smg [7mm]		Brownish grey packstone, coarse <i>Pentamerid</i> brachs, mud ~25%
	4967			Packstone	Stylolite: 7mm Fracture Stylolites [4]: 2mm	Interparticle, smg [8mm] Vuggy, smg [5mm]		Pinkish white brachiopod packstone, mud ~25% Brownish grey brachiopod packstone, mud ~30% Pink packstone, coarse <i>Pentamerid</i> brachs, bounded by stylolites Grey brachiopod packstone
	4968			Packstone	Sand/mud infill Fracture	Moldic, smg [6mm] Vuggy, smg [7mm]	T.S. ISO	Breccia with fossil and intraclast fragments Brownish yellow dolomitized packstone, coarse <i>Pentamerid</i> brachs
	4969			Grainstone	Stylolites[4]: 1.5mm	Intraparticle, lms [1mm]		Grey packstone, coarse <i>Pentamerid</i> brachs; mud along fractures and surrounding brachs
	4970			Packstone	Stylolites[6]: 1.5mm	Intraparticle, smg [6mm]		Pinkish grey packstone/grainstone, coarse <i>Pentamerid</i> brachs, mud infill brachs and stylolites; tight
	4971			Grainstone	Stylolite: 5mm Stylolite: 2mm Stylolite: 1.5mm Stylolite: 3mm	Vuggy, smg [5mm] Interparticle, lms [3mm]		Greyish white packstone, <i>Pentamerid</i> brachs, mud (~40%) Brown brachiopod packstone, mud (~35%)
	4972			Grainstone		Moldic, smg [15mm] Vuggy, smg [9mm]	T.S. ISO	Brownish yellow dolomitized grainstone, moldic porosity from <i>Pentamerid</i> brachs
	4973			Packstone	Stylolites [2]: 5mm	Intraparticle, smg [5mm] Vuggy, smg [7mm]	T.S. ISO	Greenish pink brachiopod packstone bounded by stylolites, mud between brachs
	4974			Grainstone	Vertical fracture Stylolites [6]: 2mm	Interparticle, lms [2mm]		Pinkish white grainstone, coarse <i>Pentamerid</i> brachs, tight
	4975			Packstone	Stylolite: 1mm Stylolites [3]: 2mm	Interparticle, smg [9mm] Shelter, smg [5mm]		Pinkish grey brachiopod packstone White crystalline Ls bounded by stylolites Pinkish grey brachiopod grainstone, tight
	4976			Grainstone		Shelter, lms [3mm] Interparticle, lms [3mm] Vuggy, lms [2mm]		Pinkish yellow grainstone, coarse <i>Pentamerid</i> brachs (up to 3cm), tight Brownish yellow brachiopod packstone, calcareous mud (~20%); slightly dolomitized ?
	4977			Packstone	Fracture Stylolite: 3mm Fracture	Interparticle, smg [7mm] Vuggy, smg [10mm] Shelter, smg [15mm]		Pinkish grey packstone with coarse <i>Pentamerid</i> brachs Shelter porosity partially filled with calcite crystals
	4978			Grainstone	Stylolites [2]: 4mm Stylolites [2]: 1mm	Shelter, lms [3mm]		Greyish pink brachiopod grainstone
	4979			Grainstone	Fractures	Shelter, lms [3mm] Interparticle, smg [4mm]		Pinkish grey grainstone with coarse <i>Pentamerid</i> brachs
	4980			Packstone	Fractures Stylolite: 7mm	Vuggy, smg [5mm]		Brownish pink brachiopod packstone, mud ~40% Greyish pink mudstone; tight (2" thick)
	4981			Packstone	Stylolite: 10mm	Fracture, 9cm long <1mm open	T.S.	Pinkish grey brachiopod packstone
	4982			Packstone	Vertical fracture filled with calcareous mud			Pinkish grey packstone, <i>Pentamerid</i> brachs, calcareous mud filling fractures and surrounding brachs (karsting)
	4983			Grainstone	Stylolites [2]: 3mm			Pinkish brown <i>Pentamerid</i> brachiopod packstone, mud ~5%
	4984			Packstone	Stylolites [2]: 2mm			White crystalline Ls Pinkish brown <i>Pentamerid</i> brachiopod packstone, mud ~15%
	4985			Grainstone	Stylolites [3]: 1mm Stylolite: 3mm	Vuggy, lms [1mm]		Pinkish grey brachiopod grainstone, sparse crinoid fragments
	4986			Packstone		Shelter, lms [3mm]		Brachiopod packstone with brown calcareous mud (~30%)
	4987			Packstone	Stylolite: 5mm			Pink brachiopod packstone with brown calcareous mud; tight
	4988			Packstone/grainstone	Stylolites [6]: 1mm			Pinkish grey grainstone/packstone, <i>Pentamerid</i> brachs and crinoid fragments; tight
	4989			Packstone/grainstone		Shelter, smg [4mm] Intraparticle, smg [8mm] Vuggy, lms [2mm]		Tan grainstone/packstone, <i>Pentamerid</i> brachs and some crinoids, calcareous mud (~10%)
	4990			Packstone	Stylolite: 2mm	Vuggy, lms [3mm]		Greyish pink crystalline Ls bounded by stylolites; tight
	4991			Packstone	Crystalline carbonate Stylolites [7]: 2mm	Shelter, lms [3mm]		Brachiopod crinoidal packstone with dark brown calcareous mud (~25% of mud); tight
	4992			Grainstone	Stylolites [8]: 1mm Fracture			<i>Pentamerid</i> brachiopod grainstone; tight
	4993			Packstone		Vuggy, smg [6mm]		Pinkish tan brachiopod packstone with brown calcareous mud filling porosity
	4994			Packstone	Stylolites [4]: 1mm Fracture Stylolites [2]: 1mm			Greyish tan brachiopod packstone, brown calcareous mud; tight
	4995			Packstone	Stylolite: 1mm Fractures			Greyish tan brachiopod packstone, brown calcareous mud; tight
	4996			Crystalline carbonate	Stylolites[2]: 3.5mm			Greyish tan brachiopod packstone, brown calcareous mud surrounding brachs; tight
	4997			Crystalline carbonate	Stylolites[6]: 2.5mm			Tan crystalline Ls; tight
	4998			Grainstone	Vertical stylolite Fracture			Tan brachiopod grainstone, slightly laminated; tight
	4999			Packstone	Stylolite: 7mm Stylolite: 1mm Stylolite: 3mm			Yellowish white crystalline carbonate; tight Yellowish grey brachiopod packstone (~25% mud); tight
	5000			Crystalline carbonate	Stylolites [2]: .5mm Fracture			Yellowish white crystalline carbonate; tight
	5001			Packstone	Stylolite: 1mm			Greyish brown brachiopod packstone (~30% mud); tight
	5002			Packstone	Stylolite: 0.5mm Fracture	Fracture, 8cm long 3mm open		Brachiopod packstone, brachs up to 4 cm, calcareous mud infill surrounding brach shells and filling fractures (~40% mud); tight
	5003			Packstone	Stylolite: 3mm			Greyish white packstone, brachs > crinoids, calcareous mud infill (~30% mud); tight
	5004			Packstone	Fracture			Greyish brown packstone, crinoids (up to 3.2cm) and brachs (up to 3cm), calcareous mud infill (~45% mud)
	5005			Grainstone	Stylolite: 1mm			Pinkish white grainstone with crinoids and brachs; tight
	SYLVAN	4997						Greenish brown dolomitized mudrock, slightly calcareous, fractured, pyrite, wavy discontinuous lamination
		4998						

- Brachiopod
- Crinoid
- Coral
- Oil shale
- Shaly sandstone
- Limestone
- Dolomitized limestone
- Dolomite
- Dolomitized mudrock
- smg - small mesopore
- lms - large mesopore
- T.S. - Thin Section
- ISO - isotope geochemistry

CORE DESCRIPTION

Fm.	Depth	Lithology	Fossils	Fabric	Diagenetic Features	Pore type	Sample	Descriptions
WOODFORD SHALE	4950							
	4951							Dark grey organic shale, carbonaceous, pyrite
	4952							
MISENER	4953							Dark grey very fine to fine grained sandstone, abundant large brachiopods, sharp unconformable contact with the underlying Cochrane Fm.
LOWER COCHRANE MEMBER - CHIMNEYHILL SUBGROUP - HUNTON GROUP	4954			Packstone/ grainstone				Coral fragments (<i>Favosites</i> sp.)
	4955			Packstone/ grainstone	Vertical fractures	Vuggy		Coral fragments (<i>Favosites</i> sp.)
	4956			Packstone/ grainstone		Interparticle		Pinkish grey packstone/grainstone, coarse <i>Pentamerus</i> brachs, sand infill in open vertical fractures and vugs (Misener); chaotic breccias, calcite crystals partially filling vugs
	4957			Packstone/ grainstone				
	4958			Packstone				
	4959			Packstone		Vuggy Moldic		Pinkish grey packstone, brachs (mainly <i>Stricklandia</i> , sparse <i>Pentamerus</i>) mostly tightly cemented, little sand infill
	4960			Packstone				
	4961			Packstone			Solution enlarged molds	
	4962			Packstone	Fractures	Vuggy Moldic Vertical open fractures		Pinkish grey packstone, brachs (mixed <i>Stricklandia</i> and <i>Pentamerus</i>) short open vertical fractures
	4963			Packstone				
	4964			Packstone				
	4965			Packstone			Solution enlarged molds Moldic	Pinkish grey brachiopod packstone with sparse corals, cavern fill
	4966			Packstone/ grainstone				
	4967			Packstone/ grainstone	Fractures	Moldic Vertical open fractures		Pinkish grey packstone/grainstone, brachiopod <i>Stricklandia</i>
	4968			Grainstone				
	4969			Grainstone				
	4970			Grainstone			Moldic	Pinkish grey grainstone with <i>Pentamerid</i> brachs, mostly tightly cemented; possible recrystallized stromatoporoid (4971.5')
	4971			Grainstone				
	4972			Grainstone				
	4973			Grainstone				
	4974			Packstone				
	4975			Packstone	Fractures	Interparticle Moldic		Pale orange packstone, leached vuggy brachiopods
	4976			Packstone				
	4977			Packstone				
	4978			Packstone		Moldic		Pinkish grey packstone with crinoids and brachs, tighly cemented
	4979			Grainstone				
	4980			Grainstone			Moldic	Pinkish grey grainstone with large crinoids and sparse large brachs, tighly cemented
	4981			Grainstone				
4982			Grainstone					
4983			Grainstone					
4984			Grainstone					
4985			Grainstone					
4986			Grainstone					
4987			Grainstone	Fractures	Moldic Interparticle		Greyish orange crinoidal grainstone, sparse brachs, trace of ooids, leached collapsed grainstone	
4988			Grainstone					
4989			Grainstone					
4990			Grainstone					
4991			Grainstone					
4992			Grainstone					
4993			Grainstone					
4994			Grainstone			Interparticle	Greyish orange crinoidal grainstone, sparse brachs, tightly cemented, terra rosa	
4995			Grainstone					
4996			Grainstone		Moldic		Greyish orange grainstone, coarse brachs and crinoids (<i>Pentamerid</i> brach - <i>Stricklandia</i>), leached to fine separate vugs in interparticle pores	
4997			Grainstone			Interparticle		
4998			Grainstone	Stylolite: 3mm Stylolite: 2mm		Intraparticle, smg [4mm] Vuggy, lms [1mm]	Tan grainstone, <i>Pentamerid</i> brachs (<i>Stricklandia</i>), sparse crinoids	
4998			Grainstone	Stylolite: 1mm		Micro-vugs	T.S. slightly dolomitized; oil stained ?	
4999			Grainstone	Fractures		Shelter, lms [3mm] Fracture, 40mm long 1mm open Moldic, lms [3mm]	ISO Yellowish olive grainstone, brachs (up to 3.7cm), shelter porosity filled with calcite crystals	
4999			Grainstone			Vuggy, smg [5mm]	ISO Brownish grey dolomite, laminated	
5000			Crystalline dolomite	Stylolite: 3mm			T.S. calcite veins	
5001				Fractures			Green dolomitized mudrock pyrite laminated, fractured	

CORE DESCRIPTION

Fm.	Depth	Lithology	Fossils	Fabric	Diagenetic Features	Pore type	Sample	Descriptions	
WOODFORD	4942							Black organic shale, highly calcareous, pyrite	
	4943							Dark grey shaly sandstone with thin beds and laminae of very fine quartz sand interbedded with shale; basal contact is sharp, very irregular and sand extends deep into fractures in the underlying Cochran Fm.	
MISENER									
LOWER COCHRANE MEMBER - CHIMNEYHILL SUBGROUP - HUNTON GROUP	4944			Packstone				Light grey packstone, <i>Pentamerus</i> brachs, solution fractures and vugs filled with grey sand (Misener) occluding porosity	
	4945			Packstone					
	4946			Packstone					
	4947			Packstone		Vuggy		Pinkish grey packstone, coarse <i>Pentamerus</i> brachs with thin intervals of <i>Stricklandia</i> ; mostly tightly cemented, minor karst infill of vuggy porosity	
	4948			Packstone					
	4949			Packstone					
	4950			Packstone					
	4951			Packstone					
	4952			Packstone		Vuggy		Pinkish grey packstone, coarse <i>Pentamerus</i> brachs coquina, partly tightly cemented, partly well developed vuggy porosity filled with calcareous mud (Misener)	
	4953			Packstone					
	4954			Packstone					
	4955			Packstone					
	4956			Packstone					
	4957			Packstone					
	4958			Packstone				Pinkish grey packstone, coarse brachs (<i>Pentamerus</i>), about 60% with absent matrix, voids filled with mud (Misener); about 40% tightly cemented with calcareous mud	
	4959			Packstone					
	4960			Packstone					
	4961			Packstone					
	4962			Packstone					
	4963			Packstone					
	4964			Packstone				T.S.	
	4965			Packstone					
	4966			Packstone					
	4967			Packstone	Fracture		Vuggy		Pinkish grey packstone with coarse brachs (<i>Pentamerus</i>); much karst dissolution, large solution fracture across, and interparticle voids filled dark brown mud and quartz sand (Misener or Woodford)
	4968			Packstone					Porosity largely occluded by karst infill, mainly fine calcite with minor quartz sand
	4969			Packstone					
	4970			Packstone					
	4971			Packstone					
	4972			Packstone					
	4973			Wackestone					
	4974			Wackestone	Fracture		Vuggy		Pinkish grey wackestone with large thin brachs, discontinuous vertical-incline and horizontal solution fracture, partially healed
	4975			Packstone					Pinkish grey brachiopod packstone, <i>Pentamerid</i> brachs, abundant karst infill in interparticle porosity
	4976			Packstone					
4977			Grainstone				T.S.	Light grey to pinkish grey grainstone, sparse coarse brachs (<i>Stricklandia</i>) with very fine coral - brach fragments	
4978			Crystalline carbonate Grainstone	Stylolite: 8mm Stylolite: 3mm Stylolite: 2mm		Shelter, smg [5mm] Vuggy, smg [8mm] Moldic, smg [12mm]	T.S. T.S.	Tan crystalline Ls Tan brachiopod grainstone, brachs up to 4cm	
4979			Grainstone	Stylolite: 1mm Stylolite: 1mm		Vuggy, smg [20mm] Intraparticle, smg [8mm]	ISO	Grey dolomite grainstone, abundant moldic porosity from brachs oil stained ? Greyish tan dolomitized grainstone, brachs up to 4 cm	
4980			Grainstone	Fracture Stylolite: 1mm		Intraparticle, smg [7mm] Vuggy, lms [3mm]		oil stained ? Greyish tan brachiopod grainstone/packstone, brachs up to 4 cm, fine fossil fragments filling shelter porosity, dolomitized	
4981			Grainstone	Stylolite: 1mm		Shelter, lms [2mm] Intraparticle, smg [4mm]	T.S. ISO	oil stained ? Greyish tan dolomitized grainstone/packstone with fine <i>Pentamerus</i> brachs (up to 4 cm); shelter porosity filled with fossil fragments	
4982			Packstone Grainstone/ crystalline carbonate	Stylolite: 3mm Fracture Stylolite: 1mm		Shelter, lms [3mm] Vuggy, lms [1mm] Moldic, lms [1mm] Fracture, 17mm long <1mm open	T.S. T.S. ISO	Grey packstone with <i>Pentamerus</i> brachs (up to 3.5 cm); dolomitized	
4983			Grainstone/ crystalline carbonate	Fracture			T.S.	Yellow dolomitized grainstone/crystalline carbonate with a grey level of dolomite; tight	
4984				Fracture Fractures				Grey laminated dolomite mudstone on unconformable contact with the Sylvan mudrock Green dolomitized mudrock pyrite laminated, fractured	
SYLVAN	4985								